

For Reference

NOT TO BE TAKEN FROM THIS ROOM

Ex libris
UNIVERSITATIS
ALBERTAENSIS





Digitized by the Internet Archive
in 2019 with funding from
University of Alberta Libraries

<https://archive.org/details/Deroy1976>

THE UNIVERSITY OF ALBERTA

RELEASE FORM

NAME OF AUTHOR JEAN-MARC DEROY.....
TITLE OF THESIS SETTLEMENT BEHIND ANCHORED WALLS.....
.....
.....
DEGREE FOR WHICH THESIS WAS PRESENTED MASTER.OF.SCIENCE.
YEAR THIS DEGREE GRANTED .1974.....

Permission is hereby granted to THE UNIVERSITY OF
ALBERTA LIBRARY to reproduce single copies of this
thesis and to lend or sell such copies for private,
scholarly or scientific research purposes only.

The author reserves other publication rights, and
neither the thesis nor extensive extracts from it may
be printed or otherwise reproduced without the author's
written permission.

THE UNIVERSITY OF ALBERTA

SETTLEMENT BEHIND ANCHORED WALLS

by

JEAN-MARC DEROY

A THESIS

SUBMITTED TO THE FACULTY OF GRADUATE STUDIES AND RESEARCH
IN PARTIAL FULFILMENT OF THE REQUIREMENTS FOR THE DEGREE
OF MASTER OF SCIENCE

DEPARTMENT OF CIVIL ENGINEERING

EDMONTON, ALBERTA

SPRING, 1976

THE UNIVERSITY OF ALBERTA

FACULTY OF GRADUATE STUDIES AND RESEARCH

The undersigned certify that they have read, and recommend to the Faculty of Graduate Studies and Research for acceptance, a thesis entitled "Settlement Behind Anchored Walls," submitted by Jean-Marc Deroy in partial fulfilment of the requirements for the degree of Master of Science.

ABSTRACT

With the increasing use of anchors in excavation engineering, particularly in urbanized areas, it is of great interest to be able to minimize the ground surface settlements around such excavations.

A parametrical study of the characteristics of the soil and anchoring conditions with respect to ground surface settlements is investigated in this report.

The Finite Element Analysis, with plane strain conditions, was selected for the study of effects of the angle of anchoring, the length of anchoring, the prestress load in the anchor, the coefficient of earth pressure at rest (K_0) and the Young's modulus (E) of the soil on a typical excavation.

In order to verify the validity of this numerical method, a back analysis was performed on an outstanding case history and gave reasonable agreement between observed and predicted settlements of the ground surface.

The parametrical study proved that the characteristics of the soil (K_0 and E) dictate the magnitude of the settlements of the ground surface. However, some design considerations can minimize these deformations.

The general shape of the ground surface settlements presents two maxima.

The first maximum settlement situated close to the wall of the excavation is not affected by the length or angle of anchoring but will be reduced by an increase in the prestress load.

The second maximum settlement, situated at the level of the grouted part of the anchors is, on the contrary, not affected by changes in the prestress load, but will be reduced by an increase in the length or angle of anchoring.

ACKNOWLEDGEMENTS

The research presented in this study has been carried out at the Department of Civil Engineering, The University of Alberta, under the direction of Dr. Z. Eisenstein. The author wishes to express his appreciation to Dr. Z. Eisenstein for his guidance throughout this study.

Acknowledgements are also due to the professors of the Department of Civil Engineering for their informative lectures in the field of soil mechanics. Particular thanks are expressed to Dr. N. R. Morgenstern and Dr. D. W. Murray for their advice, particularly at the beginning of this research; to Dr. A. V. G. Krishnayya for his help with the Finite Element programs, and to Mr. R. F. Howells for advice with respect to the computer operations.

The author expresses his gratitude to the Canada Council which supported him financially during the time of this study. The financial assistance of the University of Alberta and the Department of Civil Engineering is also gratefully acknowledged.

The opportunity for advanced education came from the Ministère de l'Équipement et du Logement of France, and is greatly appreciated.

Finally, the author presents his acknowledgements to his family and friends for their encouragement and moral

support during the entire time of this research. In particular, the interesting discussions with Mr. S. Law, the proof reading and editing of Mr. J. Simmons and Mr. M. Dusseault were deeply appreciated. Special thanks are extended to Mrs. Wahl for her typing expertise.

TABLE OF CONTENTS

CHAPTER		PAGE
I	INTRODUCTION	1
	1.1 The Use of Anchors for Excavations . . .	1
	1.2 Importance of the Ground Surface Deformations	4
	1.3 Analysis and Prediction of the Ground Surface Deformation	5
	1.4 The Finite Element Method	6
II	PARAMETRICAL STUDY	9
	2.1 Outline of the Parametrical Study	9
	2.1.1 Soil and Excavation Conditions . . .	9
	2.1.2 Characteristics of the Anchoring . .	10
	2.1.3 Choice of Earth Pressure Coefficient K_o	13
	2.1.4 The Finite Element Mesh	16
	2.2 Stability Analysis and Factors of Safety	21
	2.2.1 Free Earth Support Analysis	21
	2.2.2 Limiting Position for the Anchors . .	22
	2.2.3 Required Length for the Grouted Part of the Anchors	23
	2.2.4 Overall Stability of the Chosen Anchors	25
	2.2.5 Safety Factors of the Chosen Anchors With Respect to the Overall Stability	27
	2.2.6 Determination of Anchor Prestress Limits	33

CHAPTER		PAGE
2.3	Results of the Parametric Study	34
2.3.1	Presentation of the Results	34
2.3.2	Influence of the Geometry	36
2.3.3	Influence of the Coefficient of Earth Pressure at Rest (K_0)	44
2.3.4	Influence of the Prestress in the Anchors	48
2.3.5	Influence of Young's Modulus	55
2.4	Conclusions of the Finite Element Analysis	62
2.4.1	General Shape of the Ground Surface Deformations	62
2.4.2	The First Maximum Settlement	63
2.4.3	The Second Maximum Settlement	63
2.4.4	Relative Importance of the Various Factors Studied	65
III	ANALYSIS OF A CASE HISTORY	68
3.1	The Selection of a Case History	68
3.2	Analysis of Entertainment Center and Theme Towers Excavation	69
3.2.1	Situation and Characteristics of the Excavation	69
3.2.2	Procedure Used for the Analysis	71
3.2.3	Values Assumed for the Analysis	73
3.2.4	Results of the Finite Element Analysis	78
3.3	Measured Displacements	81
3.4	Comparison of Actual and Predicted Behaviour	83

CHAPTER	PAGE
IV CONCLUSIONS AND RECOMMENDATIONS	87
4.1 Conclusions	87
4.1.1 The Reliability of the Finite Element Analysis	87
4.1.2 The Assumption of Plane Strain	88
4.1.3 The Advantages of a Finite Element Analysis	90
4.1.4 The Results of the Parametrical Study	91
4.2 Recommendations	93
4.2.1 Design Considerations	93
4.2.2 Results of Model Tests	93
4.2.3 Field Measurements	95
REFERENCES	97
APPENDIX A	102

LIST OF TABLES

TABLE	PAGE
1.1.1. Comparison of Various Excavating Procedures .	2
2.1.1. Data Chosen for the Parametrical Study	11
2.1.2. Data Chosen for the Parametrical Study	12
2.1.3. Limits for the Coefficient of Earth Pressure at Rest	15
2.2.1. Verification of the Overall Stability	28
2.2.2. Factors of Safety With Respect to the Overall Stability	31
2.2.3. Prestress Values for Different Limits and Capacities	35
2.3.1. Demonstration of Proportionality Between the Second Maximum Settlement and K_O	49
2.3.2. Check of the Relations Between the Prestress Load, the Heave, the First Maximum Settlement and the Second Maximum Settlement	53
3.2.1. Parameters Drawn from the Report	76
3.2.2. Assumed Parameters	77

LIST OF FIGURES

FIGURE	PAGE
2.1.1. Discretization of an Excavation	17
2.1.2. General Mesh for the Parametrical Study . . .	18
2.1.3. Mesh for the Sheetpile Zone	19
2.1.4. Mesh for the Anchors' Zone	20
2.2.1. Limitations in Length Due to the Potential Active Slip Surface	24
2.2.2. Evaluation of Anchor Stability	26
2.2.3. Determination of the Anchor's Capacity . . .	30
2.2.4. Factors of Safety for the Nine Anchors With Respect to the Design Capacity	32
2.3.1. Influence of the Length of Anchoring on the Ground Surface Settlements	37
2.3.2. Influence of the Angle of Anchoring on the Ground Surface Settlement	38
2.3.3. Position and Amplitude of the First Maximum Settlement for the Nine Anchors	40
2.3.4. Position and Amplitude of the Second Maximum Settlement for $K_0 = 0.67$	41
2.3.5. Position and Amplitude of the Second Maximum Settlement for $K_0 = 1.0$	42
2.3.6. Position and Amplitude of the Second Maximum Settlement for $K = 1.50$	43
2.3.7. Influence of the Value of the Coefficient of Earth Pressure at Rest on the Settlement of the Ground Surface	45
2.3.8. Variation in Amplitude and Position of the Second Maximum Settlement for Different Values of K_0 for ($E = 15,000$ psi and $A_p = 19,200$ lbs.)	46

FIGURE	PAGE
2.3.9. Variation in Amplitude and Position of the Second Maximum Settlement for Different Values of K_o for ($E = 15,000$ psi and $A_p = 19,200$ pds.)	47
2.3.10. Proportionality of the Amplitude of the Second Maximum Settlement and Different Values of K_o for ($E = 15,000$ psi and $A_p = 19,200$ pds.)	50
2.3.11. Influence of the Value of Prestressing on the 1st and 2nd Maximum Settlement for Anchor 5 with $K = 1.0$ and $E = 15,000$ psi.	52
2.3.12. Representation of the Proportionality Between the Anchor Prestress and the Amplitude of the First Maximum Settlement for Anchor 5 with $K = 1.0$ and $E = 15,000$ psi.	54
2.3.13. Influence of the Value of Prestressing on the Amplitude of the 2nd Maximum Settlement for Anchor 5 with $K = 1.0$ and $E = 15,000$ psi.	56
2.3.14. Influence of Young's Modulus (E) on the Amplitude and Position of the 1st Maximum Settlement for Anchor 5 with $K = 1.0$ and $A_p = 19,200$ lbs.	58
2.3.15. Influence of Young's Modulus (E) on the Amplitude and Position of the 2nd Maximum Settlement for Anchor 5 with $K = 1.0$ and $A_p = 19,200$ lbs.	59
2.3.16. Relation Between the Amplitude of the 1st Maximum Settlement and Young's Modulus (E) for Anchor 5 with $K = 1.0$ and $A_p = 19,200$ lbs.	60
2.3.17. Relation Between the Amplitude of the 2nd Maximum Settlement and Young's Modulus (E) for Anchor 5 with $K = 1.0$ and $A_p = 19,200$ lbs.	61
2.4.1. Factors Influencing the 1st Maximum Settlement (P = prestressing, E = Young's Modulus, K = coefficient of Earth Pressure)	64

FIGURE	PAGE
2.4.2. Factors Influencing the 2nd Maximum Settlement (P = prestressing, E = Young's Modulus, K = coefficient of Earth Pressure at rest, A = angle of anchoring, L = Length of Anchoring).	66
3.2.1. Geometry of the Excavation for Entertainment Center and Theme Towers	70
3.2.2. Finite Element Mesh Used to Represent the Excavation for Entertainment Center and Theme Towers	74
3.2.3. Detail of the Soldier Piles and Anchor	75
3.2.4. Predicted Settlement of the Ground Surface . .	79
3.2.5. Predicted Deflection of the Ground Surface Towards the Excavation	80
3.3.1. Measured Deformations at the Level of the Soldier Piles S-15 and N-42.	82
3.4.1. Comparison of Measured and Predicted Settlements at the Level of S.P. N-42.	84
3.4.2. Comparison of Measured and Predicted Deflections of the Ground Surface Towards the Excavation at the Level of S.P. N-42.	85
4.1.1. Evaluation of the plane strain assumption . .	89

CHAPTER I

INTRODUCTION

1.1 The Use of Anchors For Excavations

Population growth and urbanization in developed countries have resulted in unprecedented growth of metropolitan centres, usually concentrated around previously existing urban centers. Land values are increasing rapidly and there is much pressure for complete and efficient use of downtown real estate. Under these pressures, large scale excavations become more necessary, yet more difficult; resulting in the increasing use of anchoring in excavation engineering (Habib, 1969).

Anchored walls have some distinct advantages compared to rigid gravity walls and knowledge of these advantages is essential to the decision making process. Table 1.1.1 summarizes the main factors influencing the choice of an anchored wall. Once the decision to use an anchored wall has been made, there is a further choice of using an anchored soldier pile wall, a sheetpile wall, or a concrete wall. Depending on the characteristics of the excavation and the possible use of a temporary wall as part of the permanent structure, one of these three solutions becomes more feasible than the others. The three basic types of walls offer different rigidities: the concrete wall being the stiffest;

TABLE 1.1.1

COMPARISON OF VARIOUS EXCAVATING PROCEDURES

(AFTER D'APPOLONIA ET AL., 1967)

Item	Flattened Slope	Rigid Wall	Flexible Sheet Pile Wall and Tension Ties
Cost	M ^a	H	L
Real Estate Loss	H	L	L
Design Difficulty	L	H	M
Construction Difficulty	L	H	L
Subsurface Investigation	L	M	H
Observation and Control During and Following Construction	L	M	H
Risk During Construction	L	M	H

^aFor comparative purposes the symbols L (low), M (medium), and H (high) denote relative degree of difficulty, expenditure, etc.

the anchored soldier piles the most flexible; the sheetpile wall having an intermediate rigidity. As an alternative to anchoring, the use of braced excavations is not a satisfactory solution in most cases, as the internal braces limit the dimensions of the excavating equipment and the walls of the foundation have to be reconcreted after removal of the braces. The choice of an anchored temporary wall is often economically more interesting than a gravity rigid wall or flattened slopes.

With all types of anchored and braced walls it is of major concern to predict their stability and deformation behavior. To better understand the stress distribution and deformations related to anchored or braced excavations, and to predict future behavior, a variety of approaches may be used: scale model laboratory tests, theoretical and numerical analyses, or a purely empirical approach based on monitoring of prototype walls. Laboratory scale models have been performed on anchored bulkheads by Browsin (1948), Rowe (1952) and Terzaghi (1953) with the point of interest being the stress distribution behind a retaining wall. In their paper on the earth pressures on flexible structures, Bjerrum, Clausen and Duncan (1972) show that the application of Finite Element Analysis to anchored sheetpile walls would be rewarding. This type of analysis, already performed for braced excavations by Palmer and Kenney (1971) gave results in agreement with the observations in the field. With respect to anchored walls

such an analysis has not been yet performed. Therefore, a Finite Element Analysis performed as a parametrical study and on an existing case history would be considered a step forward especially if the data recorded are in agreement with the stress and deformation computed by the analysis.

In order to demonstrate the reliability of this method, it is necessary to have well instrumented field cases: for example, Liu and Dugan (1972), Clough and Weber (1972) and Shannon and Strazer (1970). To increase our confidence in numerical analytic methods such as the Finite Element method, high quality field data is necessary. This data is being, and will continue to be, generated as the number of anchored excavations increases, due to the necessity for detailed monitoring to preclude the possibility of catastrophic failure. This study will explore some deformation characteristics of anchored sheetpile walls using the Finite Element method, and will include analysis of soil variability, geometrical arrangement of the anchoring, prestress of the anchor and finally a check of the validity of the method using a case history.

1.2 Importance of the Ground Surface Deformations

The existence of surrounding structures often dictates the use of braced or anchored excavations, and any movement of the ground surface will give rise to differential settlements which can lead in some cases to intolerable

deformation of such structures. The absolute value of the ground deformations must often be kept as small as possible: for example, one-fourth of an inch in the case of a bridge near an excavation in the Los Angeles area (Maljian and Van Beveren, 1974). For such critical cases, precise monitoring of the deformations is essential. In fact, with the great majority of braced or anchored excavations to date, the allowable deformation rather than stability is the crucial design parameter. In the case of braced open cuts, Caspe (1966) studied in detail the movement of the ground surface, while Meissner (1970) and Plant (1972) analysed the case of anchored excavations, the influence of the angle of anchoring and of the point of anchoring with respect to the ground surface settlement. Several parameters have an influence on the deformations of the ground surface and only a parametrical study can tell the relative contribution of each factor. To prove the reliability of such a numerical analysis it is necessary to compare it with data recorded in the field for similar types of excavations.

1.3 Analysis and Prediction of the Ground Surface Deformation

Three different groups of parameters affect the settlement of the ground surface. First, the soil stress-strain characteristics, usually represented by Young's modulus (E) and Poisson's ratio (μ) will govern the deformation response of the soil for different stress distributions.

The coefficient of earth pressure at rest (K_0) influencing the value of the stress relief due to the excavation is another characteristic of the soil independent of the anchoring conditions. The second group of parameters describes the geometric configuration of the anchor for a particular point of anchoring on the sheet pile. Within the limits dictated by the stability analysis, the neutral length of the anchor and its angle from the horizontal are two parameters which could influence the ground surface settlement. Finally, the prestress in the anchor is a major factor: as well as physically holding the retaining wall, it introduces a stress field into the ground. The range of stresses thus introduced is limited by geometry and soil parameters on the one hand, and by the stability of the retaining wall on the other.

1.4 The Finite Element Method

Due to the work of Clough (1960) and the advent of powerful digital computers, the Finite Element Method has provided engineers with a powerful tool enabling them to study previously unsolvable stress and deformation problems in continuous bodies. This type of analysis is the only possible choice for a parametrical study of this kind. After some fourteen years, there is an extensive literature on the subject and the application of the method has proven to be rewarding.

In this study, the excavation is divided into a certain number of elements connected at their nodes. For each element, properties are assigned depending on the characteristics of the material which constitutes this element; then, for every node, a set of equations representing the influence of all other elements on the displacement of this particular node is established. The entire structure may thus be represented in a set of simultaneous equations in terms of nodal displacements. Using the facilities of the digital computer, this set of equations is solved and the displacement of each node determined. Knowing the displacements of the nodes for each element, the strain for each element is evaluated; and on the assumption of a particular stress-strain relationship, the stress for every element is then calculated. The displacements and stresses for the nodes and elements give a picture of the behaviour of the entire structure under different boundary conditions. The analysis may be performed either in two or three dimensions for parts of the wall far away from the corners. It is reasonable to assume that the deformations perpendicular to the chosen section are very small, and therefore a two dimensional analysis would accurately predict the excavation deformations (despite the fact that individual anchors behave in an axisymmetric manner, which ideally would call for a three dimensional analysis). This study however is concerned mainly with deformations of

the ground surface behind the excavation where the influence of closely spaced anchors would have a rather continuous effect. Because of the factors of safety employed with respect to overall stability excavations are usually subjected to relatively small strains and it is reasonable to assume that a linear elastic stress-strain relationship is acceptable.

CHAPTER II

PARAMETRICAL STUDY

2.1 Outline of the Parametrical Study

2.1.1 Soil and Excavation Conditions

For the selection of the different values of the soil and excavation parameters, standard conditions were assumed. First of all, in this study, a sand and gravel soil was chosen as its behaviour is intermediate between a soft rock which would be stiffer and a cohesive soil which would be more deformable. The weight per cubic foot, the friction angle, Young's modulus and Poisson's ratio for this soil are taken from common values in practice. In the case of Young's modulus, its value was increased with depth to represent what usually occurs in the field.

The geometry of the excavation, with a final grade at 30 feet below the ground surface level, represents a depth commonly encountered in practice. For the choice of the type of retaining wall, the same consideration was followed. The sheetpile wall, having a rigidity less than a concrete wall but more than a soldier pile wall with lagging, will give rise to deformations of intermediate amplitude. The embedment of the pile was determined by the free earth support method as the study is concerned with the behaviour of a wall driven to a shallow depth.

As for the type of anchors, friction anchors were selected as these are the most widely used in cohesionless soils. Belled anchors are commonly used for the lower parts of retaining walls but the deformation of the ground surface is largely governed by the behaviour of the friction anchors which are closer to the ground surface. The length of these anchors is designed to resist the pull-out force acting upon them by the prestress load. The angle of the anchor with the horizontal can be as high as 65 degrees but most excavations use anchors inclined between 0 and 30 degrees: these values will serve as limits in this study. Once the angle of anchoring has been selected, the free length of the anchor is limited by the consideration of the overall stability which will be verified in section 2.2. On top of these conditions, the grouted part of the anchor must be situated beyond the active wedge for the anchor to be effective. The different values chosen for this study are presented in Tables 2.1.1 and 2.1.2.

2.1.2 Characteristics of the Anchoring

To study the effects of anchor geometry, three different angles and three different lengths were chosen for the anchoring system. These values are chosen to cover most practical ranges and they also must satisfy the overall stability conditions (as checked in item 2.2.4). The embedment of the sheetpile wall is first determined, utilizing

TABLE 2.1.1
DATA CHOSEN FOR PARAMETRICAL STUDY

Type of Soil	Sand & Gravel
Unit Weight of the Soil	130 pcf.
Angle of Internal Friction	38°
Coefficient of Active Earth Pressure, K_a (for wall friction δ_a)	0.20
Coefficient of Passive Earth Pressure, K_p (for wall friction δ_p)	9.00
Angle of Wall Friction for Active Case, δ_a	+20°
Angle of Wall Friction for Passive Case, δ_p	+25°
Depth of Excavation	30 feet
Embedment of the Wall	5 feet
Type of Sheetpile Wall	Larsen 24
Point of Anchoring on the Wall	10 feet below ground
Working Load	19200 lbs./ft
Factor of Safety With Respect to Failure of the Lower Part of the Wall G_s	1.6
Factor of Safety With Respect to Anchor Pressure	3.0
Working Load as Percentage of Design Load	95%
Factor of Safety With Respect to Pull-Out Resistance for the 9 Anchors is at Least	1.5

TABLE 2.1.2
DATA CHOSEN FOR THE PARAMETRIC STUDY

Young's Modulus of Steel	29,000,000	psi
Young's Modulus of Concrete	3,000,000	psi
Young's Modulus of Soil	<u>15,000</u>	<u>psi</u> +5,000 every 10 feet
Poisson's Ratio of Steel	0.3	
Poisson's Ratio of Concrete	0.2	
Poisson's Ratio of Soil	0.4	
Equivalent Width of the Wall	0.6	feet
Length of the Grouted Anchor	10	feet
Diameter of the Friction Anchor	1	foot
	<u>Angle</u>	<u>Length</u>
Anchor 1	0°	38'
Anchor 2	0°	45'
Anchor 3	0°	52'
Anchor 4	15°	38'
Anchor 5	15°	45'
Anchor 6	15°	52'
Anchor 7	30°	38'
Anchor 8	30°	45'
Anchor 9	30°	52'

a reasonable factor of safety (G_s) with respect to failure of the lower part of the bulkhead. This gives a minimum value to the required prestress of the anchor. Another factor of safety is then applied to the prestress of the anchor with values varying between 2 and 3. The working load is then taken as 85 to 95 percent of this value. Once this value is fixed, the minimum required length of the friction anchor is calculated to resist this pull-out force and a factor of safety with respect to pull-out resistance is chosen: common practice dictates the use of a factor of 1.5. The overall stability is then checked, first verifying that the system is in equilibrium and secondly, evaluating the maximum capacity for a particular position of the anchor (Figure 2.2.2 and Figure 2.2.3). Nine different anchoring conditions will be studied and the overall stability and maximum capacity will be calculated for each geometric configuration. It should be emphasized that the various safety factors are not compoundable in any sense: each applies only to the particular analysis in which it is involved.

2.1.3 Choice of Earth Pressure Coefficient K_0

One of the factors which has a definite influence on deformations around excavations is the coefficient of earth pressure at rest K_0 (Dibiagio, 1966). It is reasonable to expect that the vertical ground subsidence around anchored walls as well would be related to K_0 values. Therefore, a

parametric study, which investigates various effects on deformations around anchored bulkheads should include a variation of K_o .

According to the theory of elasticity, the coefficient of earth pressure at rest is given by:

$$K_o = \frac{\mu}{1-\mu} \quad (1)$$

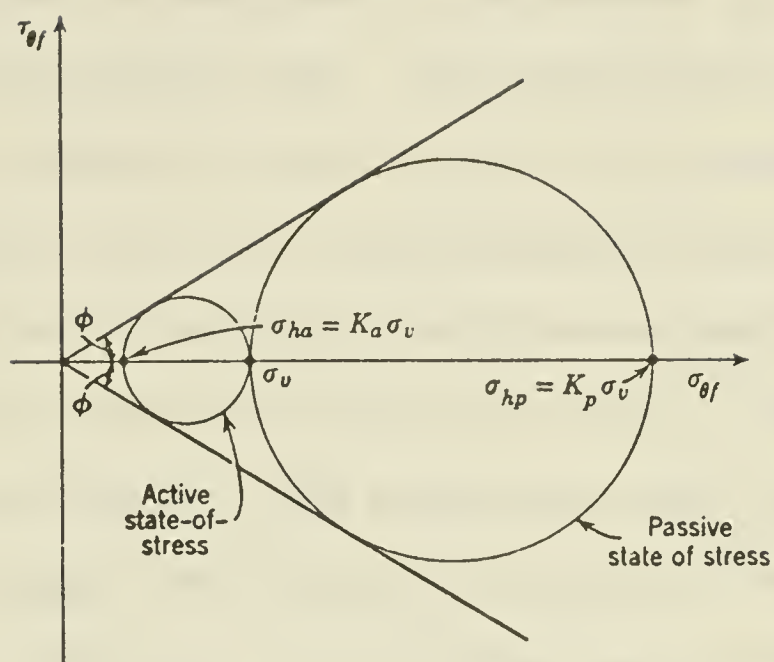
In reality, however, this is very seldom the case. Factors such as overconsolidation, tectonic stresses, etc. cause deviations from the ideal value given by equation 1. In extreme cases K_o could become equal to the active or passive earth pressure coefficients in accordance with the Rankine theory. For the particular value of the angle of internal friction chosen in this study ($\phi = 38^\circ$), the limiting earth pressure coefficients K_a and K_p can be found from Table 2.1.3.

For the purpose of the parametric study, three typical values of K_o were chosen, covering the most probable range of field values. They were:

$$K_{o1} = \frac{\mu}{1-\mu} = 0.67 \quad (\text{the "ideal" case})$$

$$K_{o2} = 1.5 K_{o1} = 1.00 \quad (\text{slightly overconsolidated soil})$$

$$K_{o3} = 2.25 K_{o1} = 1.50 \quad (\text{overconsolidated soil})$$



Rankine states of stress for geostatic condition.

Values of K_a and K_p for Rankine States of Geostatic Stress

ϕ	K_a	K_p
10°	0.703	1.42
15°	0.589	1.70
20°	0.490	2.04
25°	0.406	2.46
30°	0.333	3.00
35°	0.271	3.66
40°	0.217	4.60
45°	0.171	5.83

Table 2.1.3. Limits for the coefficient of earth pressure at rest.

(After Lambe and Whitman, 1969)

2.1.4 The Finite Element Mesh

Once the characteristics of the excavation are determined, a mesh is designed to represent this infinite media within a delimited area. The boundaries of the problem must be chosen in such a way that boundary conditions will not interfere with the displacements that are to be studied. It is not possible to eliminate completely the effect of the boundary conditions and in order to represent the excavation, the dimensions and conditions of a discretized boundary are chosen according to the recommendations of Desai (1972) (Figure 2.1.1). Then the problem is to represent the shape of the sheetpile wall in a 2D analysis. The flexibility of the wall as determined by EI (E = Young's modulus, I = moment of inertia), will be kept constant for the type of wall determined to resist the bending moment (calculated from the free earth support method) and for the equivalent continuous wall considered in the mesh. Assuming the same Young's modulus for both, the equivalent continuous wall is then a plain steel plate whose width is calculated from the inertia of the sheetpile wall chosen to resist the bending moment. The same mesh is used for the study of the nine geometric conditions of anchoring. During design, the aspect ratio (ratio of the longest side to the shortest side of each element) was kept as close as possible to unity. The Figures 2.1.2, 2.1.3, 2.1.4 represent the general mesh, the sheetpile zone and the anchor zone. This mesh is then

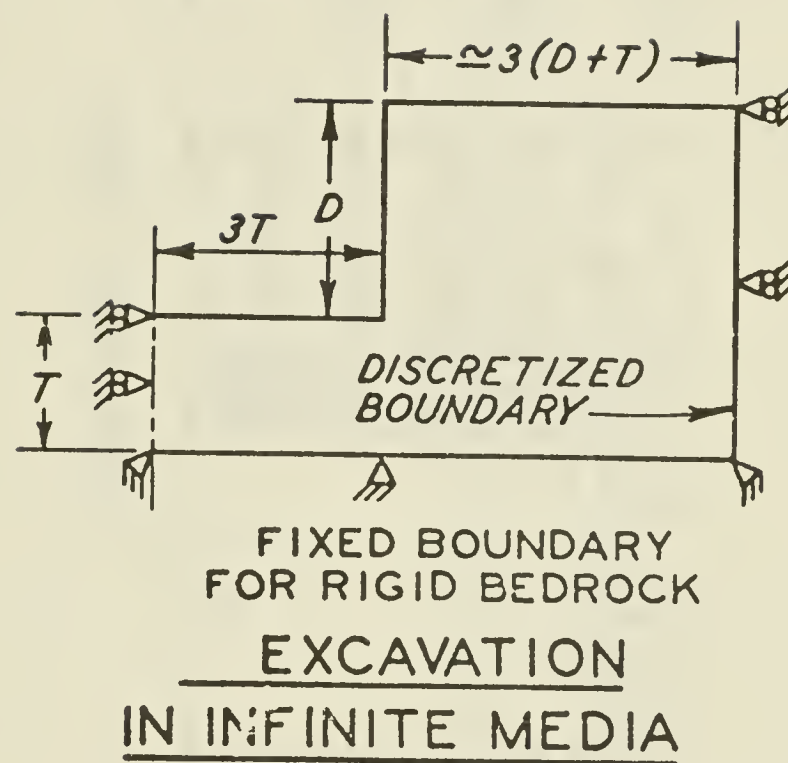


Figure 2.1.1 Discretization of an excavation
(After Desai, 1972)

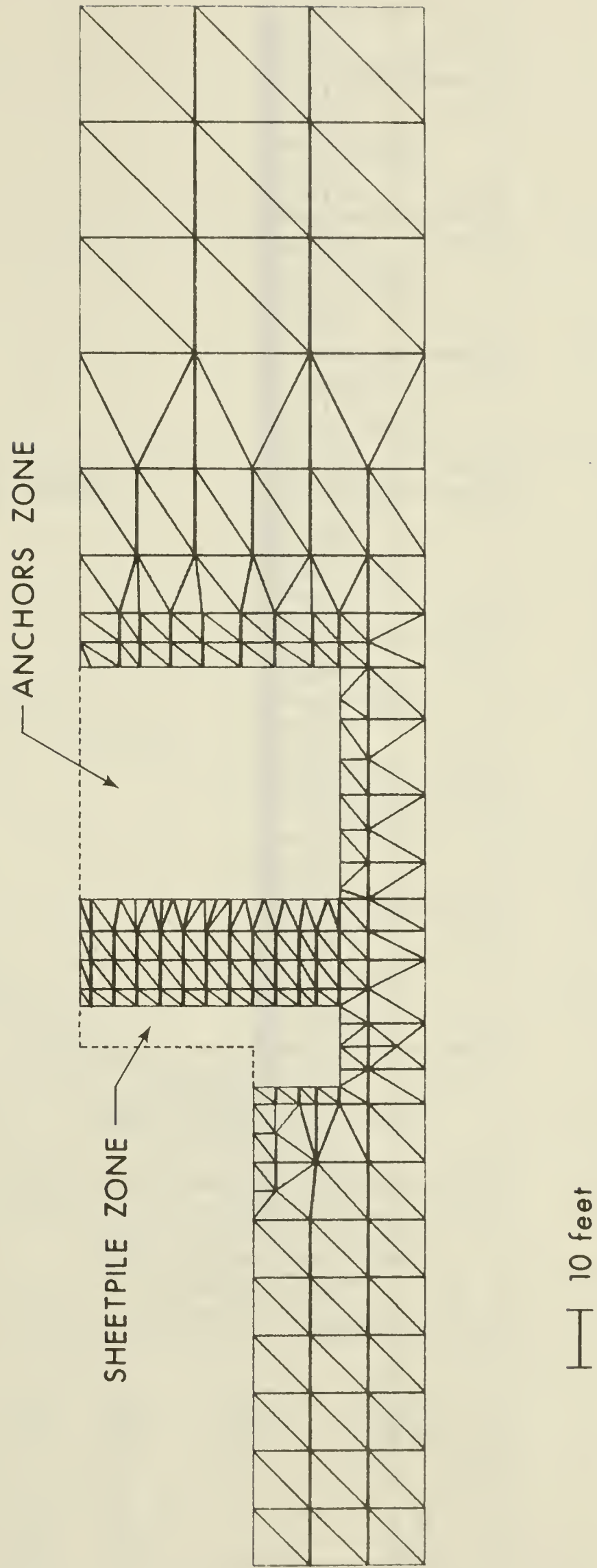


Figure 2.1.1.2. General mesh for the parametrical study

2 feet

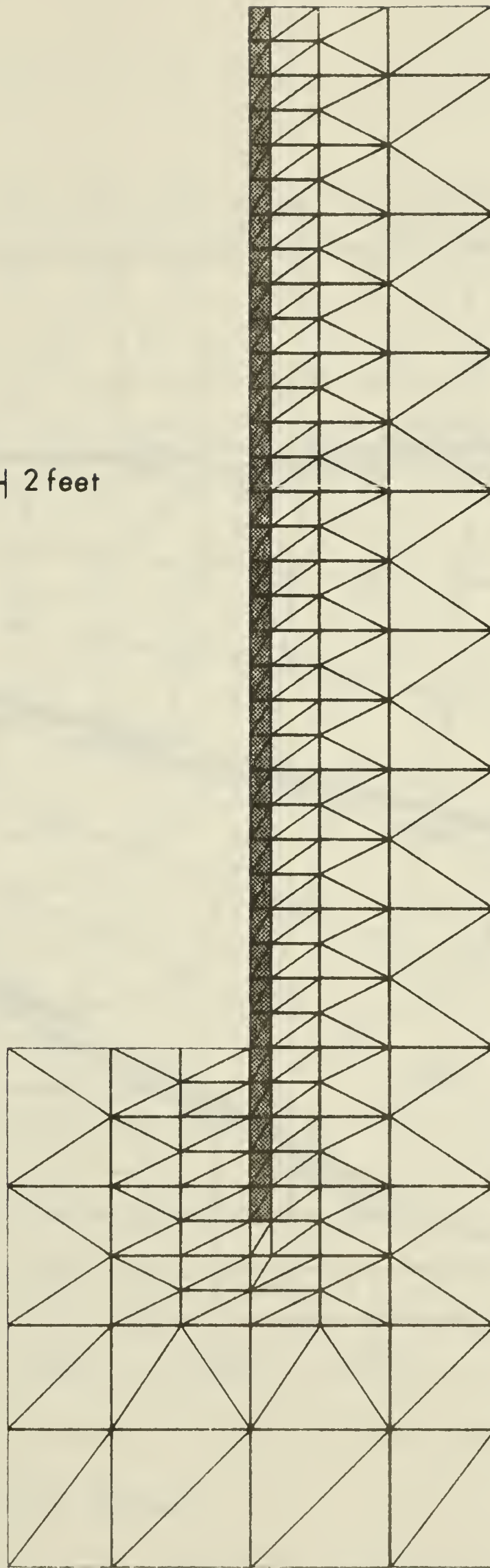
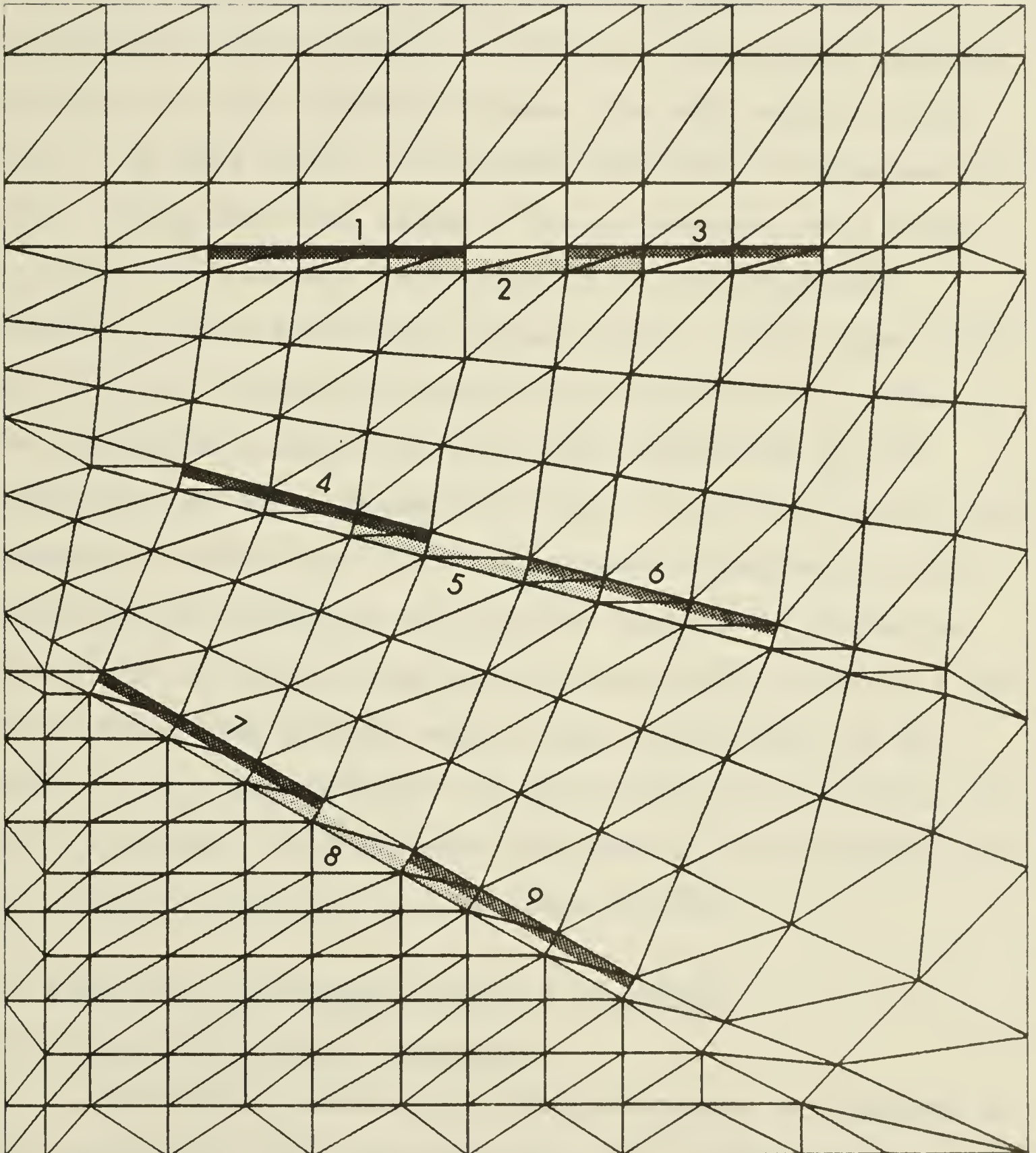


Figure 2.1.1.3. Mesh for the sheetpile zone



|-----| 10 feet

Figure 2.1.4. Mesh for the anchor zone

used with the computer program described in Appendix A to simulate the excavation. On the boundaries of the excavation (along the sheetpile wall and the final grade of the excavation), stress boundary conditions are applied assuming that prior to the excavation phase, the soil was in a rest state. We thus obtain the deformations due to the excavation only. Along the final grade of the excavation, this change in stress ($\Delta\sigma$) is equal and opposite to the overburden pressure at that particular ground depth. On the sheet pile wall and at a particular depth, this relief ($\Delta\sigma$) is equal to the overburden pressure at this level multiplied by the coefficient of earth pressure at rest. This force is directed towards the excavation. For the stress introduced into the ground by the anchoring, the working load of the anchor is applied on one side at the point of anchoring on the wall and on the other side at both ends of the grouted part of the anchor. For each geometry, the bulk density of the whole soil mass is ignored. The material characteristics are determined as indicated in Table 2.1.2 for each element.

2.2 Stability Analysis and Factors of Safety

2.2.1 Free Earth Support Analysis

The free-earth support analysis method was applied to this excavation since the sheetpile wall is driven to a shallow depth beneath the final grade of the excavation.

Assuming the sand and gravel have an angle of internal friction of 38 degrees, the analysis was performed using the coefficients of active and passive earth pressure (K_a and K_p) as indicated by Terzaghi (1953). These values described in Table 2.1.1 are representative of a clean dense sand and indeed, for the case of a dense sand and gravel, the coefficient of passive earth pressure (K_p) could be almost twice as high. In this case the embedment of the wall could be smaller but the values for a clean dense sand were considered in the analysis as they are on the safe side. Assuming a factor of safety $G_s = 1.6$ with respect to failure of the lower support of the wall and choosing an anchoring point at 10 feet below the ground surface, moment equilibrium gives an embedment depth of 5 feet for this excavation. The horizontal equilibrium of the forces then gives a minimum value of 6800 lbs. for the prestress of the anchor. Considering a permanent anchoring situation, we have to apply a factor of safety of two to three to this minimum prestress. In this study a factor of safety of three is chosen and this gives a prestress of 20,400 lbs. The working load is then taken as 85 to 95 percent of this prestress which yields a working load $A_p = 19200$ lbs.

2.2.2 Limiting Position for the Anchors

Once the embedment of the wall has been determined, it is possible to delimit the active wedge beyond which the anchors must be situated. This wedge is delimited by the

ground surface, the wall and a plane at $45^\circ + \frac{\phi}{2}$ with the horizontal from the base of the wall (Figure 2.2.1). This condition gives a lower value to the free length of the anchors. On top of this condition, it is reasonable to place the anchors at a certain distance behind the plane of potential active slip surface and in this case, a minimum of 20 feet beyond the active wedge was chosen, allowing mobilization of the full capacity as determined by the position of the anchor.

2.2.3 Required Length for the Grouted Part of the Anchors

Considering a friction anchor subjected to a pull force A_p , the grouted part has to satisfy the equation:

$$F_s A_p = \pi d \ell \tau \quad (1)$$

where:

- F_s = Factor of safety with respect to pull-out force.
- A_p = Pull-out force (equal to the working load).
- d = Diameter of the grouted part of the anchor.
- ℓ = Length of the grouted part of the anchor.
- τ = Skin friction resistance per unit area.

The skin friction resistance per unit area (τ) can be taken as:

$$\tau = K_o \sigma_v \tan \phi_a \quad (2)$$

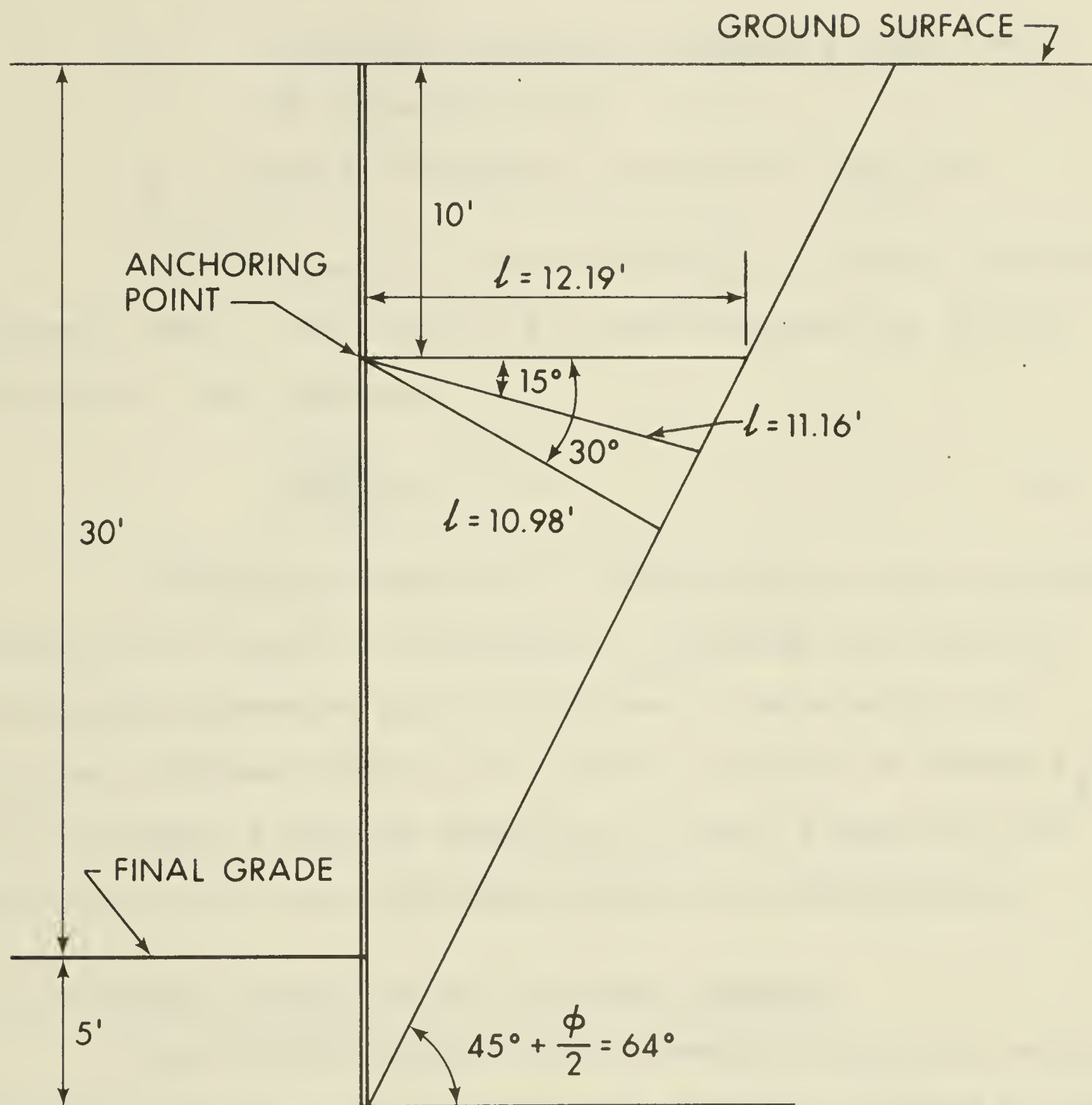


Figure 2.2.1. Limitations in length due to the potential active slip surface.

where:

$K_o = 1$ for the case of dense sand.

σ_v = effective overburden pressure at the level of the anchor zone.

ϕ_a = Angle of internal friction of the sand.

These values are chosen according to Swedish practice (Broms, 1968). The equation for the determination of the length (ℓ) then becomes:

$$\ell = \frac{F_s A_p}{\pi d \gamma h \tan \phi} \quad (3)$$

Considering equation (3), the maximum length required occurs at an angle of anchoring of 0 degrees for then the overburden pressures are at a minimum. The equation (3) yields a minimum length of 9 feet for a factor of safety $F_s=1.5$. In the study, a grouted length of 10 feet is used for the analysis of the nine different geometric configurations.

2.2.4 Overall Stability of the Chosen Anchors

The failure surface for the overall stability analysis will be approximated by a composite surface delimited by the prism of active failure at the back of the anchors, the prism of passive failure situated in front of the structure, and the plane surface between these two (Figure 2.2.2). This method is proposed by the Bureau Sécurité (1972) and frequently used in practice. For the study of the equilibrium, the force diagram consists of:

- P_a → active pressure at the back of the anchors.
- P_p → passive pressure in front of the structure.
- W → the weight of the wedge of soil.
- Q_f → the reaction of the underlying soil upon the wedge of soil.

To satisfy equilibrium, the vector diagram of these forces must close, and as all forces are known in direction and amplitude except for Q_f , we can determine both the direction and the absolute value of the soil's reaction. The direction of Q_f has to be situated within an angle of 90 degrees to 90 degrees + ϕ (angle of internal friction) with the direction of the bottom of the wedge of soil in order to assure stability. As it can be seen from Table 2.2.1, all the nine anchor positions satisfy the overall stability conditions and as the angle or the length increase, the less we mobilize friction between the wedge of soil and the underlying soil.

2.2.5 Safety Factors of the Chosen Anchors With Respect to the Overall Stability

Once the overall stability has been checked for the nine anchors, the anchor capacity for each anchoring condition is determined on the condition of mobilization of the full friction resistance between the wedge of soil and the underlying mass. The method proposed by the Bureau Securitas (1972) is used in this evaluation and serves to prevent the anchored

TABLE 2.2.1

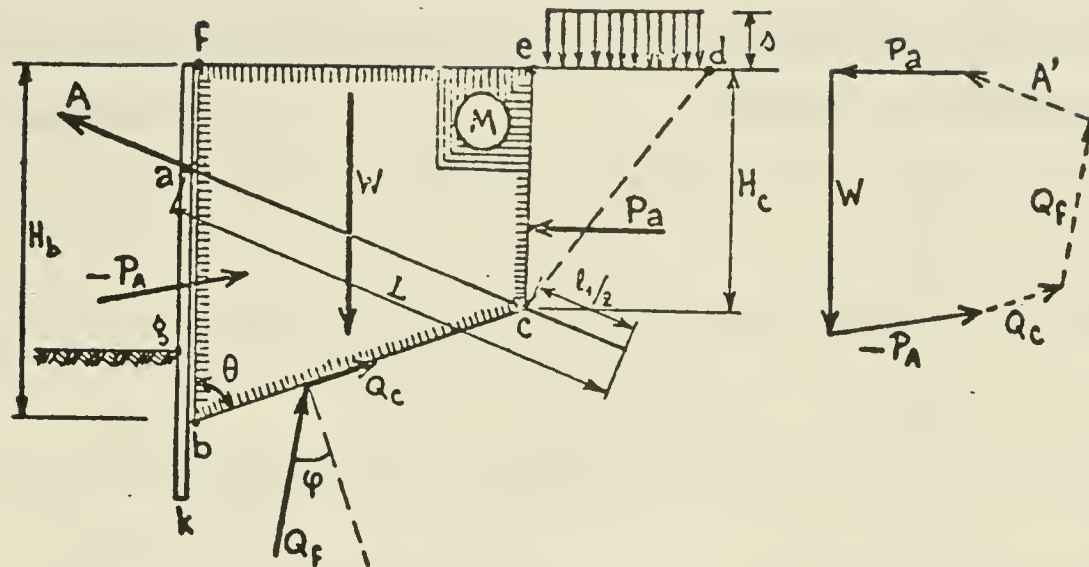
VERIFICATION OF THE OVERALL STABILITY

Anchor No	Angle for Qf Not Mobilized	Angle of Qf Mobilized	Angle for Qf Fully Mobilized
1	-33.3°	-7.1°	+4.7°
2	-29.0°	-6.0°	+8.9°
3	-25.7°	-5.1°	+12.3°
4	-22.4°	-3.9°	+15.6°
5	-17.1°	-2.7°	+20.9°
6	-12.9°	-1.9°	+25.0°
7	-10.3°	-0.7°	+27.7°
8	-3.7°	+0.6°	+34.3°
9	+1.3°	+1.6°	+39.3°

mass from overturning. Using the wedge of soil delimited in the same way as for the stability analysis (2.2.2), the equilibrium was studied in a different way. In this case, the wall was replaced by its reaction on the wedge of soil. This reaction is composed of first, the prestress load of the soil anchor and secondly, the active pressure on the full length of the wall, both reversed in direction. This analysis, represented on Figure 2.2.3, consists of the following vector quantities:

- $W \rightarrow$ the weight of the wedge of soil.
- $P_a \rightarrow$ the active pressure at the back of the anchors.
- $-P_A \rightarrow$ the opposite of the active pressure on the full length of the wall.
- $Q_f \rightarrow$ the reaction of the underlying soil on the wedge, fully mobilized.
- $A \rightarrow$ the maximum allowed prestress in the anchor.

To assure equilibrium at the limit, this diagram of forces must close. The directions of all forces here are known. The only unknowns are the amplitude of the maximum prestress allowed and the amplitude of the fully mobilized reaction of the underlying soil on the wedge. This determinate problem is then solved for the prestress (A_p) and the solutions as presented in Table 2.2.2. The different factors of safety for the nine anchors are calculated from the working load of 19200 lbs. Figure 2.2.4 gives a three dimensional view of the



Verification of the stability for the case of one row of anchors. The known forces are in solid lines (P_a , W , $-P_A$), the unknown forces in broken lines (Q_c , Q_f , A').

(Q_c = reaction due to cohesion)

Figure 2.2.3. Determination of the anchor's capacity.
(After Bureau Sécurité, 1972).

TABLE 2.2.2

FACTORS OF SAFETY WITH RESPECT TO THE OVERALL STABILITY

FOR $A_p = 19200$ lbs.

Anchor No	Factor of Safety
1	1.2
2	1.8
3	2.4
4	2.2
5	3.1
6	4.4
7	2.9
8	4.2
9	5.7

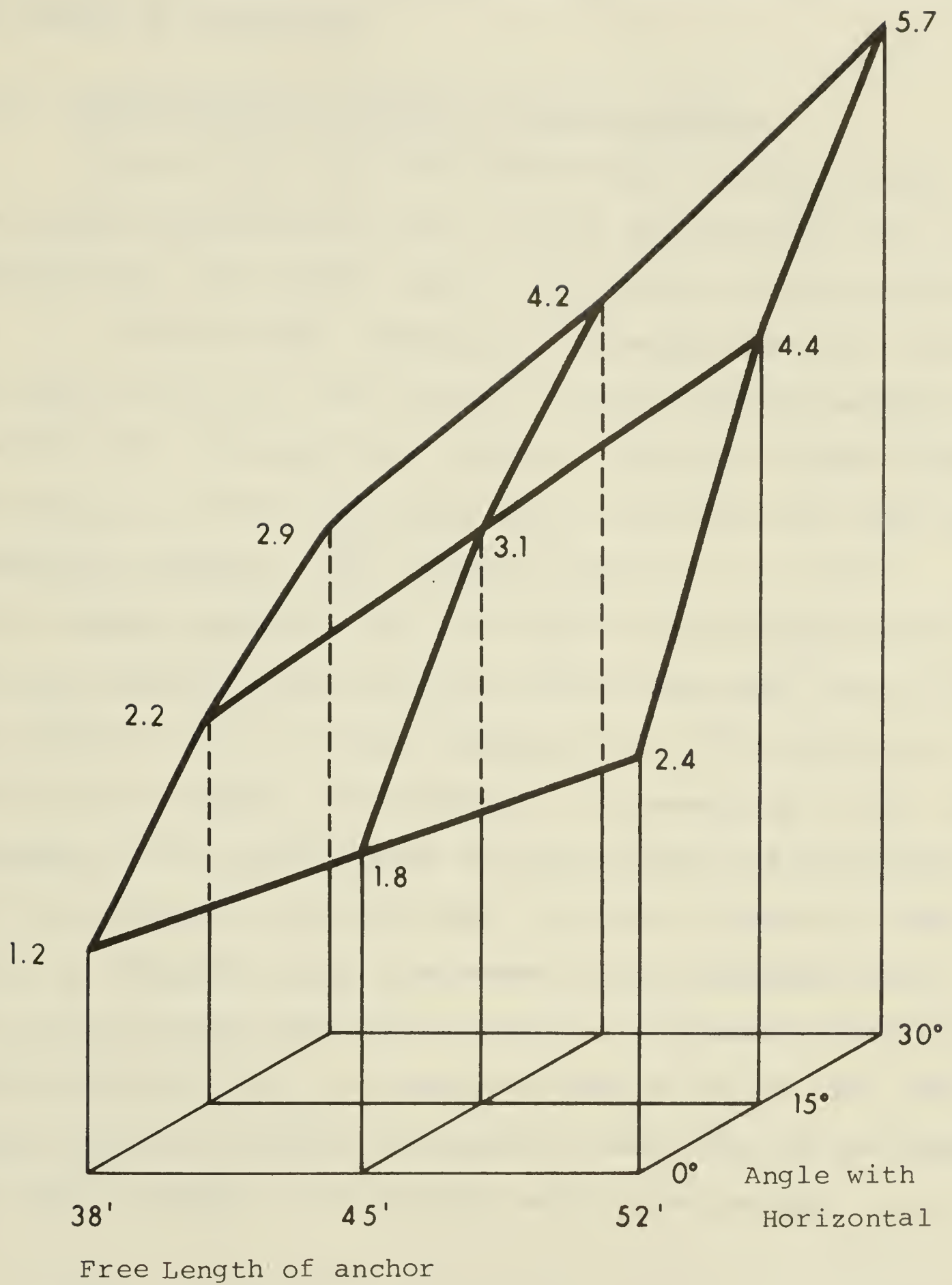


Figure 2.2.4. Factors of safety for the nine anchors with respect to the design capacity

variation of the factor of safety with respect to the angle and length of anchoring.

2.2.6 Determination of Anchor Prestress Limits

First of all, the free-earth support method yields the minimum prestressing value to hold the retaining wall in equilibrium. The bending moment calculated on this assumption is $M = 1090$ in-kips. Assuming an allowable bending stress for steel of 20 ksi, this yields a required section modulus of $s = 54.5$ in³. Considering a Larsen 24 sheetpile whose moment of inertia is 384 in⁴ per foot, we can calculate for this wall a flexibility number $p = \frac{H^4}{EI}$ which is equal to 1.4×10^{-4} . Rowe's moment reduction for this value is then equal to 0.8 and the required section modulus will be now equal to 43.5 in³. The Larsen 24 with a section modulus of 47 in³ will then be sufficient to support the structure. In paragraph 2.3.4, the influence of the prestressing will be studied and the prestress will be increased to 40,000 lbs. In order to check if this choice is adequate, first the moment in the sheetpile wall will be calculated from the deformation yielded by the Finite Element Analysis for a prestress load of 40,000 lbs. The Finite Difference Method is applied to the nodes of the sheetpile wall and the moment at each point will be valued as:

$$\frac{M_i}{E I} = \frac{1}{h^2} [\Delta_{i-1} - 2 \Delta_i + \Delta_{i+1}] \quad (1)$$

- i → point at which the moment is calculated.
- E → Young's modulus of the steel.
- I → Moment of Inertia of the sheetpile.
- h → distance between two adjacent nodes.

This equation, applied to anchor 5 with a prestress load of 40,000 lbs., yields a required section modulus $s = 7.1 \text{ in}^3$ which shows that the Larsen 24 is adequate to retain the excavation wall. In Table 2.2.3, the prestress limits and capacities for anchor 5 are reported.

2.3 Results of the Parametric Study

2.3.1 Presentation of the Results

The influence of many factors was investigated in this parametric study, and, as in any parametric study, one parameter is studied while the others are kept constant. First of all, the effects of the geometry of the anchoring are studied using nine different anchoring conditions (3 angles and 3 neutral lengths). In addition, the influence of the coefficient of earth pressure at rest (K_0) was examined for three different values of K_0 with respect to the nine geometric configuration of anchoring. For the study of the variation in geometry and coefficient of earth pressure at rest, the value of the prestress load was kept at 19,200 lbs. and the Young's modulus of the soil at 15,000 psi increasing by 5,000 psi every 10 feet

TABLE 2.2.3

PRESTRESS VALUES FOR DIFFERENT LIMITS & CAPACITIES
FOR ANCHOR 5

Case Considered	Prestress in lbs.
Free Earth support	6841
Working load	19158
Design capacity	62455
Pull out resistance	66732

in depth. Then, for the above value of Young's modulus and for the specific case of $K_o = 1.0$, the effect of variation of the prestress load was investigated. Anchor 5 was chosen for this study as it represents an intermediate configuration with respect to anchoring geometry. The limits of the variations of the prestress load are taken as described in Table 2.2.3. Finally, the influence of the variations in Young's modulus is studied for the particular case of anchor 5 with $K_o = 1.0$ and with a prestress load of 19,200 lbs. In this section, results are largely normalized by expressing them as a percentage of a value " Δ ". This value is arbitrarily defined as the first maximum settlement when anchor 9 alone is used, with $K_o = 1.5$, 19,200 lbs. anchor prestress load, and a soil's Young's Modulus as in Table 2.1.1. The absolute value of Δ was 2.2 mm (0.09 inch). The amplitude and location of the maximum settlements are referred to the original position of the ground surface and from the original location of the sheetpile wall.

2.3.2 Influence of the Geometry

The two following figures represent the settlement of the ground surface for different lengths of anchoring (Figure 2.3.1) and different angles of anchoring (Figure 2.3.2). In the first case, there is a maximum settlement situated about 50 feet from the wall of the excavation. This maximum settlement is reduced by an increase in the length of anchoring

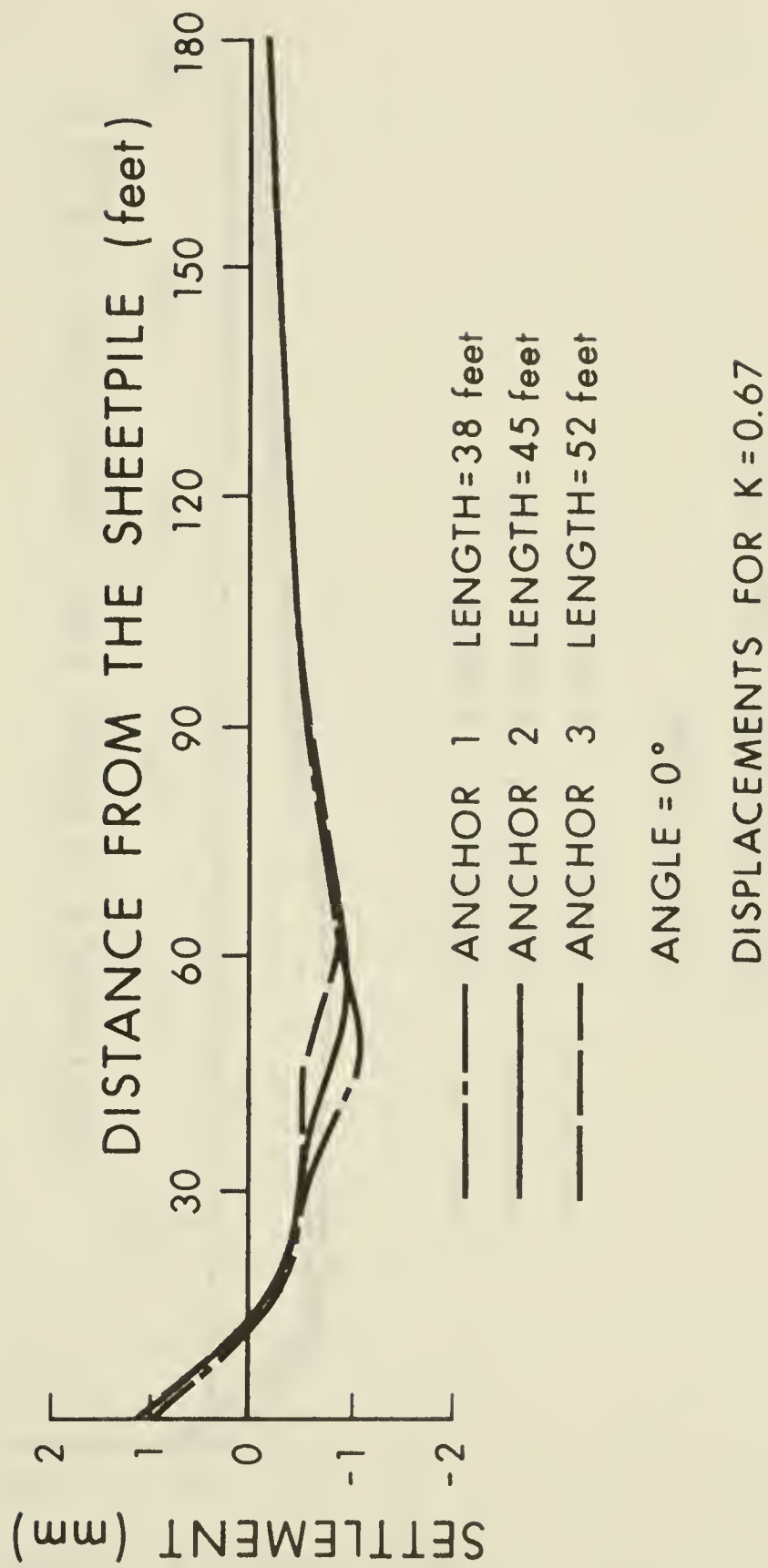


Figure 2.3.1.1. Influence of the length of anchoring on the ground surface settlements

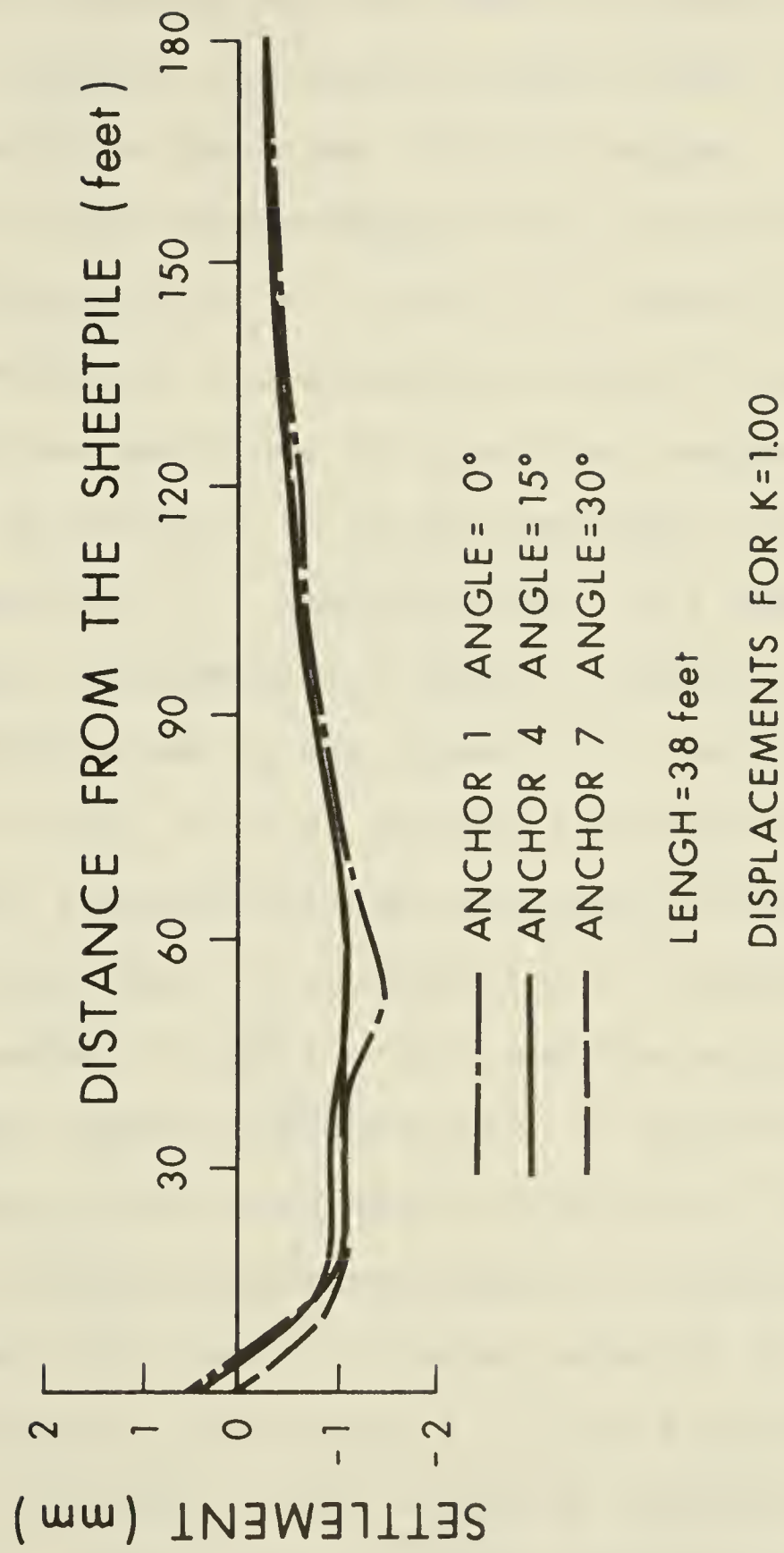


Figure 2.3.2. Influence of the angle of anchoring on the ground surface settlement

and the position of the maximum settlement is moved further from the wall. In the case of Figure 2.3.2, an increase in the angle of anchoring has the effect of reducing the maximum settlement; however, the general shape of the settlement of the ground surface shows two distinct maxima. A more precise examination of the settlements of the ground surface shows that for the case of $K_o = 1.0$ and 1.5 , there is a first maximum settlement situated at a distance of about 20 feet from the wall. The position and amplitude of this first maximum settlement (as it will be referred to in the remainder of the report), is shown on Figure 2.3.3. The amplitude, as a percentage of Δ (first maximum settlement for anchor 9 and $K_o = 1.50$), does not seem to be influenced by the geometry of the anchoring. In the case of $K_o = 0.67$, no first maximum settlement was noticed. On the contrary, a second maximum settlement situated between 50 and 70 feet from the wall is recorded for all anchoring geometry except for anchor 9 with $K = 1.00$ and the anchors at 30° for $K = 1.50$. For these configurations, no second maxima was observed (due to the large depth of burial of the anchor).

The second maximum settlement is influenced by the anchor geometry for each particular value of K_o and, as can be seen from Figure 2.3.4, Figure 2.3.5 and Figure 2.3.6, an increase in the angle or the length of anchoring reduces its amplitude. The position of this second maximum settlement does not follow a regular behaviour but it is situated approximately above the grouted portion of the anchor. The

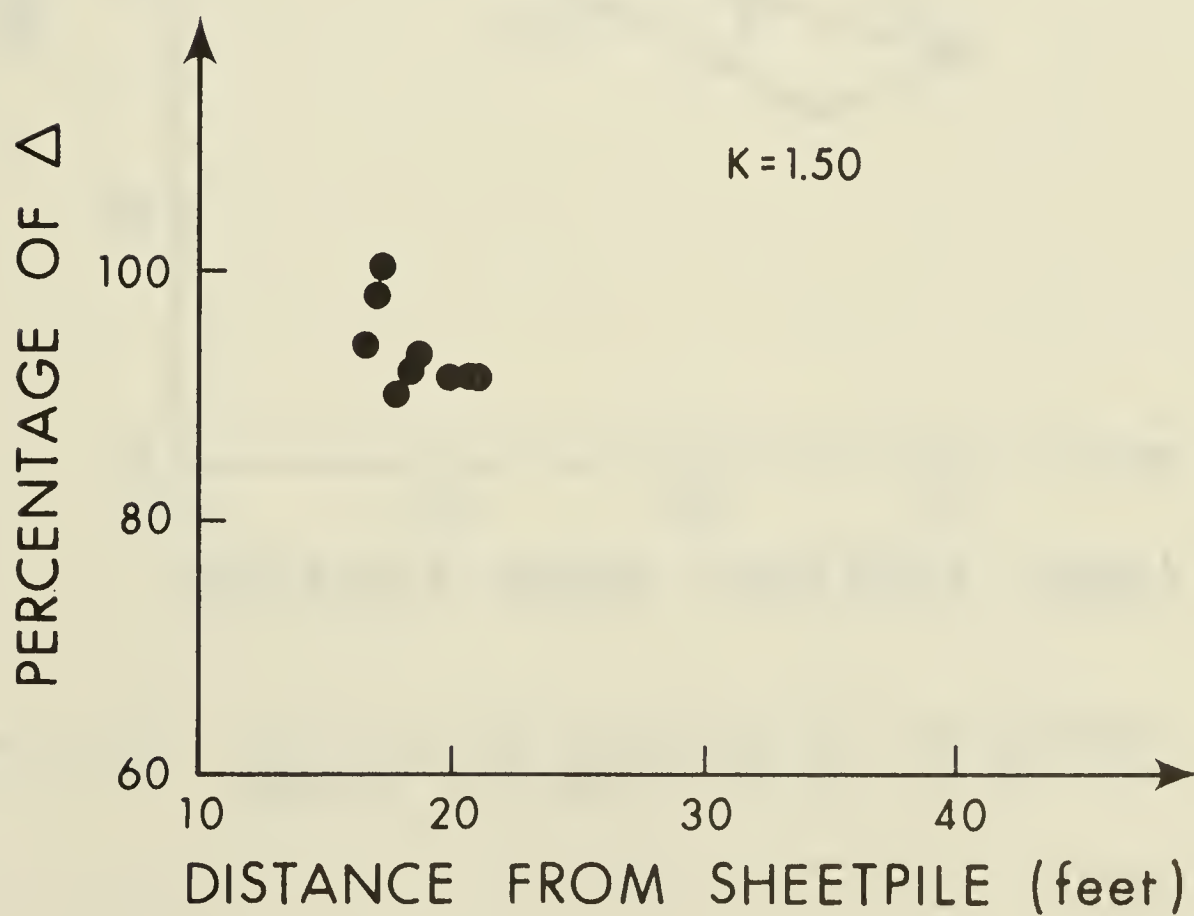
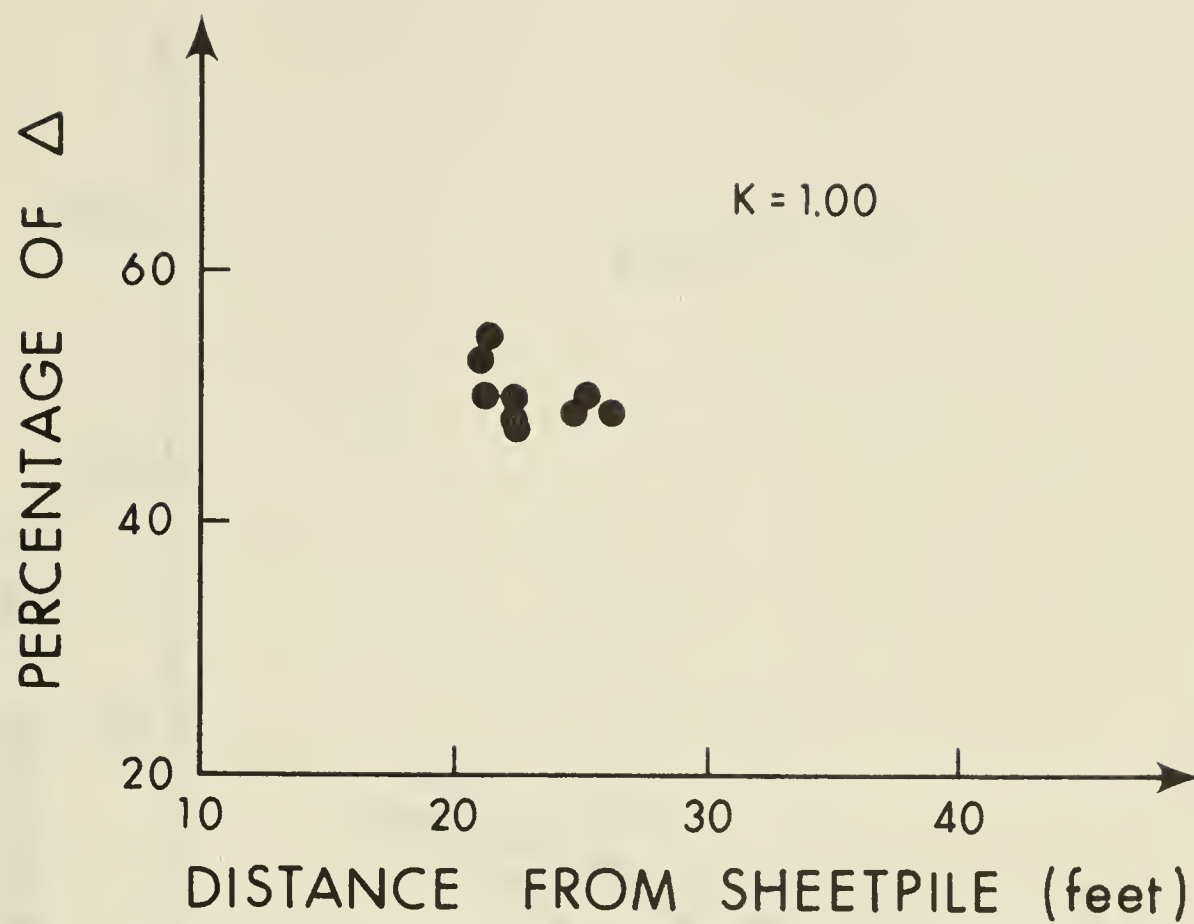


Figure 2.3.3. Position and amplitude of the first maximum settlement for the nine anchors

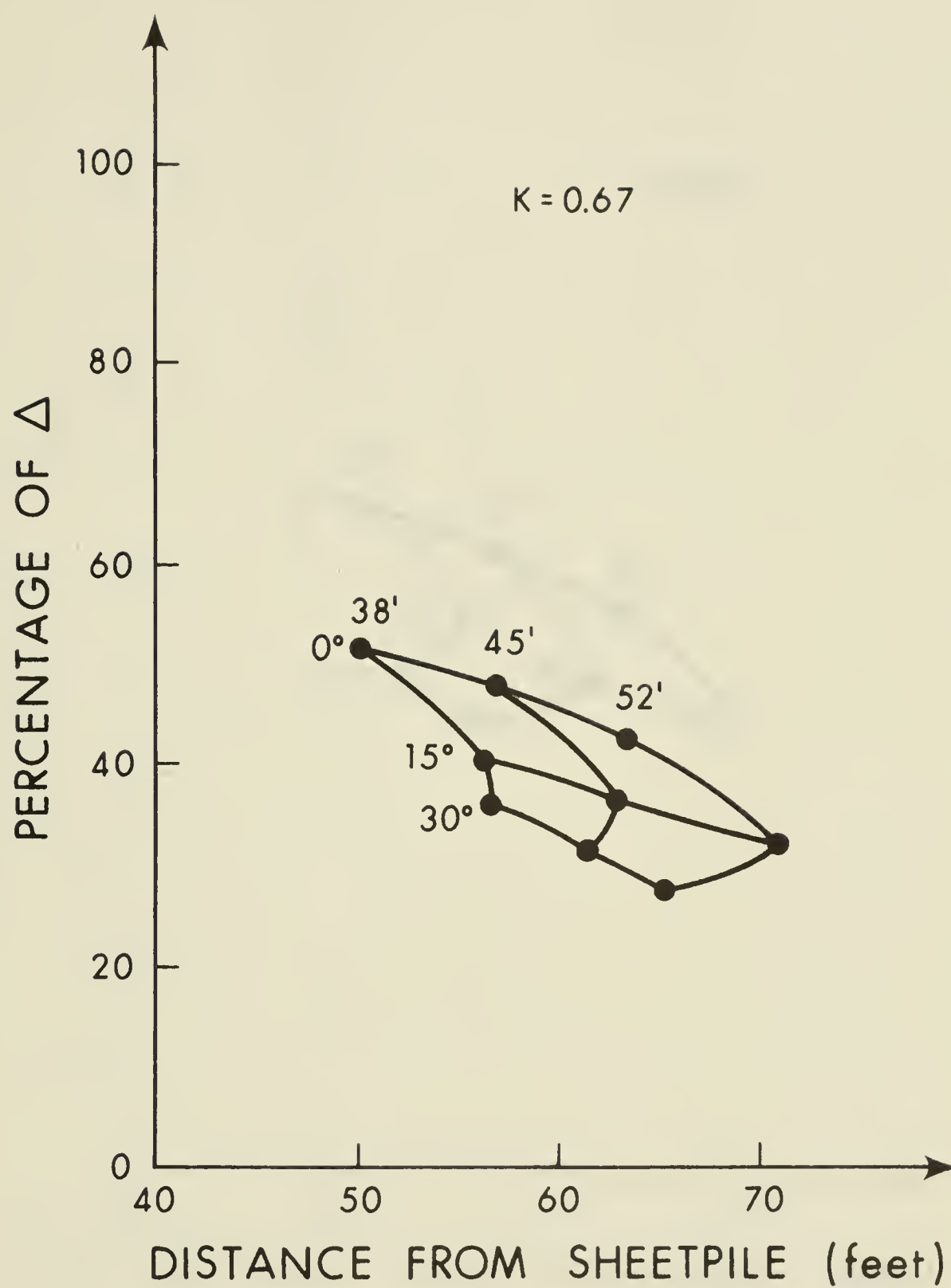


Figure 2.3.4. Position and amplitude of the second maximum settlement for $K_O = 0.67$

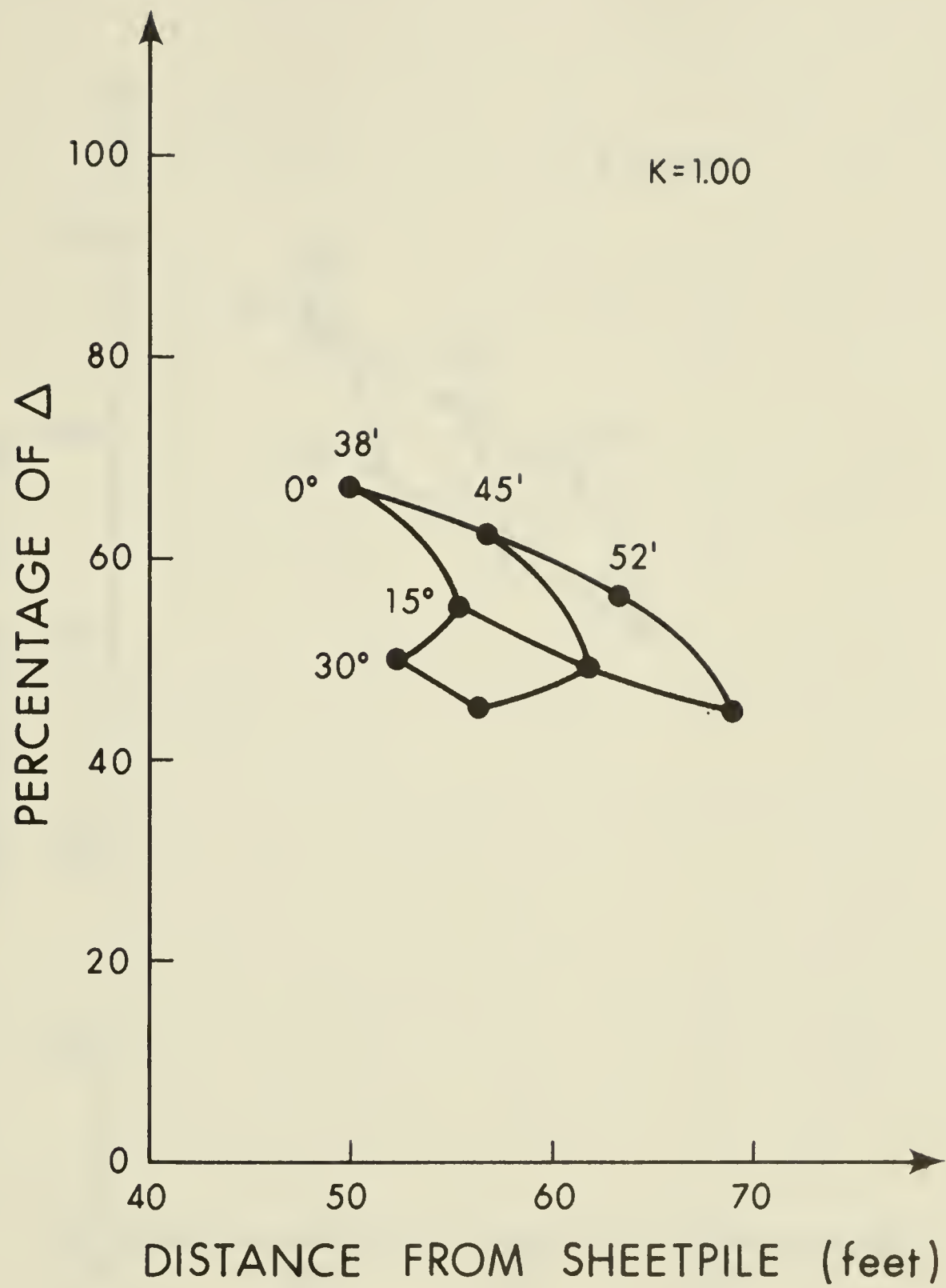


Figure 2.3.5. Position and amplitude of the second maximum settlement for $K_O = 1.0$

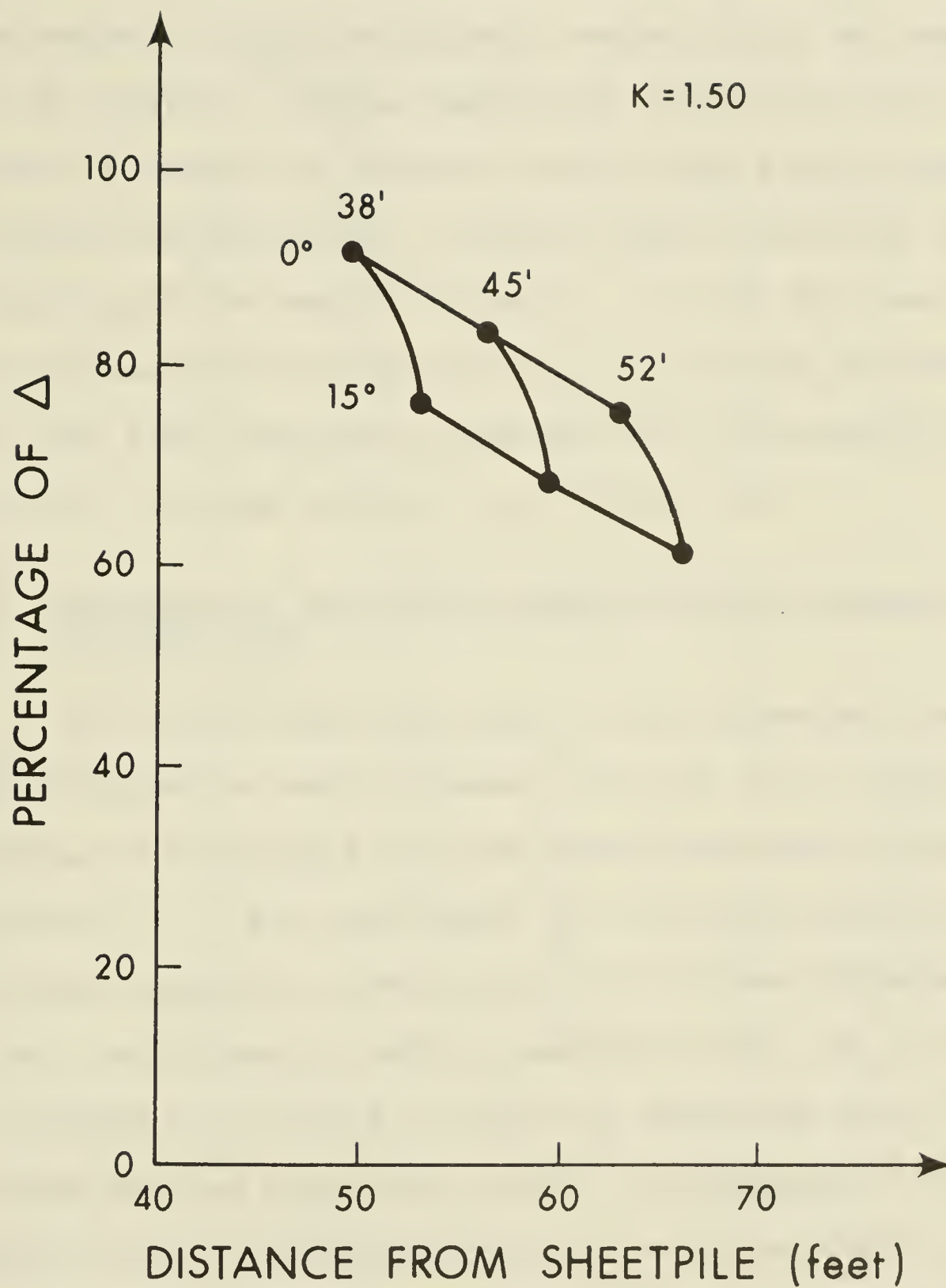


Figure 2.3.6. Position and amplitude of the second maximum settlement for $K = 1.50$

first maximum, situated close to the wall (about 20 feet) is attributed to the outward movement of the wall. The amplitude of the second maximum settlement, which occurs at about the point of grouting, can be reduced by increasing the length or angle of anchoring, thereby burying the anchor deeper into the ground and mobilizing a larger wedge of soil in the deformation of the excavation wall. In all this analysis of the influence of the geometry on the ground surface settlements, the same horizontal component of the prestress is chosen for the nine anchors ($A_p = 19,200$ lbs.).

2.3.3 Influence of the Coefficient of Earth Pressure at Rest (K_o)

As has already been seen in the preceding items, the coefficient of earth pressure at rest (K_o), has an influence on both the first and second maximum settlements. On Figure 2.3.7, the settlement of the ground surface for a particular anchoring geometry but with three different values for the coefficient of earth pressure at rest (K_o), shows that both maximum settlements increase in amplitude as K_o increases. The first maximum settlement, which is independent of the geometry, almost doubles when K_o is increased from 1.0 to 1.5 (Figure 2.3.3). The influence of K_o on the second maximum settlement is investigated more deeply on Figure 2.3.8 and Figure 2.3.9. For the anchors at 0° with the horizontal it is seen that an increase in K_o increases the amplitude but

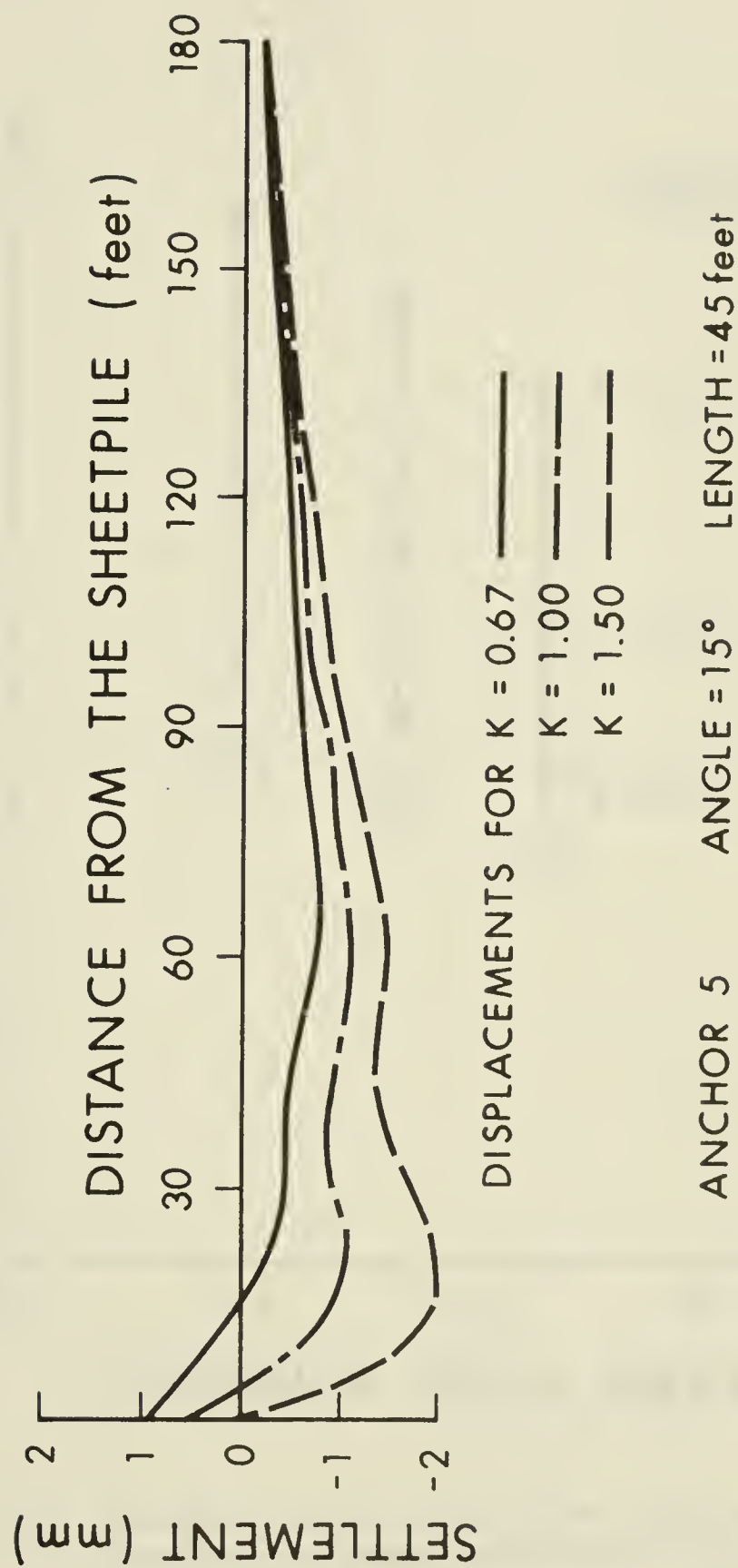


Figure 2.3.7. Influence of the value of the coefficient of earth pressure at rest on the settlement of the ground surface. ($E = 15,000$ psi and $A_p = 19,200$ lbs.)

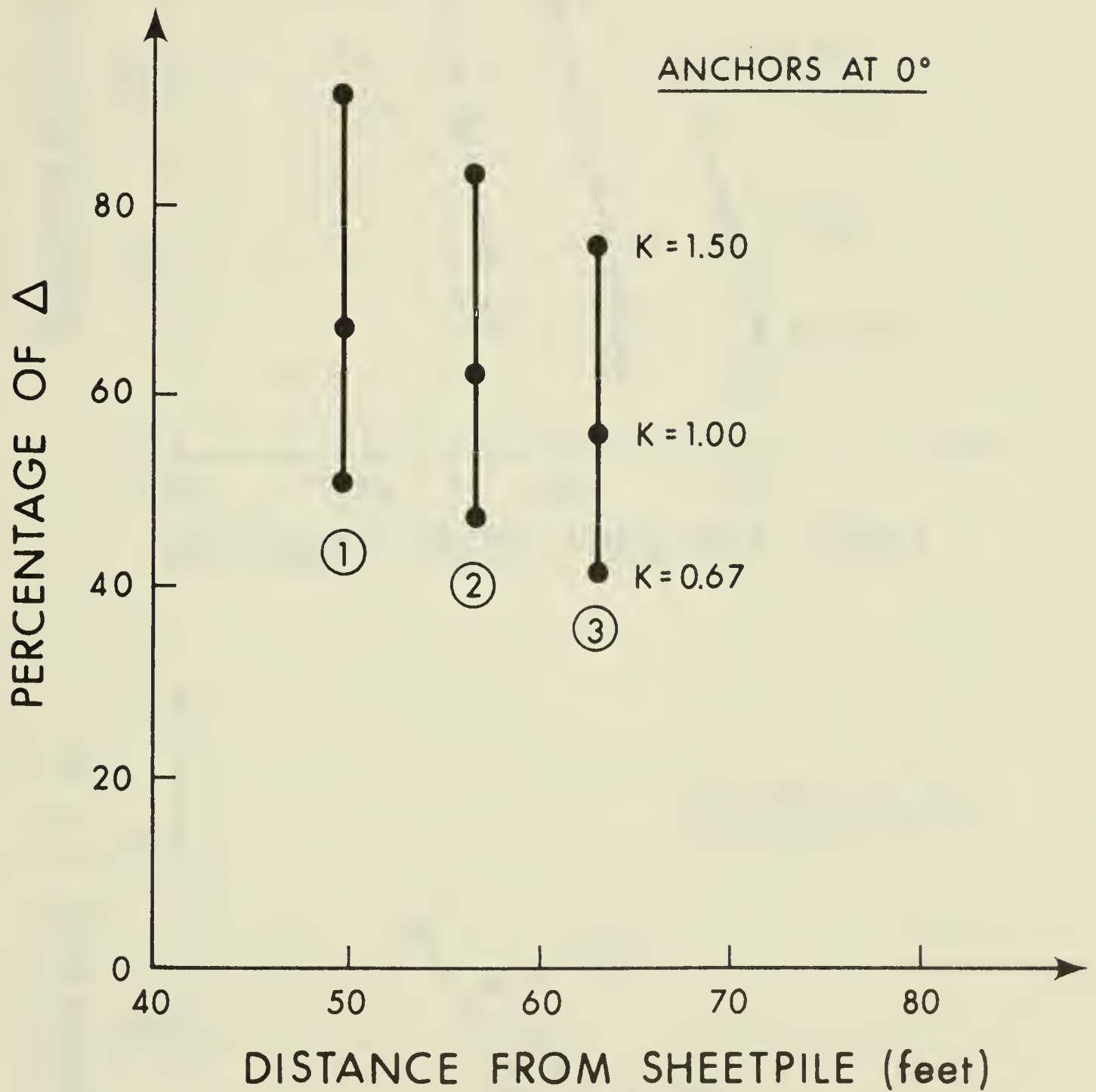


Figure 2.3.8. Variation in amplitude and position of the second maximum settlement for different values of K_o for
($E = 15,000$ psi and $A_p = 19,200$ lbs.)

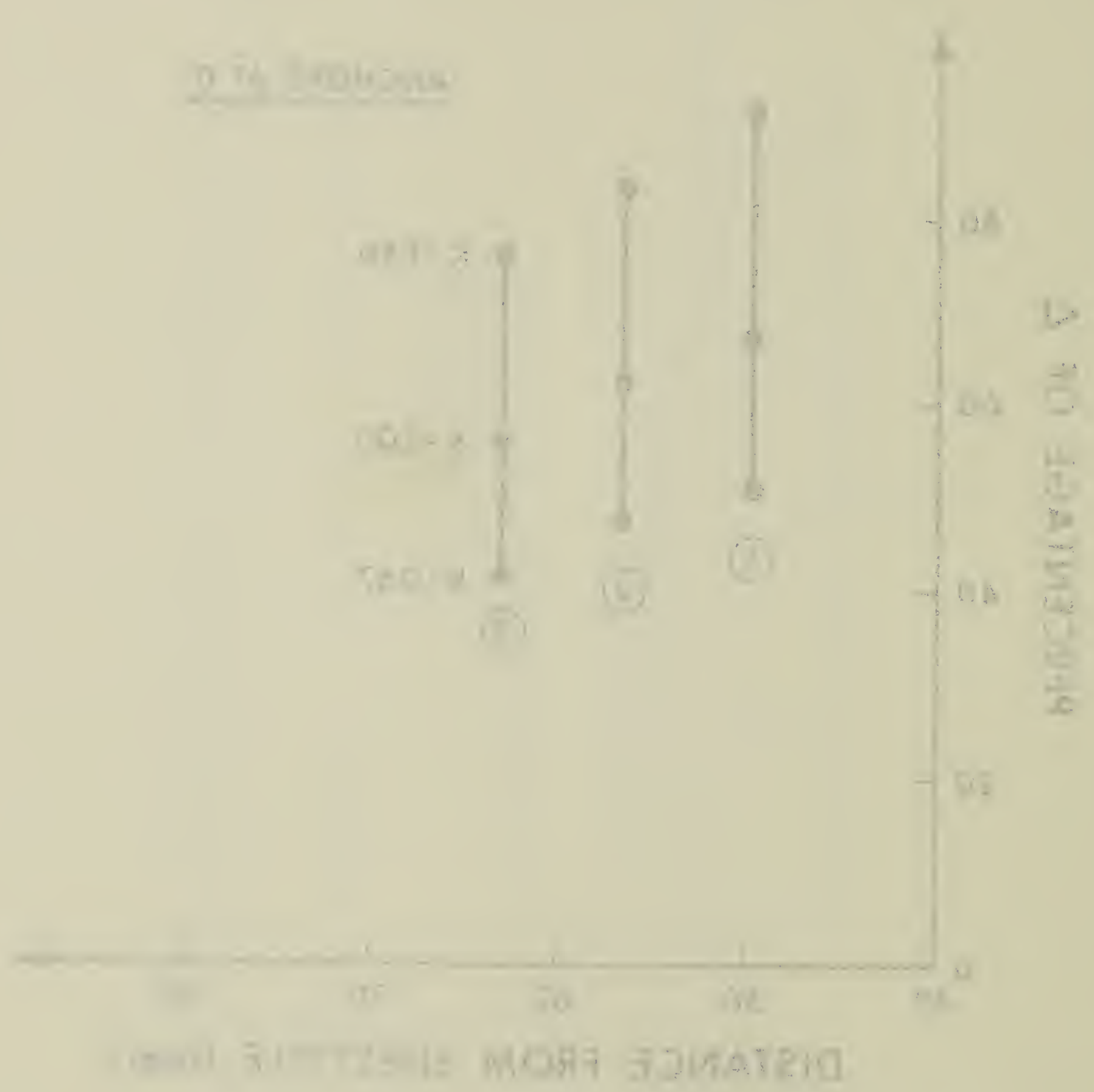


FIGURE 1. Relationship between distance from electric line and percentage of T. The data were obtained from a series of tests conducted in the laboratory of the U.S. Bureau of Reclamation, Washington, D.C. The tests were conducted at a constant voltage of 110 volts and a constant frequency of 60 cycles per second. The results of the tests are shown in the figure.

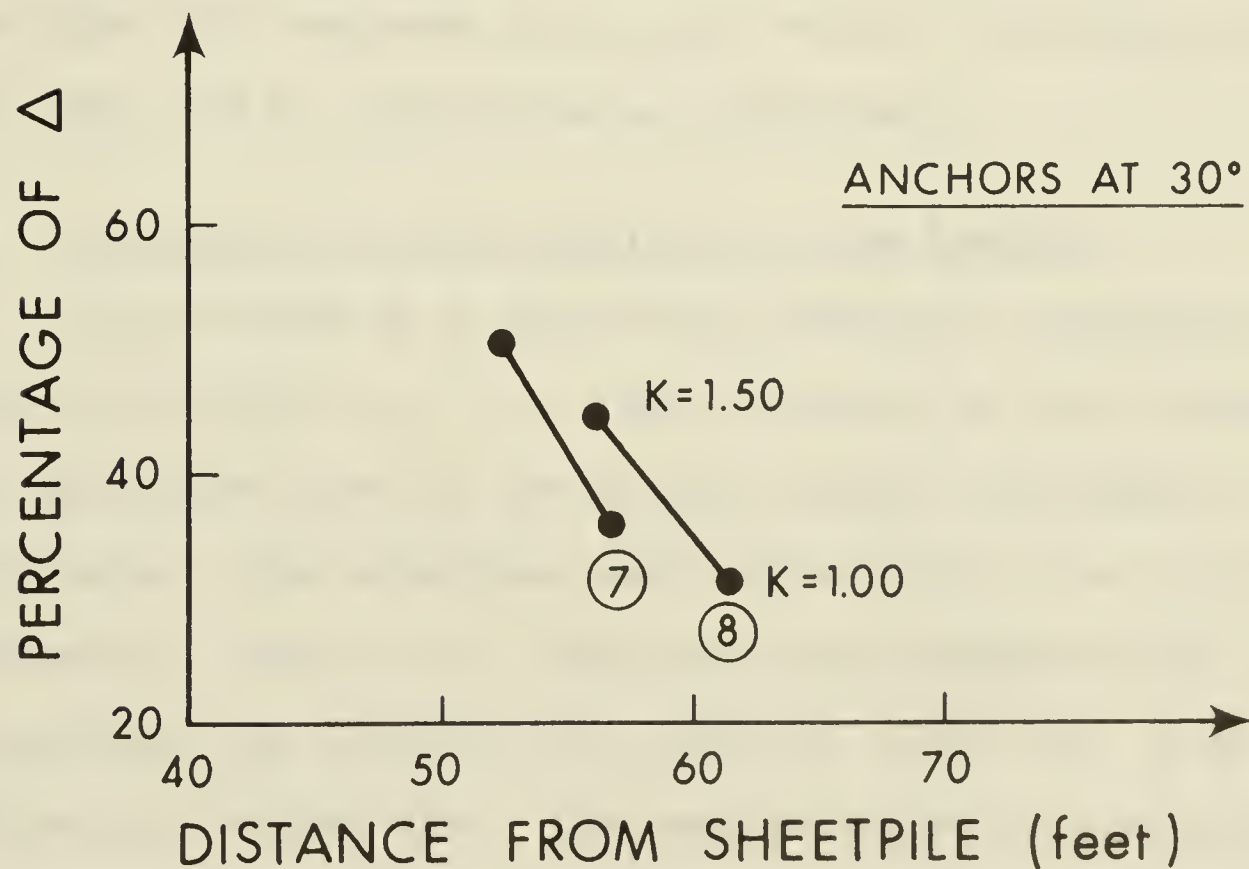
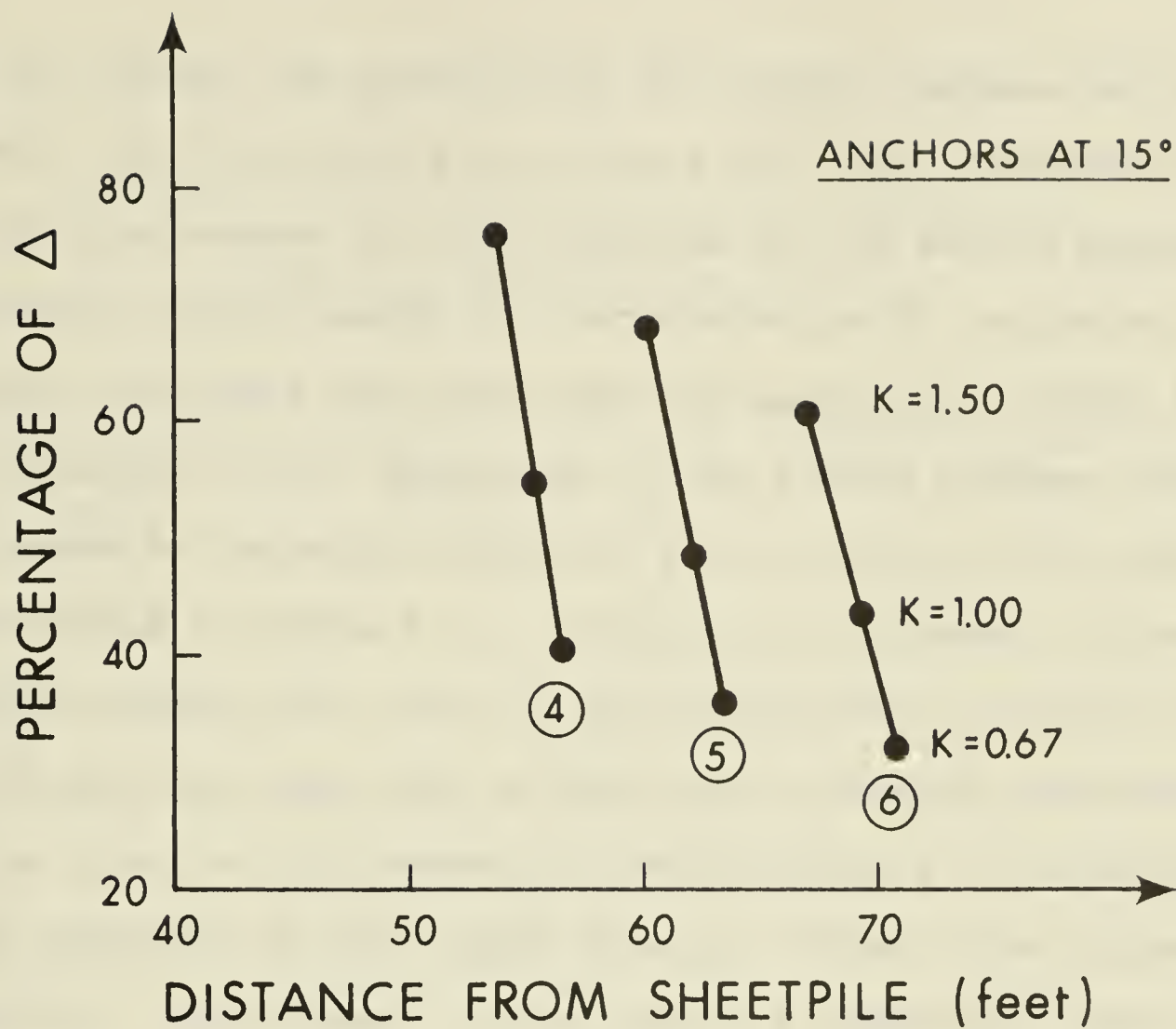


Figure 2.3.9. Variation in amplitude and position of the second maximum settlement for different values of K_o for ($E = 15,000$ psi and $A_p = 19,200$ pds.)

does not affect the position of the second maximum settlement. However, for the anchors at 15° and 30° , the amplitude increases in a similar manner but the position of the second maximum settlement moves towards the excavation as K_o increases. This movement increases with the angle of anchoring (Figure 2.3.9). The variation of the amplitude of the second maximum settlement seems to be proportional to the variation of K_o and is demonstrated in Table 2.3.1. Figure 2.3.10 shows a direct relation between the value of the coefficient of earth pressure at rest and the amplitude of the second maximum settlement. This is true for all geometric configurations of anchoring, and an increase in the length does not affect this proportionality. An increase in the angle of anchoring shows a rate of increase in the second maximum settlement somewhat faster than the increase in K_o , but within the limits of this study, they can be considered as equivalent.

2.3.4. Influence of the Prestress in the Anchors

In the case of a particular geometric configuration (anchor 5) and for $K_o = 1.0$, the influence of the variations of the prestress load on the ground surface settlement was investigated. The prestress was varied within the limits determined in item 2.2.6. The horizontal component of the prestress was increased by steps of 5,000 lbs. from 19,200 lbs. to 40,000 lbs. The general shape of the ground surface settlement presents a first and a second maximum

TABLE 2.3.1.

DEMONSTRATION OF PROPORTIONALITY BETWEEN THE
SECOND MAXIMUM SETTLEMENT AND K_o

Anchor Number	$\frac{K_{02} - K_{01}}{K_{01} - K_{00}}$	$\frac{\Delta_2 - \Delta_1}{\Delta_1 - \Delta_0}$
1	1.50	1.49
2	1.50	1.50
3	1.50	1.49
4	1.50	1.51
5	1.50	1.51
6	1.50	1.53

$\Delta_i \rightarrow$ settlement corresponding to K_{oi}

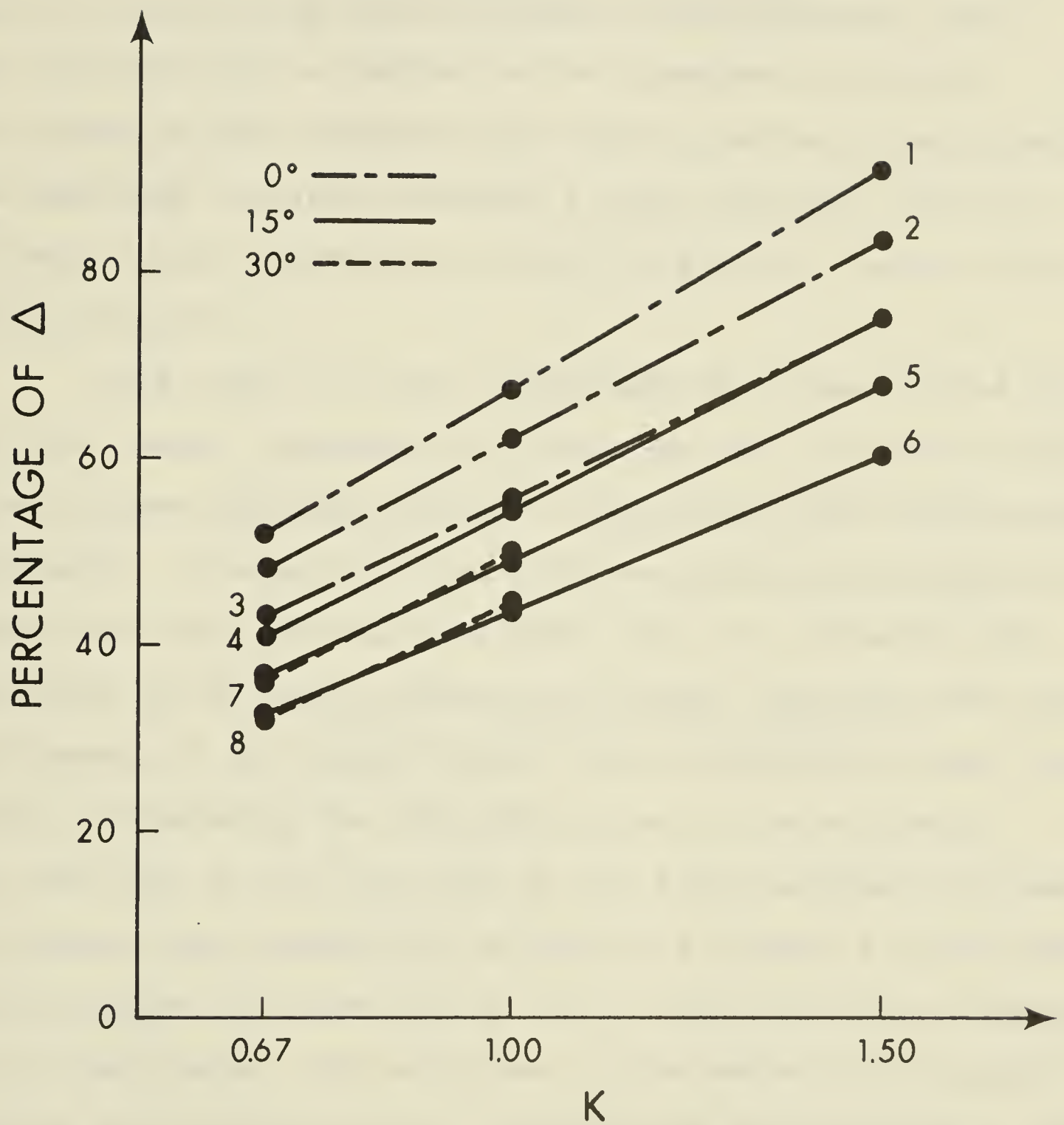


Figure 2.3.10. Proportionality of the amplitude of the second maximum settlement and different values of K_O for ($E = 15,000$ psi and $A_p = 19,200$ pds).

settlement for which the amplitude and position are plotted on Figure 2.3.11. The position of the first maximum settlement is not affected by an increase in the prestress load but its amplitude is reduced as the prestress increases. The effect on the second maximum set is precisely the opposite: the amplitude is hardly affected by the prestress, while an increase in the prestressing moves its position further from the excavation.

This result is very interesting as it was pointed out that the anchor geometry does not have any influence on the first maximum settlement while it does affect the second maximum settlement. The fact that an increase in the prestressing can reduce the first maximum settlement while not affecting the amplitude of the second maximum settlement indicates that all settlements of the ground surface can be minimized within the limits indicated by the characteristics of the soil mass. The reduction of the amplitude of the first maximum settlement is reported more accurately in Table 2.3.2 where a proportionality between the prestressing and the amplitude may be observed. In the same table, the variations in the heave of the ground surface next to the wall are investigated in the same way and a proportionality is also established. On Figure 2.3.12, the absolute values of the first maximum settlement and of the heave are plotted. The relative settlement (equal to the difference in level between the heave next to the wall and the first maximum settlement) is also reduced by an increase in the

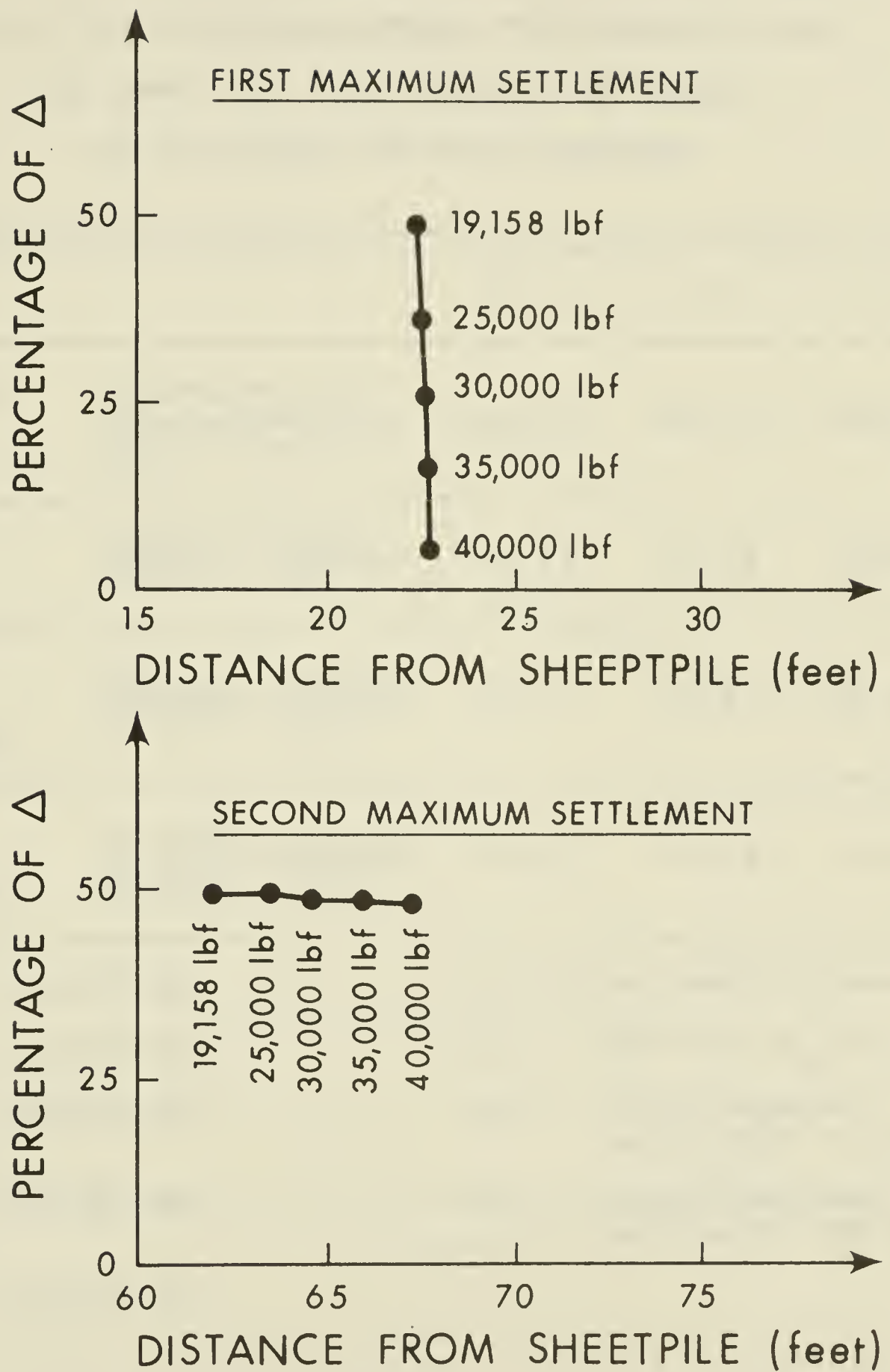


Figure 2.3.11. Influence of the value of prestressing on the 1st and 2nd maximum settlement for anchor 5 with $K = 1.0$ and $E = 15,000$ psi.

TABLE 2.3.2

CHECK OF THE RELATIONS BETWEEN THE PRESTRESS LOAD,
THE HEAVE, THE FIRST MAXIMUM SETTLEMENT
AND THE SECOND MAXIMUM SETTLEMENT

		i = 1	i = 2	i = 3
Prestress Load	$\frac{A_p(i+2) - A_p(i+1)}{A_p(i+1) - A_p(i)}$	85.6%	100.0%	100.0%
Heave	$\frac{H(i+2) - H(i+1)}{H(i+1) - H(i)}$	85.8%	99.8%	99.9%
First Maximum Settlement	$\frac{S1(i+2) - S1(i+1)}{S1(i+1) - S1(i)}$	85.7%	99.8%	100.0%
Second Maximum Settlement	$\frac{S2(i+2) - S2(i+1)}{S2(i+1) - S2(i)}$	75.0%	73.9%	73.5%
$A_p(1)$	= 19,158 lbs.	$A_p(i)$ → Prestress for case i		
$A_p(2)$	= 25,000 lbs.	$H(i)$ → Heave for $A_p(i)$		
$A_p(3)$	= 30,000 lbs.	$S1(i)$ → First Maximum settlement for $A_p(i)$		
$A_p(4)$	= 35,000 lbs.	$S2(i)$ → Second Maximum settlement for $A_p(i)$		
$A_p(5)$	= 40,000 lbs.			

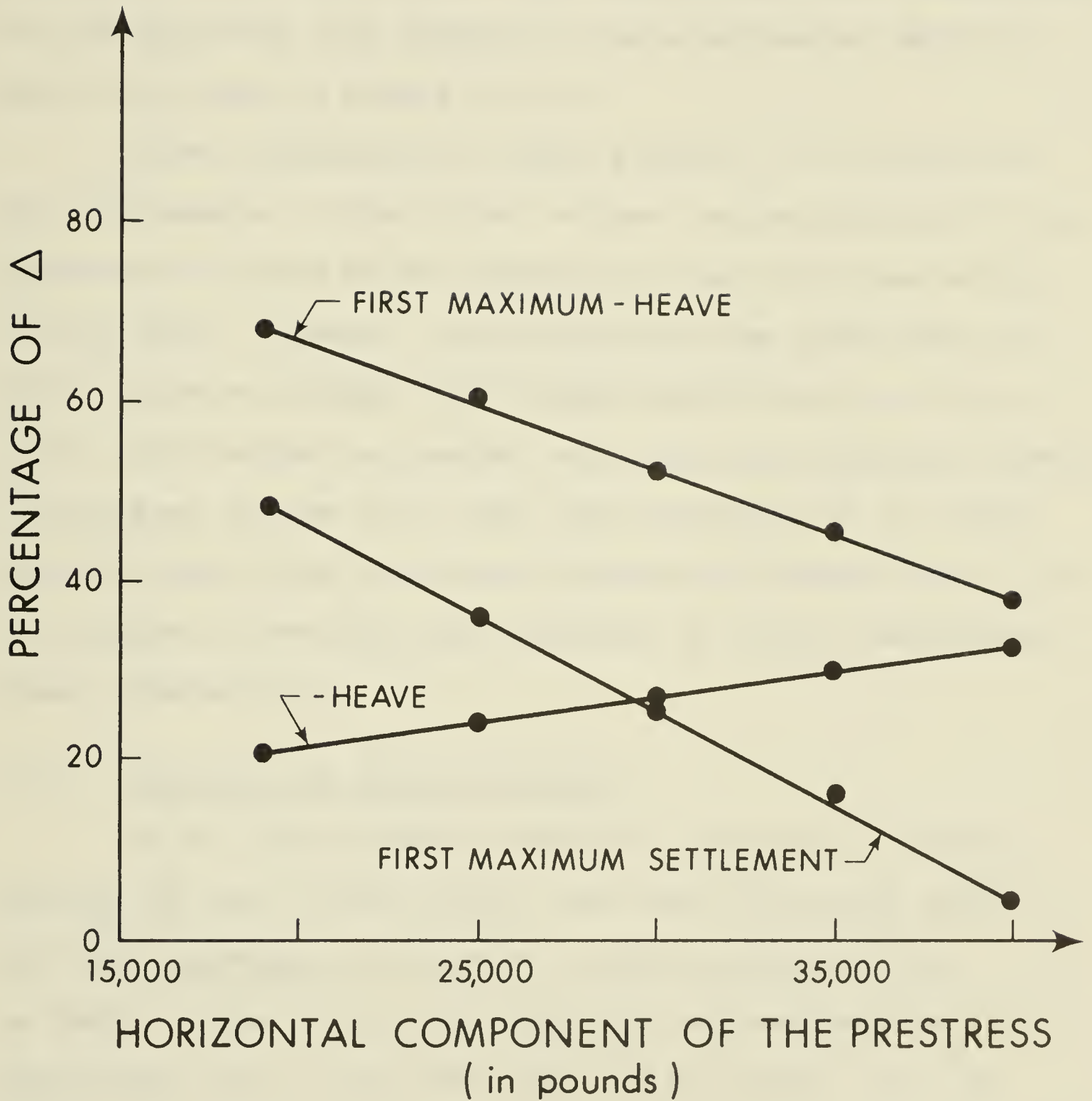


Figure 2.3.12. Representation of the proportionality between the anchor prestress and the amplitude of the first maximum settlement for anchor 5 with $K = 1.0$ and $E = 15,000$ psi.

prestress. The variations of the amplitude of the second maximum settlement for different prestress loads are also represented in Table 2.3.2. The results show the independence of the amplitude with respect to the prestressing which is best visualized on Figure 2.3.13.

After examination of these factors, it is seen that the settlements of the ground surface can be minimized by an appropriate choice of the geometry of the anchor and of the prestressing. However, factors such as the coefficient of earth pressure at rest (K_0) or the Young's modulus of the soil, which cannot be changed, are still the governing factors. It was seen in item 2.3.3 that the variations of K_0 affect directly both first and second maximum settlements and it is of interest to evaluate the influence of Young's modulus on these deformations.

2.3.5 Influence of Young's Modulus

In all the preceding analysis, the value of Young's modulus (E) was 15,000 psi for the first 10 feet of soil and then increased in value by 5,000 psi every 10 feet in depth. This value of E , which can be considered as approximate for a very dense sand and/or gravel, will be varied in this analysis from 15,000 psi to 3,000 psi for the first layer (10 feet deep) of soil. The ratio of the new value of E to the initial one in the upper layer will be used to determine the new E for the underlying layers. The general shape of the ground surface settlements presents two

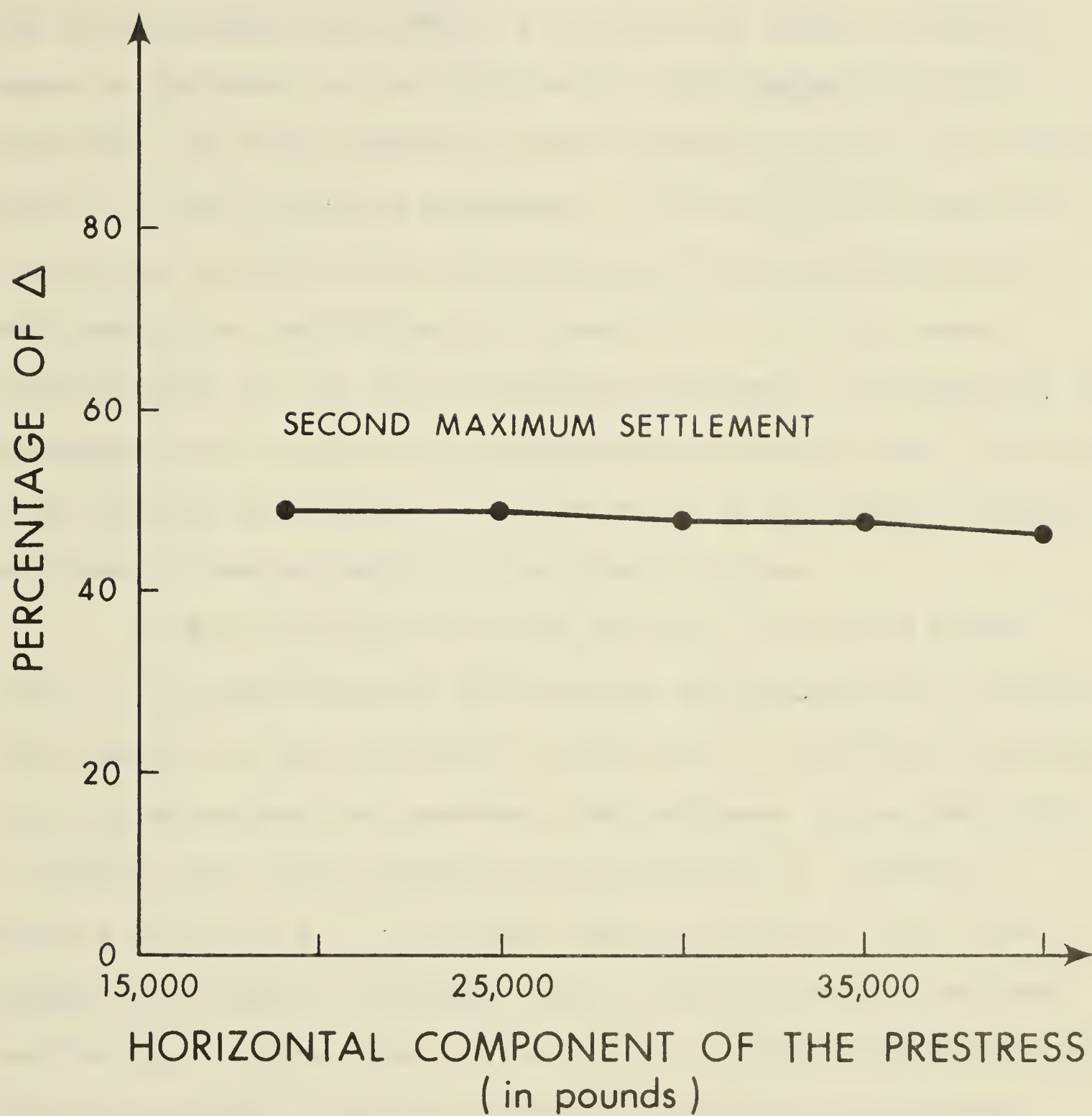


Figure 2.3.13. Influence of the value of prestressing on the amplitude of the 2nd maximum settlement for anchor 5 with $K = 1.0$ and $E = 15,000$ psi.

maximum settlements for the different values of Young's modulus assumed. On Figure 2.3.14, the curve shows that for the first maximum settlement a decrease in Young's modulus means an increase in its amplitude. With respect to the position, the first maximum moves slightly towards the excavation wall as Young's modulus decreases. Figure 2.3.15, shows the variations in amplitude and position of the second maximum settlement for the different values of E . In this case, the amplitude of the second maximum settlement increases as E decreases but the rate of increase seems smaller than for the first maximum settlement. The position of the second maximum settlement however hardly moves when E varies.

On the following figures (Figure 2.3.16 and Figure 2.3.17), the amplitude of the maximum settlements are plotted with respect to the different values of E . For both the first and second maximum settlements, the increase in the amplitude is faster than the decrease in the value of E . However, below a value of $E = 7,500$ psi, the amplitude of the first maximum settlement increases faster than the second maximum settlement. In the case of the anchor for which the variation of E was studied (anchor 5 with $K = 1.0$), a first maximum settlement of 1.0 mm (0.04 inch) for $E = 15,000$ psi becomes a settlement of 12.5 mm (0.5 inch) for $E = 3,000$ psi. This shows the utmost importance of the determination of the soil characteristics in order to be able to reasonably predict the

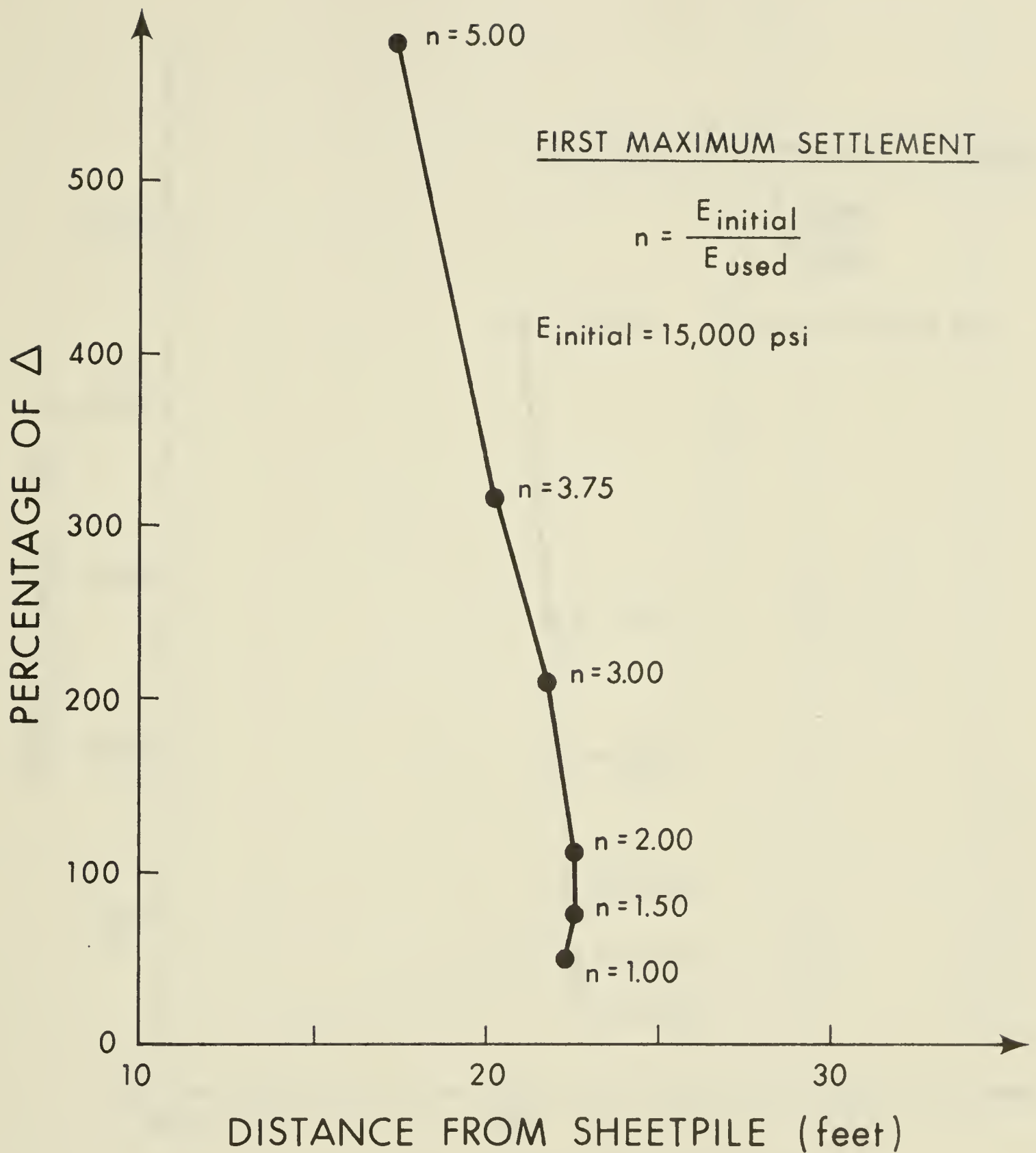


Figure 2.3.14. Influence of Young's modulus (E) on the amplitude and position of the 1st Maximum settlement for anchor 5 with $K = 1.0$ and $A_p = 19,200 \text{ lbs}$.

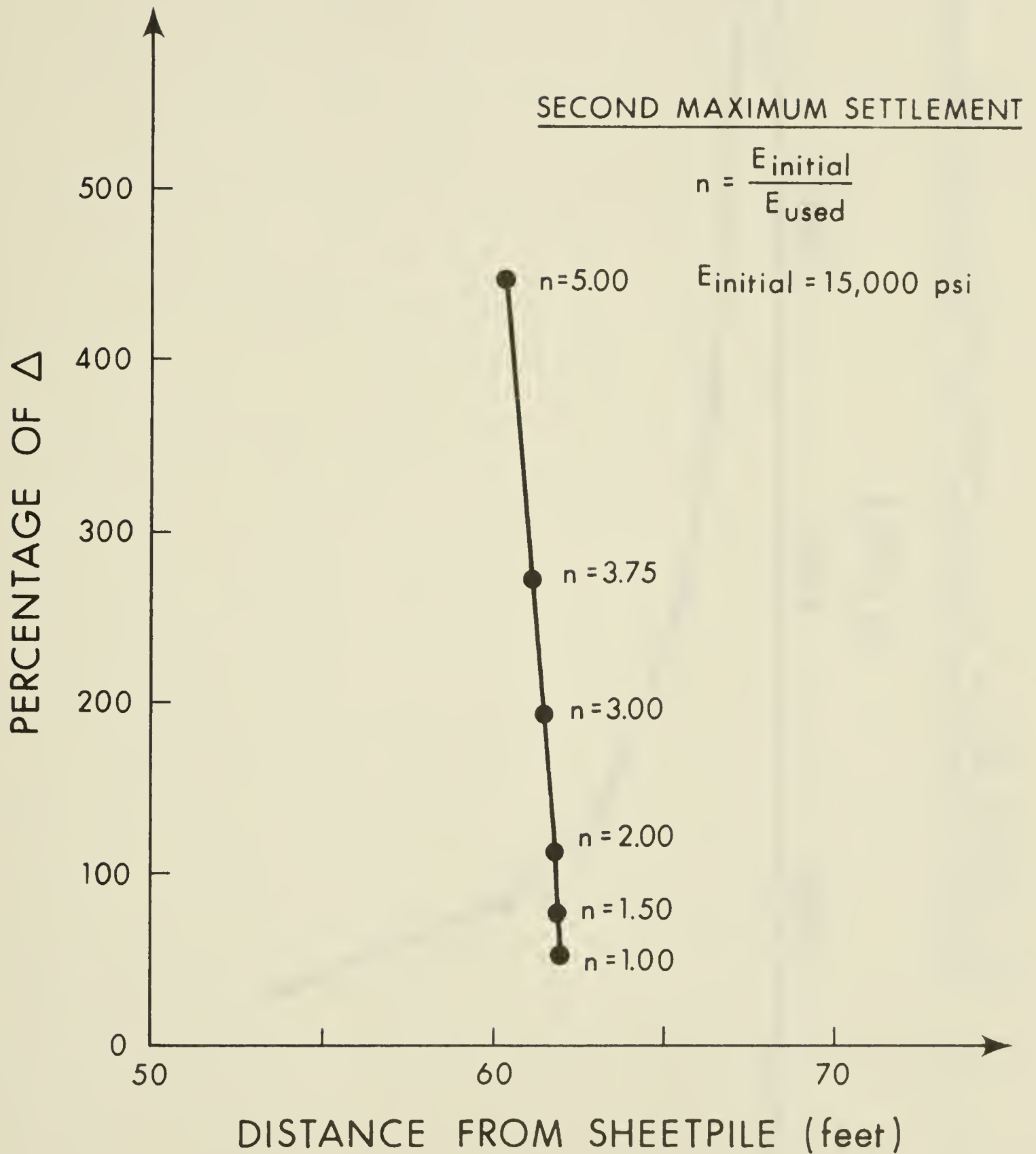


Figure 2.3.15. Influence of Young's modulus (E) on the amplitude and position of the 2nd Maximum settlement for anchor 5 with $K = 1.0$ and $A_p = 19,200 \text{ lbs.}$

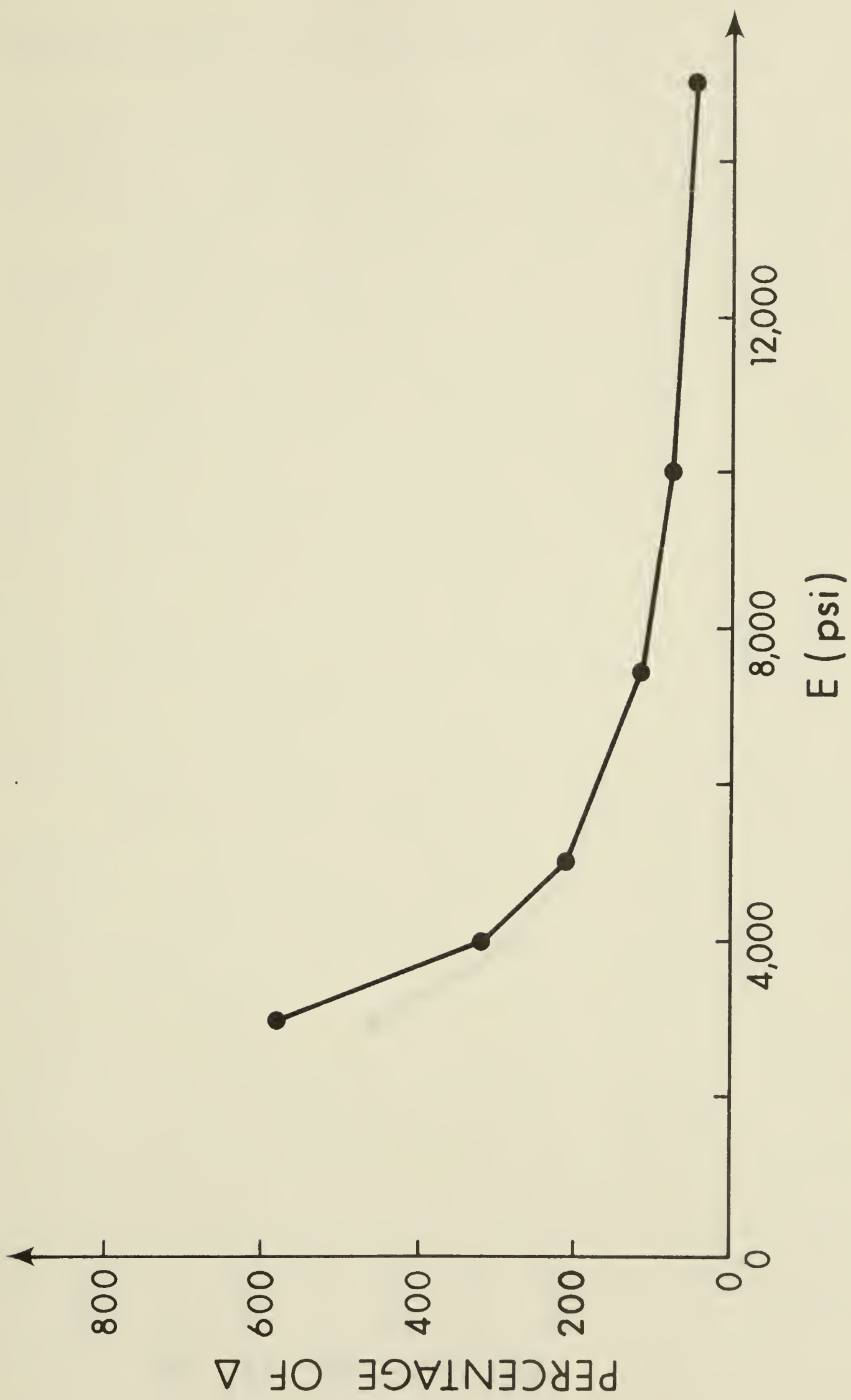


Figure 2.3.16. Relation between the amplitude of the 1st Maximum settlement and Young's modulus (E) for anchor 5 with $K = 1.0$ and $A_p = 19,200$ lbs.

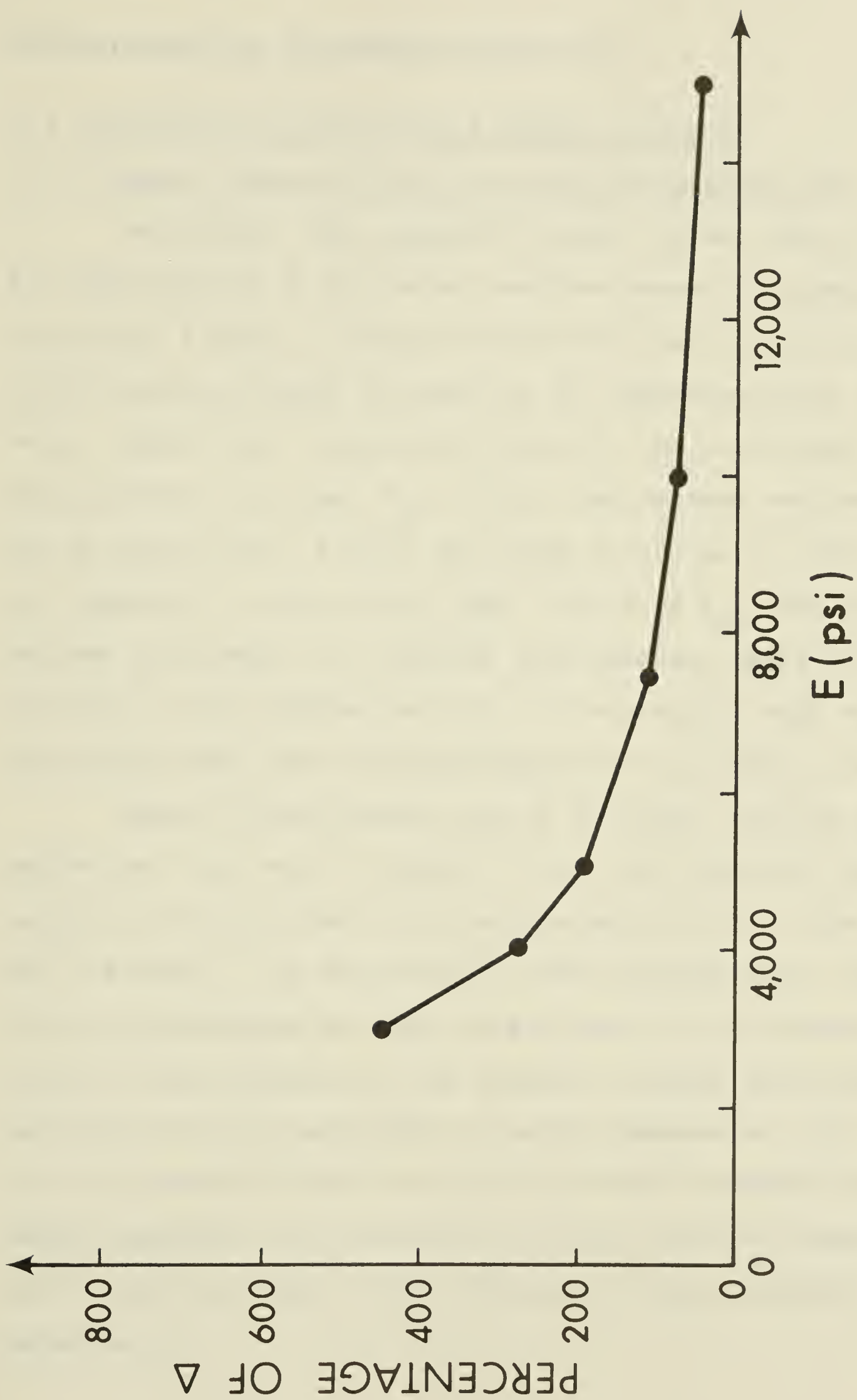


Figure 2.3.17. Relation between the amplitude of the 2nd Maximum settlement and Young's modulus (E) for anchor 5 with $K = 1.0$ and $A_p = 19,200$ lbs.

deformations for an anchored excavation.

2.4 Conclusions of the Finite Element Analysis

2.4.1 General Shape of the Ground Surface Deformations

Throughout this parametric study, it was shown that the deformations of the ground surface around an anchored excavation follow a standard pattern and can be minimized within certain limits dictated by the characteristics of the soil. Except for the smallest value of the coefficient of earth pressure at rest ($K_0 = 0.67$), two maximum settlements can be identified. A first one close to the wall, which is not apparent in the case of small values of K_0 . The second maximum settlement is, situated approximately above the position of the grouted portion of the anchors, with magnitude decreasing with the increasing depth of the anchor's burial.

These two settlements are of different origins and while the first one is typical of the wall behavior, the second is characteristic of the grouted portion of the anchor, and its depth. The amplitude of these deformations, which could be considered as small in the case of the parametrical study of the influence of the geometry, anchor prestress, and variation of the coefficient of earth pressure at rest, are in fact relative to the value of the Young's modulus and it seems reasonable to have used a relative scale of comparison with Δ for the study of the influence of the different parameters.

2.4.2 The First Maximum Settlement

This settlement, the closest to the wall of the excavation and characteristic of the behaviour of the excavation wall, is influenced by three parameters: Young's modulus (E), the coefficient of earth pressure at rest (K_o), and the anchor prestress. Young's modulus (E) and the coefficient of earth pressure at rest (K_o) determine the state and stress history of the soil and may be considered invariant. Given a certain soil, it is however possible to minimize the settlement amplitude by way of an adequate prestressing of the anchor within the limits of the stability analysis and the design capacity. It is desirable to use the highest possible prestress load compatible with the section modulus of the wall used for the excavation. The geometric configuration of the anchoring however has no effect on the amplitude of the first maximum. The different parameters affecting the amplitude and position of the first maximum settlement are presented on Figure 2.4.1.

2.4.3. The Second Maximum Settlement

This settlement, occurring about the level of the grouted portion of the anchors, is more characteristic of the specific anchor behaviour. In this case, the geometry of the anchoring is of prime importance and is a factor to take into account when a reduction of the second maximum settlement is desired. The increase in the angle of anchoring has the effect

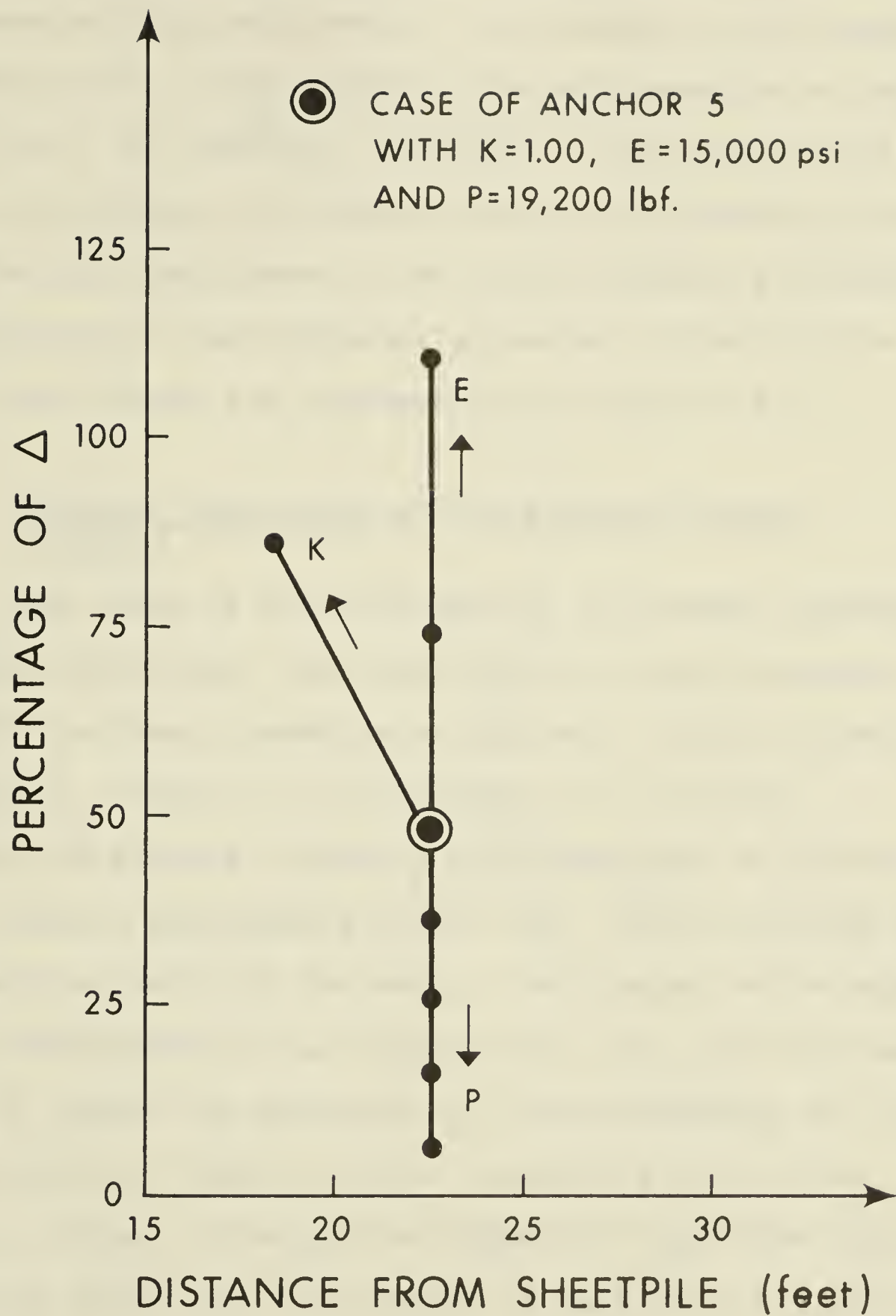


Figure 2.4.1. Factors influencing the 1st maximum settlement (P = prestressing, E = Young's modulus, K = coefficient of earth pressure).

of burying the anchor deeper into the ground and will reduce the ground surface settlement. An increase in the length of anchoring will also minimize the settlement as a larger body of soil is involved. Contrary to the case of the first maximum settlement, an increase in the prestressing does not affect the amplitude of the second maximum settlement. The influence of the different parameters affecting the second maximum settlement are represented in Figure 2.4.2.

2.4.4. Relative Importance of the Various Factors Studied

The study of the influence of the anchor geometry, the anchor prestress, the coefficient of earth pressure at rest and the Young's modulus of the soil yields two main conclusions. First, it is possible, by correctly choosing the anchors' geometry and prestress, to minimize the ground surface settlements within the limits dictated by the characteristics of the soil. The longest and steepest anchor prestressed at its highest value will give the best design to reduce the amplitude of the settlements at the ground surface. However, these parameters have to be carefully chosen and should be compatible with the stability conditions which were the subject of section 2.2. Once the best design has been made, the accurate determination of the coefficient of earth pressure at rest (K_0) and even more, the evaluation of the Young's modulus of the soil encountered

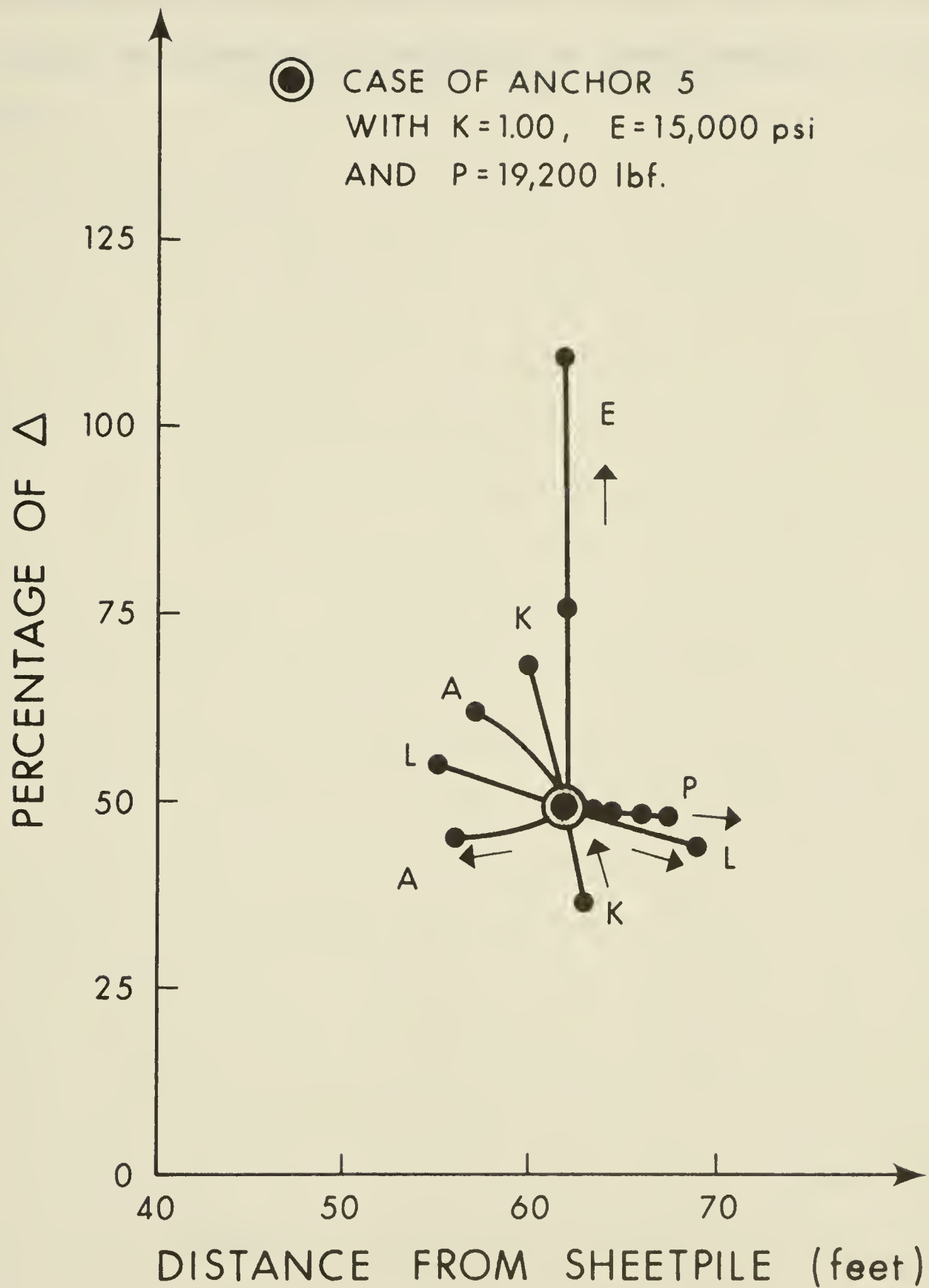


Figure 2.4.2. Factors influencing the 2nd maximum settlement (P = prestressing, E = Young's modulus, K = coefficient of earth pressure at rest, A = angle of anchoring, L = length of anchoring).

around the excavation will allow the designer to estimate the maximum settlements that have to occur and that cannot be reduced by changes in geometry or prestressing of the anchors.

CHAPTER III

ANALYSIS OF A CASE HISTORY

3.1 The Selection of a Case History

Ideally, every analytical procedure should be verified by one or more well documented case histories. Such case histories should be described not only in terms of their actual field behaviour but also in terms of other factors such as geometry, geology, loads and soil properties. Confidence in the analytical procedure is increased if the calculated behaviour of a particular case is a reasonable match to the real observed data. Information about a case history should exclude the possibility for misinterpretation of any factor: geometrical configuration, stress distribution, or material characteristics. However, this seldom is possible and there will be always some unknown that was not recorded or that could not be specified. For example: Young's modulus, Poisson's ratio and the coefficient of earth pressure at rest (K_0) are characteristics of the soil which seriously affect the settlement of the ground surface (as was shown in Chapter II). Recently, the recording of the stress distributions and of movements around excavations has been intensified (Liu and Dugan, 1972; Clough, Weber and Lamont, 1972; Shannon and Strazer, 1970; Wosser and Darragh, 1970; Maljian and Van Beveren, 1974). Due to its recentness and

its excellent descriptions of the excavation characteristics, the excavation for the Entertainment Center and Theme Towers in the Los Angeles area (Maljian and Van Beveren, 1974) was selected as a case history to verify the suitability of the Finite Element method for prediction of ground settlement around anchored excavations and also to increase confidence in results of the parametric studies presented in this thesis. The information used was obtained from the pertinent paper (Maljian and Van Beveren, 1974) and further complemented by way of personal communication with one of the authors (Maljian, 1974).

3.2 Analysis of Entertainment Center and Theme Towers Excavation

3.2.1 Situation and Characteristics of the Excavation

This excavation in the Los Angeles area is believed to be the largest such excavation in the U. S. A. The depth varies from 70 to 110 feet, and with such a depth in a city area, the use of flattened slopes was precluded, therefore an anchoring system was chosen. A mass excavation was performed first in the central part of the site and a sloped bench left on the sides (Figure 3.2.1). Soldier piles were driven at 6 foot centers, extending 15 feet below the final grade of the excavation. After installation of the soldier piles, the peripheral bench was excavated in increments of 5 feet with simultaneous installation of anchors. The anchors were placed behind an active wedge of 35 degrees (footed at

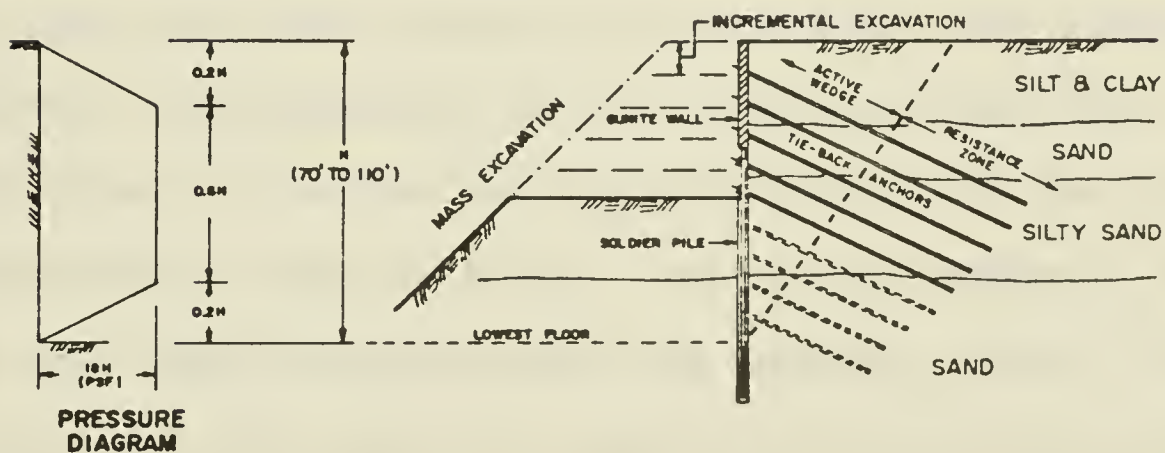
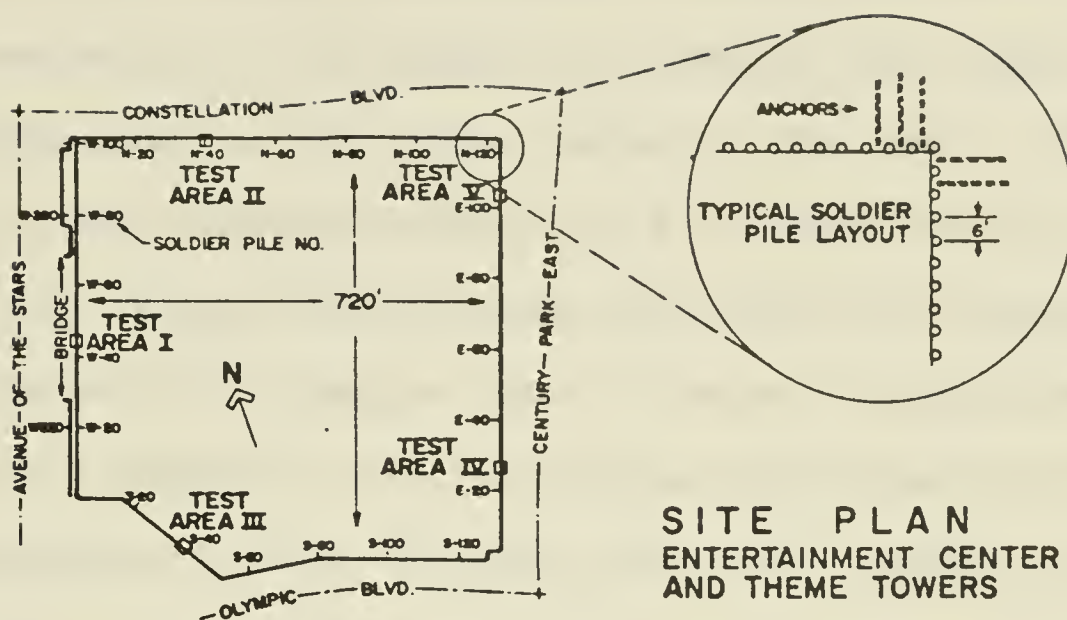


Figure 3.2.1. Geometry of the excavation for Entertainment Center and Theme Towers - After Maljian and Van Beveren (1974).

the base of the soldier piles at that point) and extended at least 40 feet behind this wedge. The anchors were mainly friction anchors, of 16 inches in diameter, but some belled anchors were used in the lower parts of the wall. These anchors all had a design capacity of 96 kips and in order to minimize the shoring deflections, they were all prestressed to approximately the design load. The soil conditions explored to a depth of 175 feet below the existing grade show 4 different layers of older alluvium (probably Tertiary (Chang and Duncan, 1970)). Undisturbed samples of all materials were collected, and direct shear tests yielded average values of cohesion and friction angle of 1000 psf and 24 degrees for the clays, and 400 psf and 32 degrees for the sands. The geometric configuration of the excavation with the different layers of soils and the disposition of the anchors are represented on Figure 3.2.1. Particular emphasis was given in the report (Maljian and Van Beveren, 1974) to a typical section, for which the settlement and deflection were published in details. This section, at the level of the soldier pile N-42, is situated about the middle of the north side wall and is then suitable for a two dimensional analysis.

3.2.2 Procedure Used for the Analysis

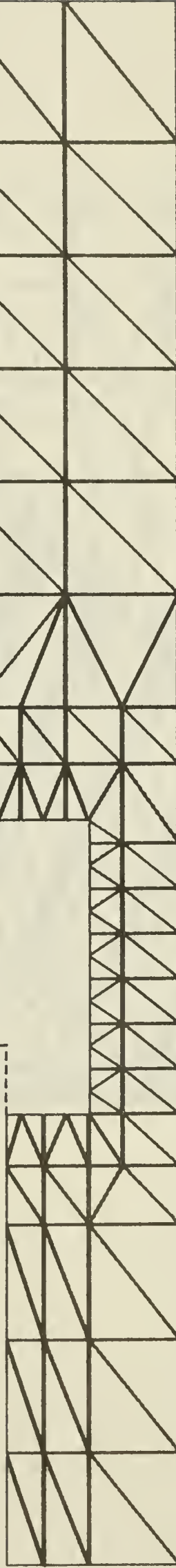
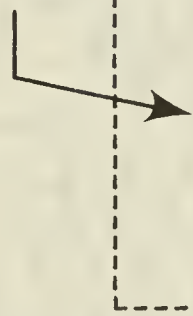
A two-dimensional Finite Element analysis using constant strain triangles was performed on this case history. Changes in bulk density due to the driving of the soldier piles

and grouting of the friction anchors are ignored. In the actual case history, deformations were recorded from the beginning of excavation, but as we are using a linear elastic analysis, stress history has no influence on obtained Finite Element deformations: therefore, attention is concentrated on final settlements only, and a "change in stress" type of analysis is used. The change in stress applied at the boundaries of the excavation in the Finite Element Analysis is equal to the relief of overburden pressure on the final grade of the excavation. For the wall of the excavation, the change in stress at a particular level is proportional to the relief in overburden pressure, but also directly proportional to the coefficient of earth pressure at rest (K_0). For this coefficient, the value must be determined on the basis of the type of deposit and on an evaluation of its stress history. The soldier piles, situated at 6 foot centers with the anchors between the piles, are replaced in this analysis by a continuous wall of equivalent rigidity, keeping the product $E \times I$ constant (E = Young's modulus and I = moment of inertia). To accommodate the two-dimensional nature of the analysis, the anchors are replaced by a continuous strip of anchoring. As for the geometry, a stress continuity was assumed, evenly distributing the prestressing of the anchors and the reactions of the pile on the 6 foot-thick equivalent slice of soil.

3.2.3 Values Assumed for the Analysis

The finite element mesh shown on Figures 3.2.2 and 3.2.3 was designed to represent the excavation. The reported data is sufficient to fix the angle of the anchors with the horizontal, the approximate length, and the spacing, of the anchors. The soldier pile characteristics as well as the stratigraphy of the soil situated around the excavation are also determined from the report by Maljian and Van Beveren (1974). However, a choice must be made regarding the Young's moduli and Poisson's ratios of the various strata as well as the coefficient of earth pressure at rest (K_0). For the lowest anchors, the information is not sufficient to distinguish between belled and friction anchors, but as the load capacities of both types are similar and since the belled anchors were placed only at the bottom of the excavation, the friction type was selected for all anchors in the analysis. The effect of this assumption on the ground surface settlements should not be significant, as the lowest anchors (of the bell or friction type) are in any case overlapped by friction anchors. The two following Tables, represent the parameters taken from the paper by Maljian and Van Beveren (1974) (Table 3.2.1) and the parameters assumed for this analysis (Table 3.2.2). The anchor lengths (Table 3.2.2) are calculated for the 7 anchors under the assumption that they all extend 40 feet behind a 35 degrees active wedge starting from the final grade level of the soldier pile. The Young's moduli of the

SOLDIER PILE AND ANCHORS ZONE



50 feet

Figure 3.2.2 Finite Element mesh used to represent the excavation for Entertainment Center and Theme Towers

Figure 3.2.3
Detail of the soldier
piles and anchors' zone

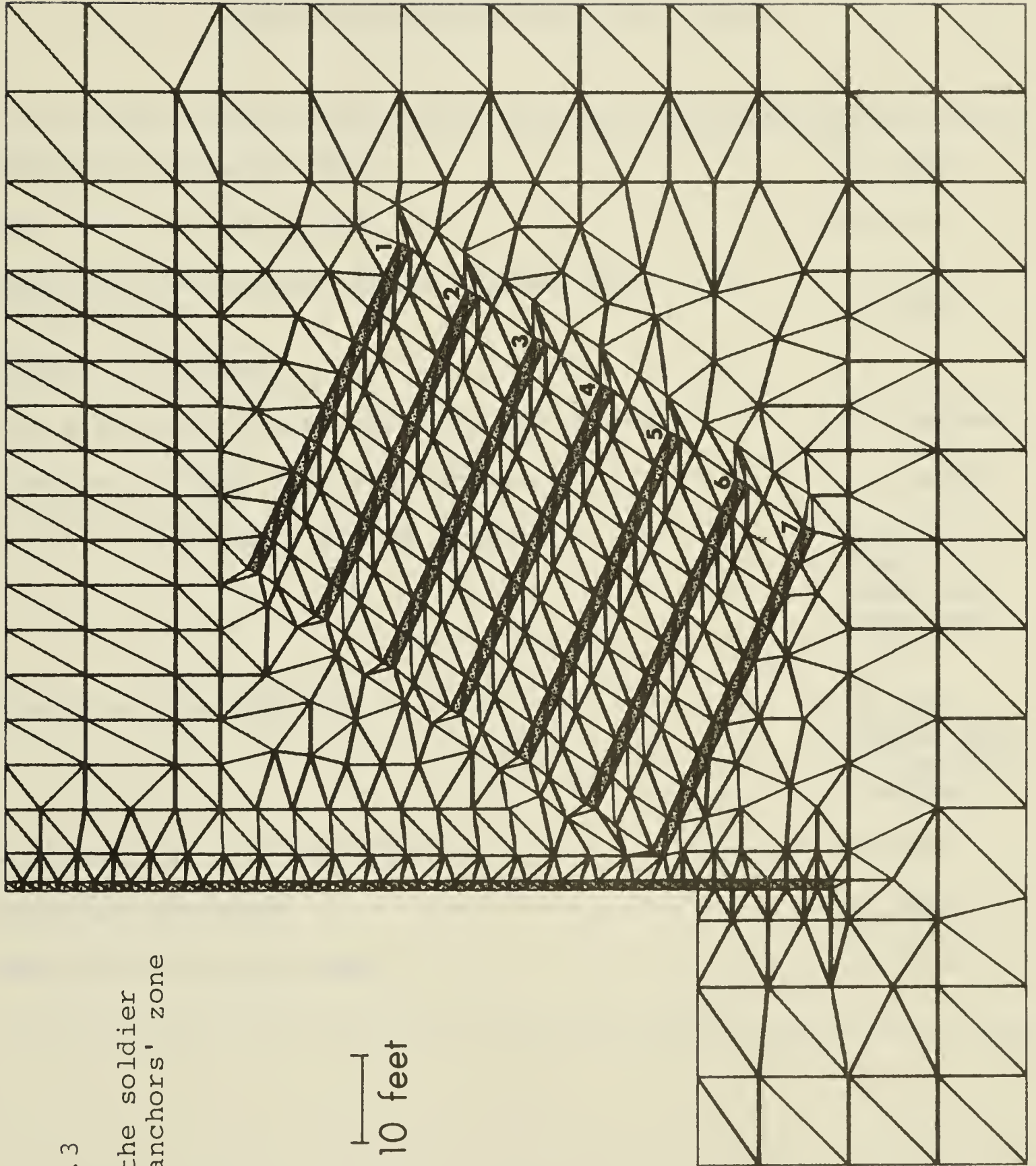


TABLE 3.2.1

PARAMETERS DRAWN FROM THE REPORT

Depth of the excavation	77 feet
Type of soldier piles	8WF32
Depth of the soldier piles beneath the final grade	15 feet
Number of anchors	7
Angle of the anchors with the horizontal	25 degrees
Diameter of the friction anchors	16 inches
Point of anchorage of the anchors	each 10 feet starting from the top
Length of the anchors	40 feet behind the 35° active wedge
Depth of the silt and clay	21 feet
Depth of the sand	13 feet
Depth of the silty sand	25 feet

TABLE 3.2.2

ASSUMED PARAMETERS

Type of anchors	friction
Length of anchor 1	80 feet
Length of anchor 2	74 feet
Length of anchor 3	68 feet
Length of anchor 4	62 feet
Length of anchor 5	56 feet
Length of anchor 6	51 feet
Length of anchor 7	45 feet
Young's modulus for the silt and clay	10,000 psi
Young's modulus for the sand No. 1	15,000 psi
Young's modulus for the silty sand	20,000 psi
Young's modulus for the sand No. 2	25,000 psi
Poisson's ratio for all soils	0.4
K_0 (coefficient of earth pressure at rest)	1.5
Unit weight of all soils	130 pcf.

different soils were chosen according to judgment based on common values found for these types of material (Lambe and Whitman, 1969). Due to the fact that this excavation is situated in older alluvium, a coefficient of earth pressure at rest of 1.5, indicating mild overconsolidation, would seem to represent quite well the state of the Tertiary sediments in the Los Angeles area (Brooker and Ireland, 1965). The unit weight of 130 pcf is also reasonable for these materials.

3.2.4 Results of the Finite Element Analysis

The general behaviour of the ground surface as indicated by Figure 3.2.4 shows two maximum settlements. The maxima are both about 12mm (0.5 inch) but one is situated at 20 feet and the other at 130 feet from the anchored wall. With the exception of a 40 foot section centered at 55 feet from the excavation edge, vertical displacement exceeded 10mm (0.4 inch) up to a distance of 210 feet from the wall. At 460 feet from the excavation, the settlement is still of the order of 3mm (0.1 inch), thereby demonstrating that a single first settlement measurement is probably inadequate for most practical purposes. The horizontal extent of the settlement is very large and several data points are necessary to delineate both the maxima, and the distribution. Figure 3.2.5 represents the horizontal movement of the ground surface towards the excavation. This displacement is 55mm (2.2 inch) at the

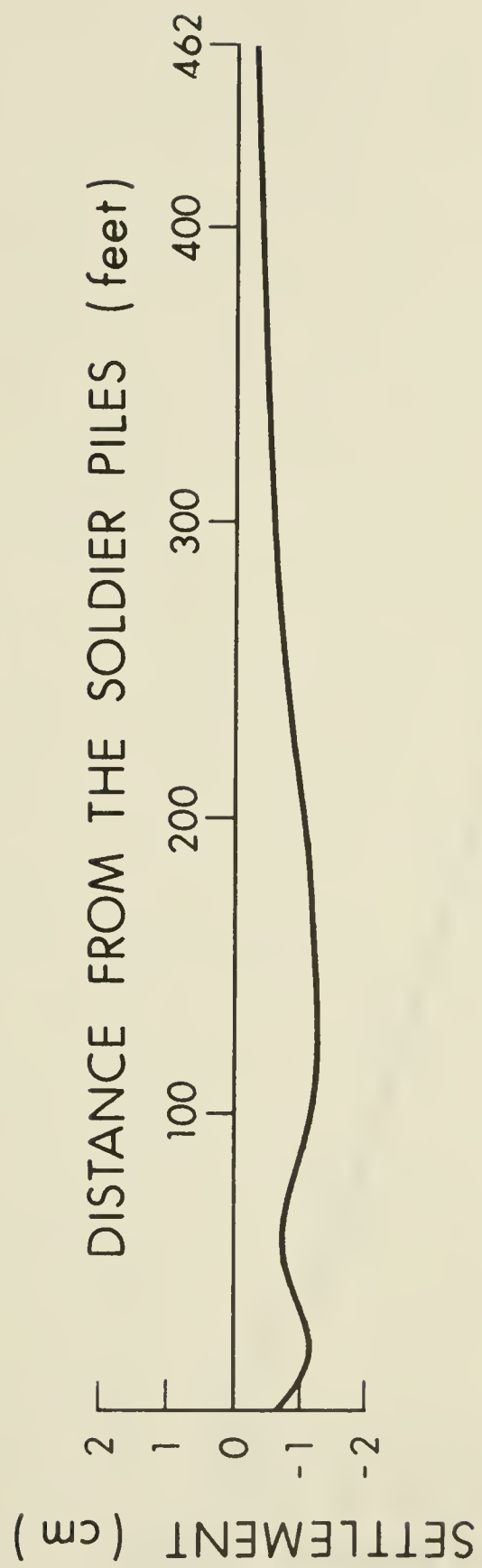


Figure 3.2.4 Predicted settlement of the ground surface

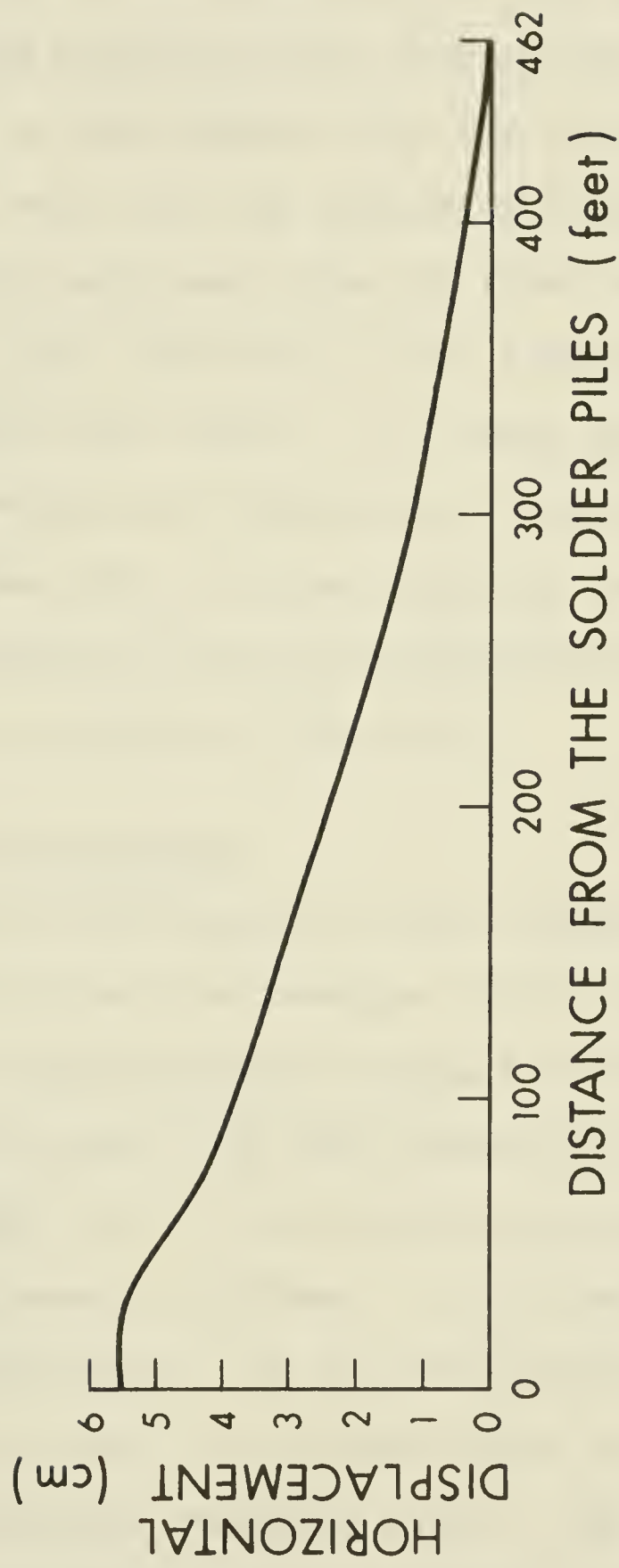


Figure 3.2.5 Predicted deflection of the ground surface towards the excavation

soldier piles, and decreases as the distance from the wall increases but at 300 feet it is still of the order of 12mm (0.5 inch). From these results, it is noted that the settlement of the ground surface presents two distinct maxima, the first close to the soldier pile and due to the outward movement of the wall, and the second of the same amplitude but more than 100 feet away from the first one and more typically due to the behaviour of the anchors. The settlement, however is greater than 10mm (0.4 inch) over more than 150 feet. The horizontal deflection towards the excavation, however, decreases more or less regularly as the distance from the pile becomes greater and demonstrates the mobilization of active pressure on the wall.

3.3 Measured Displacements

The typical deflection of the soldier pile N-42 is reported by Maljian and Van Beveren (1974) (Figure 3.3.1). For this section, the relative movement of two points on the ground surface is known with high accuracy as indicated in Figure 3.3.1. The tip of the soldier pile moves towards the excavation by an amount of 27mm (0.09 foot) but there is no measurable settlement. At 14 feet behind the wall, there is a settlement of 3mm (0.1 inch) while at 44 feet, zero settlement is recorded (Maljian, 1974). The measurements were obtained using reference points situated at 80 feet behind the soldier piles and these are absolute values only under the condition that the points of reference do not move. A first

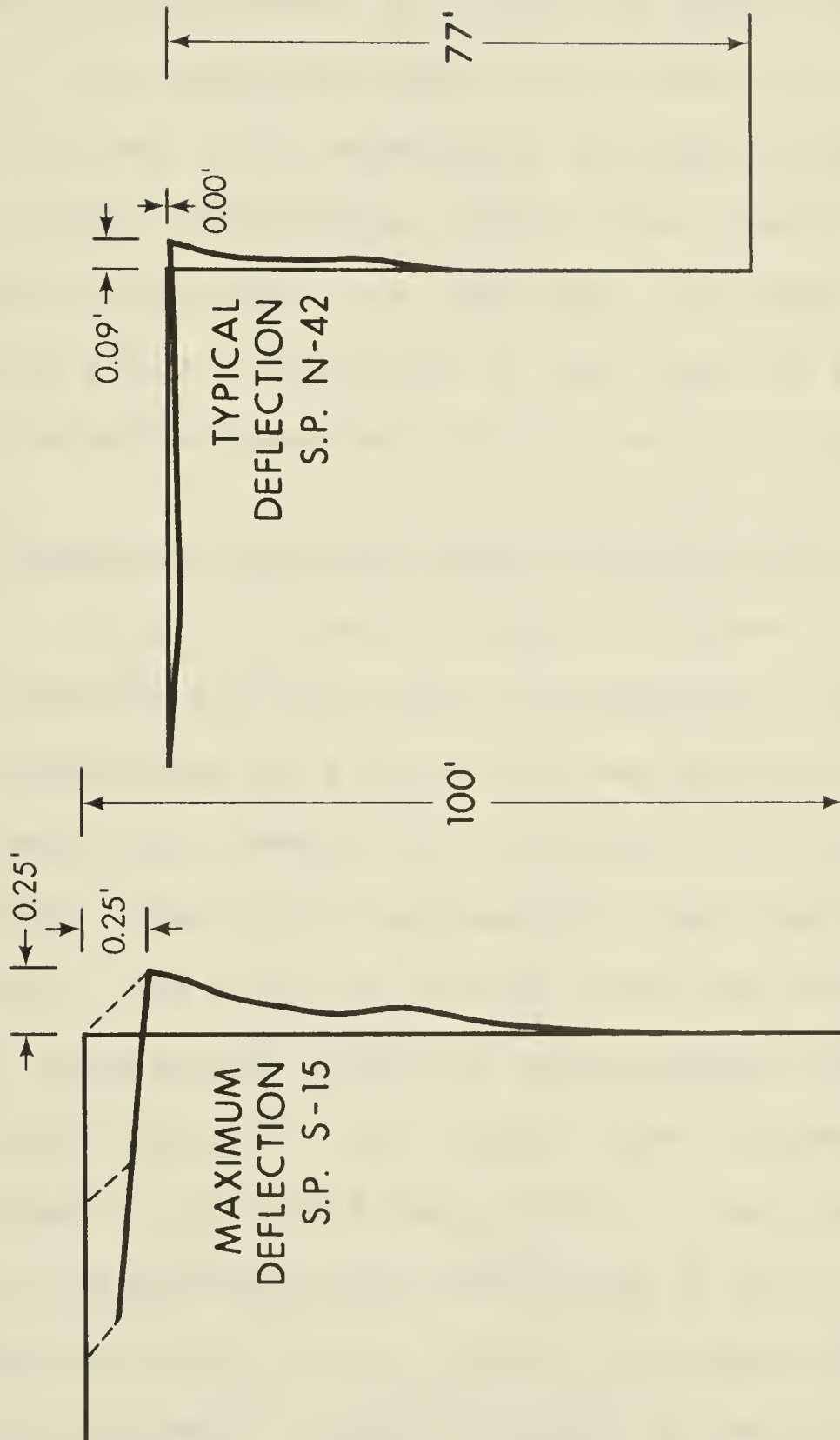


Figure 3.3.1 Measured deformations at the level of the soldier piles S-15 and N-42.

look at the deformation of the soldier pile shows that the bottom part did not move at all, an item which is quite surprising (Figure 3.3.1). Although, the soldier pile is buried at its bottom in 15 feet of sand, the stress relief due to the excavation must affect mostly the bottom part of the pile and it is reasonable to expect that there will be some slight translation towards the excavation on the full length of the pile. In any case, the reported settlements in this field record were of the order of several millimeters and the deflections were of the order of several centimeters.

3.4 Comparison of Actual and Predicted Behaviour

On the following graphs (Figures 3.4.1 and 3.4.2), the vertical and horizontal movements of the ground surface are represented by the curve drawn from the Finite Element Analysis and a second curve showing the actual deformations recorded. The curve representing the predicted behaviour was plotted. The point at 79 feet from the soldier pile, however, had a significant predicted displacement and from this new reference position, the actual curve representing the movements recorded in the field was plotted. Upon examining Figure 3.4.1 (representing the deflection of the ground surface), it is seen that the Finite Element analysis under estimates the outward movement by approximately 20 percent. On the other hand, Figure 3.4.2 shows a perfect agreement between predicted and recorded settlements. However, this agreement

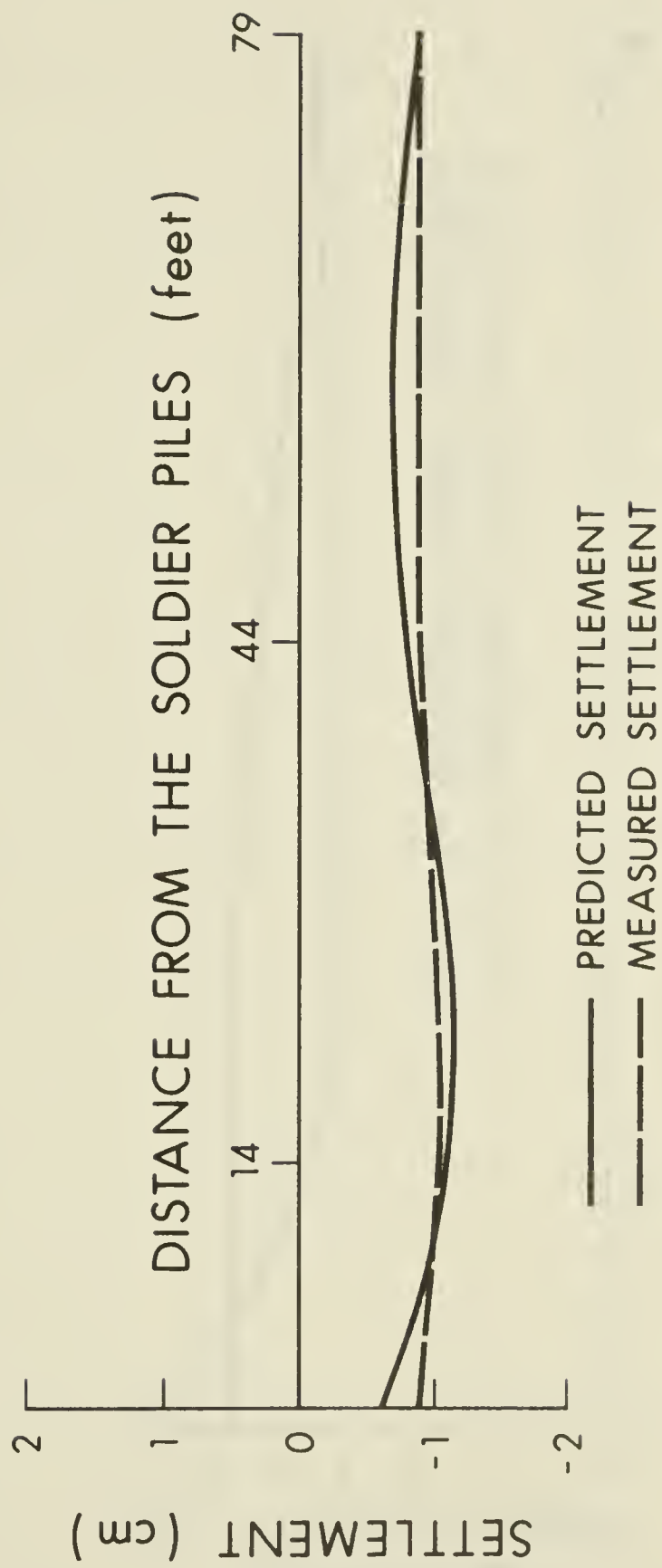


Figure 3.4.1 Comparison of measured and predicted settlements at the level of S.P. N-42.

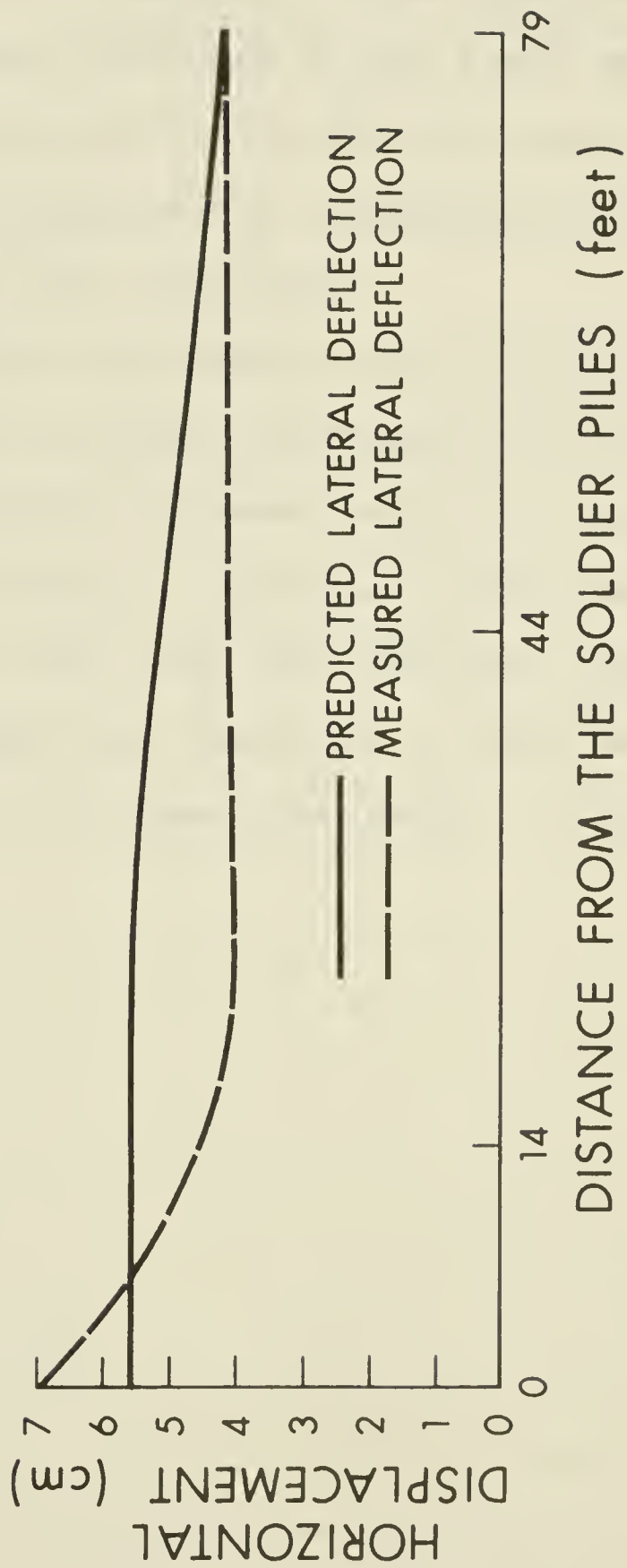


Figure 3.4.2. Comparison of measured and predicted deflections of the ground surface towards the excavation at the level of S.P. N-42.

is due to the fact that the curves were compared, assuming that the reference point had a settlement as determined by the numerical analysis. This, then, would indicate that the measurements recorded in the field were in fact relative recordings. In the Finite Element results, it is seen that a reasonable position for a reference point would be around 500 feet from the excavation.

Two main conclusions can be stated. First, the Finite Element analysis performed on this excavation gave results in general agreement with the data recorded in the field and secondly; a recording of the deformations about an excavation will give good absolute values if the reference points are chosen at a sufficient distance from the excavation (7 to 8 times the depth of the excavation).

CHAPTER IV

CONCLUSIONS AND RECOMMENDATIONS

4.1 Conclusions

4.1.1 The Reliability of the Finite Element Analysis

The back-analysis of an outstanding case history showed that the Finite Element method is capable of predicting the ground surface settlements with reasonable accuracy. Such numerical analysis based on the assumption of plane strain using an equivalent continuous wall and a continuous strip of anchoring to replace the actual complicated shape of the soldier piles and the discontinuous anchoring system prove to be reliable. It seems reasonable then, in other such analyses, to replace the actual shape of the wall by a rectangular shaped beam which is more easily introduced into a two-dimensional analysis. The major relation to be respected in this equivalence is to keep the flexibility (EI) constant, which then correctly represents the deformation behaviour of the wall. However, for a stress analysis, this assumption would not seem sufficient; as in this case, the section modulus would be of greater concern in its effect on the stress distribution. The use of a continuous strip of anchoring to replace the discontinuous actual anchoring conditions is a correct assumption under the condition that

the loads are sufficiently closely spaced so that the overlapping of pressures becomes predominant: then a simulated plane strain condition is quite representative.

4.1.2 The Assumption of Plane Strain

In their recent paper, Tsui and Clough (1974), undertook a study of the plane strain approximations in Finite Element Analyses of temporary walls. This study particularly investigates the discrepancy between the actual stress distribution and a uniform planar pressure assumption. From the determination of the "characteristic length" (ℓ_0), an important characteristic of the wall-soil system, values of which are represented on Figure 4.1.1, it is possible, knowing the spacing of the anchoring, to know the maximum percent deviation between actual and uniform planar stress distribution. The evaluation of this deviation can give in the case of the calculations in Chapter II and Chapter III, a feeling of the value of our plane strain assumption. The analysis of Tsui and Clough (1974) showed that the assumption of a continuous wall replacing the soldier piles and lagging yields accurate results for the behavior of the soldier piles but does not represent well the behaviour of the lagging. Considering the behaviour of the soldier piles, it is then interesting to evaluate from the equivalent continuous wall, the validity of assuming a uniform pressure of the anchoring. For the case history described in Chapter III, the characteristic

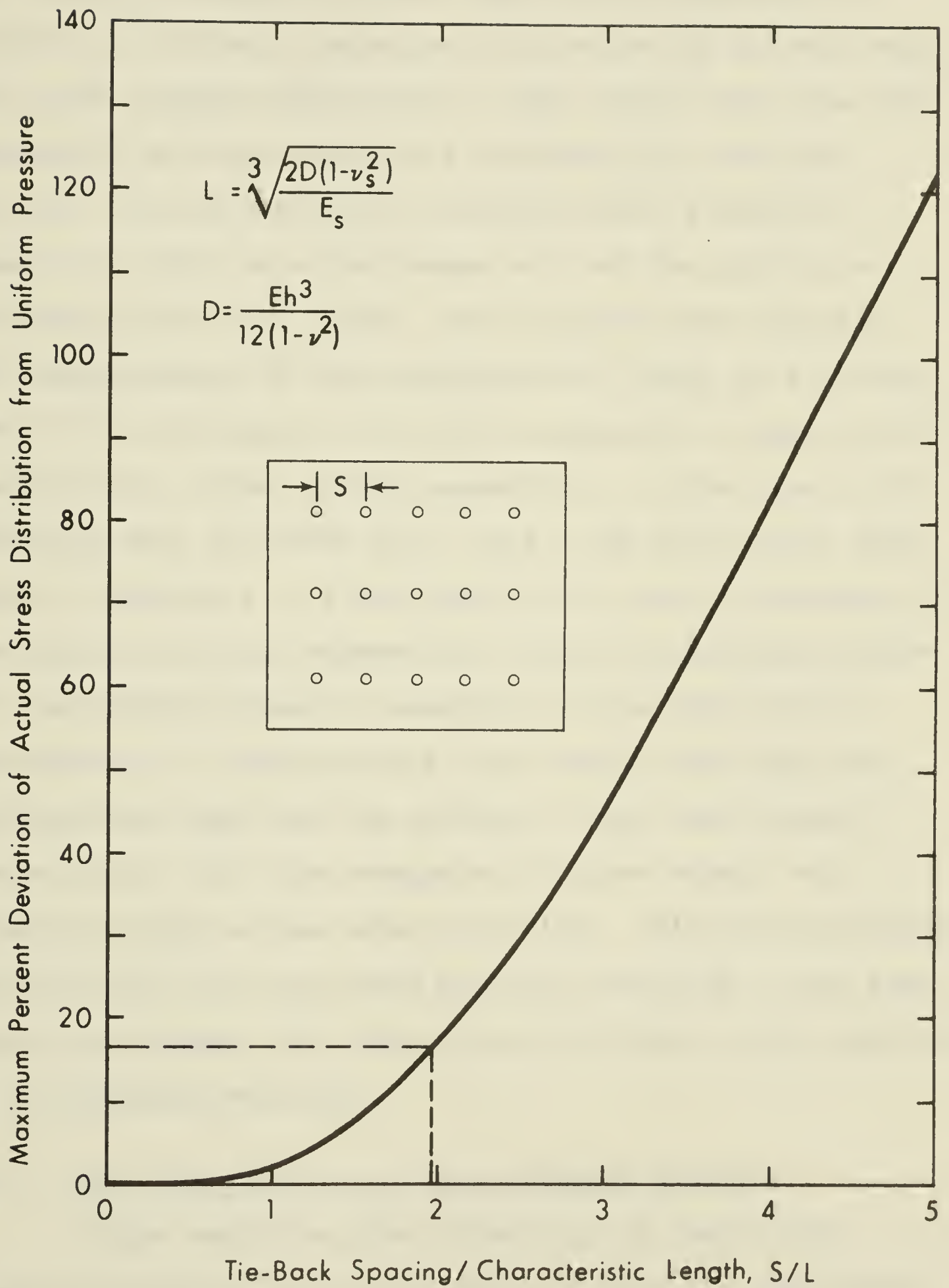


Figure 4.1.1. Evaluation of the plane strain assumption.
(After Tsui and Clough, 1974)

length is $L = 3.0$ feet. With a spacing s equal to 6 feet, the ratio $\frac{s}{L}$ is equal to 1.96. This value introduced in Figure 4.1.1 shows a deviation of less than 20 percent with the actual stress distribution. This result shows that the assumption of plane strain was acceptable for the case history. In the case of the sheetpile wall studied in Chapter II which is a continuous wall and for which the analysis of Tsui and Clough (1974) applies more directly, the determination of the characteristic length will give an idea of the spacing of the anchors necessary to yield correct results from a plane strain assumption. In the case of the sheetpile wall the value of L is 4.1 and with such a high value, a spacing $s = 8$ feet would still give a deviation of less than 20 percent between the actual stress distribution and the uniform pressure assumption of the plane strain consideration. These results show clearly that both the parametrical study and the analysis of the case history investigated under the assumption of plane strain had a behaviour close to the actual behaviour. With the correlation between actual and predicted behaviour verified on the case history in Chapter III, this gives much value to the results of the parametrical study.

4.1.3 The Advantages of a Finite Element Analysis

After verifying the reliability of the Finite Element Analysis, it is of interest to note its advantages. The design of a correct mesh represents one of the important

steps in this type of analysis. In fact, for the analysis of the different parameters which were investigated in Chapter II, the same mesh was used and designed for the nine geometric configurations. It was important to keep it the same throughout the study in order to eliminate side effects due to changes in the geometric configuration of the mesh which would have reduced the value of the parametrical study. However, limiting the aspect ratio to a value as close as possible to unity, the same mesh was then used for the whole study and it is then easy to investigate the influence of different parameters such as K_o , E , μ , and the prestress in the anchors, as there are just minor changes to implement in the input data. In the case of the mesh used to represent the case history, this was used to analyse the behaviour of a particular excavation under some precise conditions as to K_o , E , μ or the prestress load, but it should be emphasized that the same mesh could be used in a study of the influence of the number of anchors, position of the points of anchoring or length of grouted part of the anchors. This indicates the flexibility of this type of analytical procedure for practical design purposes and in particular the study of the variations of the different parameters.

4.1.4 The Results of the Parametrical Study

Of the various types of deformations around an anchored excavation, the settlement of the ground surface

adjacent to the excavation is the most important. The parametrical study indicated the relative importance of the various factors involved:

- (a) the geometry of the anchoring.
- (b) the prestressing of the anchor.
- (c) the soil properties.

The general shape of the settlement of the ground surface presents two maximum settlements. One which is close to the wall and called the first maximum settlement. One situated at the level of the anchors and called the second maximum settlement. While the amplitude of both maximum settlements is dictated by the characteristics of the soil, they can be minimized independently to a certain extent as dictated by the soil properties. The first maximum settlement related to the movement of the wall will be reduced by an increase in the prestressing but a change in the angle or length of anchoring will not change its amplitude. The second maximum settlement which is more characteristic of the behaviour of the anchors, will be correspondingly influenced by the characteristics of the geometry of the anchoring: the longest and deeper anchor will give the best minimization in this case. The value of the prestress load, however, has no influence on its amplitude.

4.2 Recommendations

4.2.1 Design Considerations

In view of the results presented in paragraph 4.1.4, while it is not possible to change the soil properties for a particular site, a designer can make an intelligent choice of the anchoring conditions in order to minimize the settlements of the ground surface. In the case of a single anchor retaining a flexible wall, which was the object of this study, the best results are given by the longest anchor, buried deeply into the ground and prestressed at the highest possible load. In this case, the length and maximum angle of anchoring will be limited by the stability analysis and the maximum prestress load will then be limited by the upper bound of the design load determined by the geometric configuration of the anchoring. The length of the grouted part of the anchor should then be calculated to resist the corresponding pull-out force applied by the prestressing.

4.2.2 Results of Model Tests

Some investigation of the anchoring conditions and particularly, the influence of the geometry of the anchoring, has been performed by the use of model tests. One of the most interesting contributions was made by Plant (1972). However, it is important to note the representation of the anchoring condition in these tests. The boundaries of the wall, the final grade of the excavation and the ground surface level are

representative of the actual conditions but, in these studies, the anchors, fixed at one end to the excavation wall, were fixed at the other end at a sloping back (Plant, 1972) or vertical back (Tsui and Clough, 1974). This condition, which seems to be satisfactory in the study of the behaviour of the wall will, however, fail to include the behaviour of the anchors since they are definitely fixed to the back of the model. This assumption fails to represent the behaviour of the soil away from the excavations and is a problem of boundary conditions. In addition, the configuration cannot represent the yield of the anchors. In fact, the estimation of the first maximum settlement recorded (which would be then the maximum settlement) could indeed be relevant, but no indication of the second maximum settlement is possible. In the case of Plant's analysis, the anchor prestress was kept constant while the inclination was increased, and an increase in settlement amplitude was attributed to the inclination increase. However, within the limits of the present analysis, it has been demonstrated that this increase is in fact due to the decrease in the horizontal component of the anchor prestress (Chapter III).

In conclusion, and with respect to model tests, it is of utmost importance to represent correctly the anchors in a physical sense to be able to notice the second maximum settlement whatsoever. The boundary conditions at the back of this excavation should also be representative of field conditions,

which is not the case in most model tests studied. However, the model tests based on assumptions such as those of Plant (1972) or Tsui and Clough (1974) will give reliable results for the first maximum settlement.

4.2.3. Field Measurements

The influence of other factors may readily be introduced into a Finite Element Analysis: for example, position of the point of anchoring, number of anchors, wall stiffness, stress-strain relationships of the soil. Effects studied may be extended as well: wall deflections, stress distributions, etc. There is however, a need for high quality field measurements to facilitate case history computer modeling in order that we may gain confidence in the analytic method.

The case history selected in Chapter III was one of the best instrumented available and most of the data were well described in the paper by Maljian and Van beveren (1974). In view of the many but not yet sufficient number of case histories reported in the literature, two points should be emphasized. First, the field measurements should be undertaken with much more accuracy, particularly for the recording of the ground surface settlements. A method such as the one prescribed by Jackson and Kirby (1974) could given an accuracy of ± 0.25 mm (± 0.01 inch), which would be certainly sufficient for most cases. Secondly, it is noted that most of the time, settlements and deflections are recorded from a reference point which is too

closely situated to the excavation and this yields only relative values for both settlements and deflections. A distance of 8 times the height of the excavation would seem a reasonable distance at which a reference point should be situated from the wall of an excavation. In the view of these conditions it would be then of great interest to expect also a precise determination of the soil properties which are definitely the important parameters affecting the amplitude of the ground surface settlements.

REFERENCES

REFERENCES

- Bjerrum, L., Frimann Clausen, C. J. and Duncan, J. H., 1972, "Earth Pressures on Flexibles Structures. A State-of-the-Art Report". Proc. 5th European Conf. Soil Mechs. Found. Eng., 2, 169-196.
- Booth, W. S., 1966, "Tie-backs in soil for unobstructed deep excavation". Civil Engineering, 36, 46-49.
- Bowles, J.E., 1968, "Foundation Analysis and Design". McGraw-Hill, New York.
- Broms, B. B., 1968, "Swedish Tie-Back Systems for Sheet Pile Walls". Acta Technica Academiae Scientiarum Hungaricae Tomus, 63 (3), 410-411.
- Brooker, E. W. and Ireland, H. O., 1965, "Earth pressures at rest related to stress history". Canadian Geotechnical Journal, 2, No. 1, 1-15.
- Browzin, B. S. 1948, "Upon the Deflection and Strength of Anchored Bulkheads". Proc. 2nd Int. Conf. Soil Mechs. Found. Eng., 3, 302-308.
- Bureau Securitas, 1972, "Recommandations Concernant la Conception, le Calcul, L'Exécution et le Controle Des Tirants D'Ancrage". Eyrolles, Paris.
- Caspe, M. S., 1966, "Surface Settlement adjacent to Braced open Cuts". J. Soil Mechanics Division, Proc. ASCE, 92, SM4, 51-59.
- Chang, C. Y. and Duncan, J. M., 1970, "Analysis of soil movement around a deep excavation". J. Soil Mechanics Division, ASCE, 96,
- Clough, R. W., 1960, "The finite element in plane stress analysis". Proc. 2nd A.S.C.E. Conf. on electronic computation, Pittsburgh, Pa.
- Clough, G. W., Weber, P. R. and Lamont, J., 1972, "Design and observation of a tied-back wall". Proc. ASCE Speciality Conf. on Performance of earth and earth supported structures, New York, 1367-1389.

- Cornfield, G. M., 1969, "Direct-reading nomograms for design of anchored sheet-pile retaining walls". Civil Engineering and Public Works Review, 64, 753-755.
- Costet, J. and Sanglerat, G., 1969, "Cours Pratique de Mécanique des Sols". Dunod, Paris.
- D'Appolonia, E, Alperstein, R. and D'Appolonia, D. J., 1967, "Behavior of a Colluvial Slope". J. Soil Mechanics Division, Proc. ASCE, 93, SM4, 447-473.
- Desai, C. S., 1972, "Applications of The Finite Element Method in Geotechnical Engineering". Proc. of the Symposium held at Vicksburg, Mississippi, 61.
- Desai, C. S. and Abel, J. F., 1972, "Introduction to the Finite Element Method". Van Nostrand, New York.
- Dibiagio, E. L., 1966. "Stresses and Displacements Around an Unbraced Rectangular Excavation in an Elastic Medium". Ph.D. Thesis, University of Illinois.
- Egger, E. P., 1972, "Influence of Wall Stiffness and Anchor Prestressing on Earth Pressure Distribution". Proc. 5th European Conf. Soil Mechs. Found. Eng., 1, 259-264.
- Habib, P., 1969, "Anchorage especially in soft ground". International Conference Mexico 1969 Speciality Sessions No. 14 and 15, 113-118.
- Haliburton, T. A., 1968, "Numerical Analysis of Flexible Retaining Structures". J. Soil Mechanics Division, Proc. ASCE, 94, SM6, 1233-1251.
- Hanna, T. H., Sparks, R. and Yilmaz M., 1972, "Anchor Behavior in Sand". Proc. ASCE, 98, SM11, 1187-1208.
- Healy, K. A., 1971, "Pullout Resistance of Anchors Buried in Sand". Proc. ASCE, 97, SM11, 1615-1622.
- Hoesch Hüttenwerke, A.G., 1969, "Profiltafeln für Stahlspundwände". Dortmund.
- Jackson, W. T. and Kirby, R. C., 1974, "A method of measuring settlements more accurately and at lower cost". Ground Engineering, 7, 18-19.
- Lambe, T. W., and Whitman, R. V., 1969, "Soil Mechanics". John Wiley & Sons, New York.

- Littlejohn, G. S., Jack B. J., Struet M. I. and Sliwinski, Z. J., 1971, "Anchored Diaphragm Walls in Sand - Some Design and Construction Considerations". Journal of Inst. of Highway Engineers, 18, 15-29.
- Liu, T. K. and Dugan, J. P., 1972, "An instrumented tied-back deep excavation". Proc. ASCE Speciality Conference on Performance of earth and earth-supported structures, New York, 1323-1339.
- Maljian, P. A., 1974, "Personal communication with the author". Letter May 8th, 1974.
- Maljian, P. A. and Van Beveren, J. L., 1974, "Tied-back deep excavations in Los Angeles area". ASCE National meeting on water resources engineering, Meeting reprint 2158, Los Angeles.
- Meissner, H., 1970, "The anchorage of retaining walls with little deformation". Der Bauingenieur, 45, 337-339.
- Palmer, J. H. L. and Kenney, T. C., 1971, "Analytical Study of a Braced Excavation in Weak Clay". Proc. 24th Canadian Geotechnical Conf. Halifax, Nova Scotia.
- Plant, G. W., 1972, "Anchor inclination - its effect on the performance of a laboratory scale tied-back retaining wall". Proc. Int. of Civil Engineers, 53, 257-274.
- Rowe, P. W., 1952, "Anchored Sheet-Pile Walls". Proc. Int. of Civil Engineers, 1, 27-70.
- Rowe, P. W., 1955, "A Theoretical and Experimental Analysis of Sheet-Pile Walls". Proc. Int. of Civil Engineers, 4, 32-69.
- Salvadori, M. G. and Baron, M. L., 1961, "Numerical Methods in Engineering". 2nd edition, Prentice-Hall, New Jersey.
- Shannon, W. L. and Strazer, R. J., 1970, "Tied-back excavation wall for Seattle First National Bank". Civil Engineering, 40, 62-64.
- Teng, W. C., 1964, "Foundation Design". 2nd edition, Prentice Hall, New Jersey.
- Terzaghi, K., 1953, "Anchored Bulkheads". Proc. ASCE, 79, 262.

- Terzaghi, K., 1966, "Theoretical Soil Mechanics". 14th edition, John Wiley and Sons, New York.
- Tsui, Y. and Clough, G. W., 1974, "Plane Strain Approximations in Finite Element Analyses of Temporary Wall". Proc. of Conf. on Analysis and Design in Geotechnical Engineering, ASCE, 1, 173-198.
- Wosser, T. D. and Darragh, R. D., 1970, "Tiebacks for Bank of America Building excavation wall". Civil Engineering, 40, 65-67.
- Zienkiewicz, O. C., 1971, "The Finite Element Method in Engineering Science". McGraw-Hill, London.

APPENDIX A


```

C      COMMON E(6),PR(6),RO(6),X(650),Y(650),U(650),V(650),TH(1200),
1      1STIF(150,1300),AP(1300),ESTIF(6,6),ECM(3,3),EBM(3,6),ESM(3,6),WT
      COMMON NUMNP,NUMEL,NUMAT,KODE(650),NP(3,1200),MAT(1200),MBAND,
1      1 NEQ,M,LM(6)
C
1      CALL READIN
C
      CALL ASTIF
C
      CALL BAND1
C
      GO TO 1
      END
      SUBROUTINE READIN
C      THIS SUBROUTINE READS AND PRINTS MATERIAL DATA, NODAL DATA, ELEMENT DATA.
C      IT GENERATES COORDINATES OF INTERMEDIATE NODAL POINTS AND CALCULATES
C      THE BAND WIDTH AND NUMBER OF EQUATIONS
      COMMON E(6),PR(6),RO(6),X(650),Y(650),U(650),V(650),TH(1200),
1      1STIF(150,1300),AP(1300),ESTIF(6,6),ECM(3,3),EBM(3,6),ESM(3,6),WT
      COMMON NUMNP,NUMEL,NUMAT,KODE(650),NP(3,1200),MAT(1200),MBAND,
1      1 NEQ,M,LM(6)
C
      DIMENSION HED(18)
C      READ PRELIMINARY INFORMATION
      READ(5,1000,END=998) HED,NUMNP,NUMEL,NUMAT
      WRITE(6,2000) HED,NUMNP,NUMEL,NUMAT
C
C      READ AND WRITE MATERIAL PROPERTIES
C
      WRITE(6,2005)
      DO 10 M=1,NUMAT
      READ(5,1010) E(M),PR(M),RO(M)
10      WRITE(6,2010) M,E(M),PR(M),RO(M)
C
C      READ AND WRITE NODAL DATA AND GENERATE INTERMEDIATE NODAL DATA
C
      WRITE(6,2014)
      WRITE(6,2015)
      L=1
      READ(5,1020) N,KODE(N),X(N),Y(N),U(N),V(N)
      GO TO 40
C
20      READ(5,1020) N,KODE(N),X(N),Y(N),U(N),V(N)
      DN = N-L
      DX = (X(N)-X(L))/DN
      DY = (Y(N)-Y(L))/DN
25      L=L+1
C
      IF(N-L) 50,40,30
30      X(L) = X(L-1)+DX
      Y(L) = Y(L-1)+DY
      KODE(L)= 0
      U(L) = 0
      V(L)= 0
      GO TO 25
C

```



```

      40 WRITE (6,2020) N,KODE(N),X(N),Y(N),U(N),V(N)
         IF (NUMNP-N) 50,60,20
C
50      WRITE (6,2025) N
         CALL EXIT
C
      60 WRITE (6,2016)
         WRITE (6,2015)
         WRITE (7,2021) (N,X(N),Y(N),N=1,NUMNP)
C
C      READ AND WRITE ELEMENT DATA
C
         WRITE (6,2031)
         WRITE (6,2030)
         ML=0
51      IF (ML.GE.NUMEL) GO TO 70
         READ (5,1035) M,NP(1,M),NP(2,M),NP(3,M),MAT(M),TH(M)
         WRITE (6,2035) M,NP(1,M),NP(2,M),NP(3,M),MAT(M),TH(M)
         MM=ML+1
         IF (MM.EQ.M) GO TO 65
C
      55 ML1=ML+1
         IF (ML1.EQ.M) GO TO 65
         ML2=ML+2
         MLM1=ML-1
         IF (MLM1.LE.0) GO TO 85
         DO 62 I=1,3
            NP(I,ML2)=NP(I,ML)+1
      62 NP(I,ML1)=NP(I,MLM1)+1
            MAT(ML2)=MAT(M)
            MAT(ML1)=MAT(M)
            TH(ML2)=TH(M)
            TH(ML1)=TH(M)
            ML=ML2
            GO TO 55
C
      65 ML=M
         GO TO 51
      70 CONTINUE
         WRITE (6,2032)
         WRITE (6,2030)
         WRITE (6,2035) (M,(NP(J,M),J=1,3),MAT(M),TH(M),M=1,NUMEL)
C
C      DETERMINE BAND WIDTH AND NUMBER OF EQUATIONS
C
         L=0
         DO 80 M=1,NUMEL
            DO 80 I=1,2
               II=I+1
               DO 80 J=II,3
                  K= IABS(NP(I,M)-NP(J,M))
                  IF (K.GT.L) L=K
      80 CONTINUE
C
         MBAND = 2*(L+1)
         NEQ= 2*NUMNP
C
         WRITE (6,2040) MBAND,NEQ
         IF (MBAND.LE.150.AND.NEQ.LE.1300) GO TO 90
         WRITE (6,2050)

```



```

      CALL EXIT
85   WRITE(6,2060)
998  CALL EXIT
C
90   WRITE(6,3000)
3000 FORMAT( ' READIN COMPLETED ' ///)
      RETURN
C
C  FORMAT STATEMENTS
1000 FORMAT(18A4/ 3I6)
2000 FORMAT(1H1,10X,18A4,////)
      1 1H ,      26H NUMBER OF NODAL POINTS = ,I6/
      2 1H ,      26H NUMBER OF ELEMENTS      = ,I6/
      3 1H ,      26H NUMBER OF MATERIALS      = ,I6/
2005 FORMAT(///,1H ,10X, 21H MATERIAL PROPERTIES //
      11X, 8HMAT. NO.,4X, 9HMODULUS E,4X,14HPOISSONS RATIO,4X,11HUNIT WEI
      2GHT,/)
1010 FORMAT(6X,F12.0,2F6.0)
2010 FORMAT(1H ,I5,F17.0,F15.3,F17.3)
2014 FORMAT( '1', 5X, 'OUTPUT OF INPUT NODAL DATA ')
2015 FORMAT(///,10X,19H NODAL POINT OUTPUT,///
      11H ,59H NODE   KODE      X COORD      Y COORD      X FORCE      Y FORCE
      2//)
2016 FORMAT('1', 5X, 'OUTPUT OF COMPLETE NODAL DATA ')
1020 FORMAT(2I6,2F12.2,2F12.2)
2020 FORMAT(I4,I6,F13.3,3F12.3)
2021 FORMAT(I6,2F12.2)
2025 FORMAT(1H0,28H ERROR IN NODAL DATA,NODE = ,I4)
2030 FORMAT(///,10X, 13H ELEMENT DATA ///,
      1' 40H ELEM   I      J      K      MAT THICKNESS //)
2031 FORMAT('1',5X, 'OUTPUT OF INPUT ELEMENT DATA' )
2032 FORMAT( '1', 5X, 'OUTPUT OF COMPLETE ELEMENT DATA ' )
1035 FORMAT (5I6,F6.0)
2035 FORMAT (1X,I4, 4I6,F11.4)
2040 FORMAT (///10X, 22H BAND WIDTH      = ,I6/
      1      10X, 22H NUMBER OF EQUATIONS = ,I6)
2050 FORMAT(///10X, 33H PROBLEM EXCEEDS SPECIFIED LIMITS )
2060 FORMAT( 'MLM1 IS LESS THAN OR EQUAL TO ZERO ')
C
      END
      SUBROUTINE ASTIF
C
C  THIS SUBROUTINE TAKES EACH ELEMENT IN TURN AND FORMS THE ELEMENT STIFFNESS
C  MATRIX (BY CALLING ELSTIF).IT ASSEMBLES THE ELEMENT STIFFNESSES INTO
C  KSTIF , ASSEMBLES THE APPLIED LOAD VECTOR (AP), AND MODIFIES THE
C  ASSEMBLASES FOR DISPLACEMENT BOUNDARY CONDITIONS (BY CALLING MODIFY)
C
      COMMON E(6) ,PR(6) ,RO(6) ,X(650) ,Y(650) ,U(650) ,V(650) ,TH(1200) ,
      1STIF(150,1300) ,AP(1300) ,ESTIF(6,6) ,ECM(3,3) ,EBM(3,6) ,ESM(3,6) ,WT
      COMMON NUMNP ,NUMEL ,NUMAT ,KODE(650) ,NP(3,1200) ,MAT(1200) ,MBAND ,
      1 NEQ,M,LM(6)
C
C  INITIALIZE APPLIED LOAD VECTOR AND MASTER STIFFNESS MATRIX AND ECM
C
      DO 10 I=1,NEQ
      AP(I)=0.0
      DO 10 J=1,MBAND
10   STIF(J,I)=0.0
      DO 20 I=1,3
      DO 20 J=1,3

```



```

20   ECM(I,J)=0.0
C   FORM ELEMENT CONSTITUTIVE MATRIX (ECM) IF NUMAT=1)
C
      IF (NUMAT.NE.1) GO TO 30
      EPR=PR(1)
      COM=E(1)/((1.+EPR)*(1.-2.*EPR))
      COM1=COM*(1.-EPR)
      COM2=COM*EPR
      ECM(1,1)=COM1
      ECM(2,2)=COM1
      ECM(1,2)=COM2
      ECM(2,1)=COM2
      ECM(3,3)=E(1)/(2.*(1.+EPR))
C
30   DO 45 M=1,NUMEL
C
      CALL ELSTIF(1)
C
C   ASSEMBLE ELSTIF INTO MASTER STIFFNESS MATRIX
C
      DO 35 I=1,3
      I2=2*I
      LM(I2)=2*NP(I,M)
35   LM(I2-1)=LM(I2)-1
C
C
      DO 40 I=1,6
      II=LM(I)
      DO 40 J=1,6
      JJ=LM(J)-II+1
      IF (JJ.LE.0) GO TO 40
      STIF(JJ,II)=STIF(JJ,II)+ESTIF(I,J)
40   CONTINUE
C
C   ADD GRAVITY LOADS INTO AP VECTOR
C
      DO 45 I=2,6,2
      II=LM(I)
      AP(II)=AP(II)-WT
45   CONTINUE
C
C   ADD NODAL LOADS INTO AP VECTOR
C
      DO 50 N=1,NUMNP
      N2=2*N
      AP(N2)=AP(N2)+V(N)
50   AP(N2-1)=AP(N2-1)+U(N)
C
C   MODIFY STIFFNESS AND LOAD VECTOR FOR DISPLACEMENT BOUNDARY CONDITIONS.
C
      DO 100 N=1,NUMNP
      N2=2*N
      IF (KODE(N) .NE. 80,70,60)
60   II=N2-1
      CALL MODIFY(II,N)
      CALL MODIFY(N2,N)
      GO TO 100
70   II=N2-1
      CALL MODIFY(II,N)
      GO TO 100

```



```

80      IF (KODE(N).EQ.0) GO TO 100
        CALL MODIFY(N2,N)
100     CONTINUE
C
        RETURN
        END
        SUBROUTINE ELSTIF(KOP)
C      THIS SUBROUTINE FORMS THE ELEMENT STIFFNESS MATRIX (ESTIF) OR
C      ELEMENT STRESS MATRIX (ESM) FOR THE CONSTANT STRAIN TRIANGLE
C
        COMMON E(6),PR(6),RO(6),X(650),Y(650),U(650),V(650),TH(1200),
1      STIF(150,1300),AP(1300),ESTIF(6,6),ECM(3,3),EBM(3,6),ESM(3,6),WT
        COMMON NUMNP,NUMEL,NUMAT,KODE(650),NP(3,1200),MAT(1200),MBAND,
1      NEQ,M,LM(6)
C
        DIMENSION AV(3),BV(3)
C
        DO 10 I=1,3
        DO 10 J=1,6
10      EBM(I,J)=0.0
        I=NP(1,M)
        J=NP(2,M)
        K=NP(3,M)
C
C      FORM ELEMENT DIMENSIONS
C
        AV(1)=X(K)-X(J)
        AV(2)=X(I)-X(K)
        AV(3)=X(J)-X(I)
        BV(1)=Y(J)-Y(K)
        BV(2)=Y(K)-Y(I)
        BV(3)=Y(I)-Y(J)
        AREA2=AV(3)*BV(2)-AV(2)*BV(3)
        IF (TH(M).EQ.0.) TH(M)=1.
        VOL=TH(M)*AREA2/2.
        IF (VOL.LE.0.) GO TO 75
C      FORM CONSTITUTIVE MATRIX
C
        IF (NUMAT.EQ.1) GO TO 30
        NM=MAT(M)
        EPR=PR(NM)
        COM=E(NM)/((1.+EPR)*(1.-2.*EPR))
        COM1=COM*(1.-EPR)
        COM2=COM*EPR
        ECM(1,1)=COM1
        ECM(2,2)=COM1
        ECM(1,2)=COM2
        ECM(2,1)=COM2
        ECM(3,3)=E(NM)/(2.*(1.+EPR))
C
C      FORM ELEMENT B MATRIX (EBM)
C
30      DO 40 I=1,3
        I2=2*I
        I2M=2*I-1
        EBM(1,I2M)=BV(I)/AREA2
        EBM(2,I2)=AV(I)/AREA2
        EBM(3,I2M)=EBM(2,I2)
40      EBM(3,I2)=EBM(1,I2M)
C

```



```

C   FORM ELEMENT STRESS MATRIX (ESM)
C
      DO 50 I=1,3
      DO 50 J=1,6
      ESM(I,J)=0.0
      DO 50 K=1,3
50   ESM(I,J)=ESM(I,J)+ECM(I,K)*EBM(K,J)
C
      IF(KOP.EQ.2) GO TO 80
      IF(NUMAT.EQ.1) NM=1
      WT=VOL*RO(NM)/3.
C
C   FORM ELEMENT STIFFNESS MATRIX (ESTIF)
C
      DO 70 I=1,6
      DO 70 J=1,6
      ESTIF(I,J)=0.0
      DO 60 K=1,3
60   ESTIF(I,J)=ESTIF(I,J)+EBM(K,I)*ESM(K,J)
70   ESTIF(I,J)=ESTIF(I,J)*VOL
      GO TO 80
75   WRITE(6,1000) M
      CALL EXIT
80   RETURN
C
C
1000  FORMAT (1H1, 18H VOLUME OF ELEMENT ,I4, 18H IS LESS THAN ZERO)
C
      END
      SUBROUTINE MODIFY (I,N)
C
C   THIS SUBROUTINE MODIFIES KSTIF AND AP IF A DISPLACEMENT BOUNDARY CONDITION
C   IS IMPOSED IN EQUATION I ASSOCIATED WITH NODAL POINT N
C
      COMMON E(6),PR(6),RO(6),X(650),Y(650),U(650),V(650),TH(1200),
1      STIF(150,1300),AP(1300),ESTIF(6,6),ECM(3,3),EBM(3,6),ESM(3,6),WT
      COMMON NUMNP,NUMEL,NUMAT,KODE(650),NP(3,1200),MAT(1200),MBAND,
1      NEQ,M,LM(6)
C
      DISP=U(N)
      IF((I-2*N).EQ.0) DISP=V(N)
C
      DO 50 J=2,MBAND
      IL=I+J-1
      IU=I-J+1
      IF(IU.LE.0) GO TO 10
      AP(IU)=AP(IU)-STIF(J,IU)*DISP
      STIF(J,IU)=0.0
10   IF(IL.GT.NEQ) GO TO 50
      AP(IL)=AP(IL)-STIF(J,I)*DISP
      STIF(J,I)=0.0
50   CONTINUE
      AP(I)=DISP
      STIF(1,I)=1.0
      RETURN
      END
      SUBROUTINE BAND1
C
C   THIS SUBROUTINE SOLVES FOR DISPLACEMENTS USING A GAUSSIAN ELIMINATION
C   TECHNIQUE FOR SYMMETRIC BANDED MATRICES STORED IN CORE

```



```

C
COMMON E(6),PR(6),RO(6),X(650),Y(650),U(650),V(650),TH(1200),
1A(150,1300),B(1300),ESTIF(6,6),ECM(3,3),EBM(3,6),ESM(3,6),WT
COMMON NUMNP,NUMEL,NUMAT,KODE(650),NP(3,1200),MAT(1200),MM,
1 NN,M,LM(6)
C
C TRIANGULARIZE AND REDUCE RIGHT HAND SIDE
NL=NN-MM+1
NM=NN-1
MR=MM
C
DO 100 N=1,NM
IF (A(1,N).LE.0.) GO TO 700
BN=B(N)
B(N)=BN/A(1,N)
IF (N.GT.NL) MR=NN-N+1
C
DO 100 L=2,MR
IF (A(L,N).EQ.0.) GO TO 100
C= A(L,N)/A(1,N)
I= N+L-1
J= 0
DO 50 K=L,MR
J=J+1
50 A(J,I)= A(J,I)-C*A(K,N)
B(I)=B(I)-C*BN
A(L,N)=C
100 CONTINUE
C
C BACK SUBSTITUTE
C
I=NN
C
B(NN)=B(NN)/A(1,NN)
DO 600 N=1,NM
I=I-1
IF (N.LT.MM) MR= N+1
DO 600 J=2,MR
K=I+J-1
600 B(I)=B(I)- A(J,I)*B(K)
WRITE(7,2001) ((I,B(I)),I=1,NN)
2001 FORMAT('1',I6,E15.5)
RETURN
700 WRITE (6,2000) N
CALL EXIT
2000 FORMAT(1H0, 81H ZERO OR NEGATIVE ELEMENT ON MAIN DIAGONAL OF TRIA
1NGULARIZED MATRIX FOR EQUATION ,I5)
C
END

```


B30140